Disk Cutter Drilling Performance and Optimization Methods, Rock Strength Correlation and Field Data Analysis

By

©Salum Mafazy

A thesis submitted to the School of Graduate Studies in partial fulfillment of the requirements for the degree of

Master of Engineering

Faculty of Engineering and Applied Science

Memorial University of Newfoundland

February, 2023

St. John's, Newfoundland and Labrador, Canada

Abstract

Drilling a rock near the ground surface has an increasing demand for natural resources exploration, such as the recovery of minerals or crushed rock, the application of tunneling in civil engineering, etc. A recent field mine drilling at Baie Verte, located in the North of Newfoundland, Canada, involved a diamond drilling hole (DDH) for core recovery, which was intended for lithology analysis and as a pilot hole and a large diameter hole drilling (LDH) for ore excavation. This thesis includes an investigation of mining drilling on the LDH to determine abnormal drilling low rate of penetration (ROP) performance at a specific depth interval, where drilling data was analyzed based on each lithology. Also rock material characterization was conducted on granite rock to introduce a new method of Semi-Point Load Strength Index (Semi-PLSI) for estimation of the rock strength, and a detailed analysis of the effect of microwave irradiation on rock properties as one of the influencing technology of an increasing ROP. The above studies involve several laboratory tests, which include detailed rock core logging, mechanical tests, cutting size analysis, and mineral liberation analysis (MLA). The study of drilling performance at specific interval was influenced by high rock strength which was caused by a variation of rock micro-structure determined by MLA technology. Also, the rock characterization study of a new approach of Semi-PLSI shows excellent correlation and strength estimation with standard PLSI and other strength tests. Additionally, microwave irradiation (MI) analysis shows a decrease in strength, ultrasound wave velocities and elastic constants of the rock after the rocks are exposed to MI. Also, the effects of MI observed to increase drilling rate of penetration (D-ROP) of the rocks.

Acknowledgments

All the perfect praises and thanks be to Almighty God.

First, I would like to express my sincere and deep gratitude to my respected supervisor Dr. Stephen Butt for his positive support for the entire life of my MEng program. His supervision, guidance, teaching, and other contributions were so incredible to me in accomplishing my research.

Also, I thank Novamera Inc., Memorial University of Newfoundland (MUN), and MITACs for the Sustainable Mining by Drilling (SMD) project's technical and financial support, which enable me to participate and complete my research on time.

I sincerely thank all the members of the Drilling Technology Laboratory (DTL). I am incredibly thankful to Laboratory Manager Dr. Abdelsalam Abugharara for his help, cooperation, and motivation for achieving the goals. Adding to this list, I would also like to mention my fellow group members, Zijian Li, and Michael Marsh, for their assistance in my research.

Last but not least, I am grateful to my whole family, including my mother, Aziza Salim, and my supportive wife, Ilham Ally, who have been there for my entire graduate life. Also, without forgetting my sister Maryam Omar and Amina Mafazy. I am truly thankful for having them all in my life.

Table of Contents

List of Figures

List of Tables

Nomenclatures

A_B	Bit Area
ASTM	American Society for Testing Materials
ASME	American Society of Mechanical Engineers
BE	Back-scattered Electron
BTS	Brazilian Tensile Strength
BHA	Bottom hole assembly
BSE	Backscattered electrons
Cc	Coefficient of Curvature
CCS	Confined Compressive strength
CGS	Canadian Geotechnical Society
CSA	Cutting Size Analysis
CI	Coarseness Index
Cu	Coefficient of uniformity
CMC	Carboxymethyl cellulose
CSD	Cutting Size distribution
D-ROP	Drilling Rate of Penetration
DAQ	Data Acquisition
DAQ	Data Acquisition System
DD	Diamond Drilling
DDH	Diamond Drilling Hole
DE/D.E	Drilling Efficiency

DF	Direct Flash
DOT	Drill of Test
DTL	Drilling Technology Laboratory
DSE	Drilling Specific Energy
d_b	Bit Diameter
EDX	Energy Dispersive X-ray
FFT	Full-Field Trial
GR	Granite
GHz	Gigahertz
GLF	Geomechanics Loading Frame
GSA	Grain Size Analysis
ISRM	International Society for Rock Mechanics
IT/ITS	Indirect Tensile Strength
Is	Point Load Index
KN	KiloNewtons
k	Calibration Constant
L: D	Length-to-diameter ratio
LDH	Large Diameter Hole
LVDT	Linear Variable Displacement Transducer
M.A.T	Mafic Ash Tuff
MI/MWI	Microwave Irradiation
MSE	Mechanical Specific Energy

MUN	Memorial University of Newfoundland
N	Rotary Speed
MLA	Mineral Liberation Analysis
MWD	Measurements-while-Drilling
OMAE	Offshore Mechanics and Arctic Engineering
PAM	Polyacrylamide
PDC	Polycrystalline Diamond Compacts
PLS/PLSI	Point Load Strength Index
PSD	Particle Size Distribution
PEO	Polyethylene-oxide
R/ROP	Rate of Penetration
RBM	Raise Boring Machine
RLM	Rock-like-Material
RPM	Revolution-per-Minute
RQD	Rock Quality Designation
S	In-situ Stress
SDS	Sandstone
SE	Secondary Electrons
SEM	Scanning Electron Microscope
SMD	Sustainable Mining by Drilling
SH	Schmidt Hammer
SW	Software

SS	Sandstone
T	Torque
TBM	Tunnel Boring Machine
T&D	Torque and Drag
TFA	Total Flow Area
TVD	True Vertical Depth
UCS	Unconfined Compressive Strength
Vp / vp	Primary (pressure) Wave Velocity
Vs/ vs	Secondary (shear) Wave Velocity
W/WOB	Weight-on-Bit
WBMs	Water-Based Mud
OBMs	Oil-Based Mud
SBMs	Synthetic-Base Mud
XT	Temperature Elastomer

Chapter 1: Introduction

1.1 Background of the Thesis

Rock excavation through blasting and surface drilling has been used widely in the mining industry. One breakthrough in the industry is near surface drilling using a large diameter hole (LDH). LDH involves drilling a well using a large cutter head which is considered more than 0.5 m in diameter, which was developed based on the application of other methods used in the civil and mining industry such as Tunnel Boring Machines (TBM), Raise Boring Machine (RBM), and Pile Drilling (Mafazy et al., 2022). The rate of penetration (ROP) is one of the critical drilling parameters that predict the performance of the well in the drilling industry, and it is defined as penetration depth per hour (m/h) (Hareland et al., 2010). Mining or oil and gas companies usually prefer drilling with high ROP and cost reduction per foot. Other parameters like Revolution per Minute (RPM), Weight-on-Bit (WOB), and torque are also essential for a better understanding of the drilling performance of a well and prediction ROP (Takbiri-Borujeni et al., 2019). In natural resource exploration, either mining or oil and gas, understanding the rock or lithology ahead of bit penetration is essential. An abrupt variation of ROP in conventional drilling may indicate a change in the lithology (Ashena & Thonhauser, 2018). The process of coring the rock is needed for various purposes, including conducting core analysis, i.e., core logging and mechanical tests to obtain underground geological formation, strength and hardness of the rock (Mafazy et al., 2022). In some cases, a study of the rock mineral microstructure and its composition is required. Mineral Liberation Analysis (MLA) technology is a common method used to identify and evaluate ore mineralogy and

metallurgical products (Grant et al., 2016). This analysis is important since even the same rock type has a different mineral alignment as the depth increases and may cause to change in the strength of the rock due to the variation of the hardness of each mineral.

Also, while the drill bit chips the rock, the cuttings are generated at the downhole. Several studies have evaluated the relationship between drilling performance and cutting size (Altındag, 2003), (Ersoy & Waller, 1997) and (Reyes et al., 2015). The shape of the cuttings depends on different conditions, including the drill string weight on the bit, the higher the weight, and the small size of the cuttings. Another factor is the drilling fluid circulation method, which may be reverse or direct flash circulation, the type of rock or lithology penetrated, etc. Hence, it is essential to conduct a Cutting Size Analysis (CSA) of the drill cuttings to relate the shape of the chip size with lithology, drilling parameters, and mode of circulation to evaluate the drilling performance and ROP behavior (Alsuwaidi, 2018).

A detailed determination and correlation of the strength of the rock are needed in all excavation industries. Rock strength relates to the drilling performance since the drill bit must contact the rock to establish penetration (Mafazy et al., 2022). Analysis and determination of the rock strength at the laboratory is a method that would estimate the in-situ strength and even estimate drilling ROP. Lastly, the drilling methods or technology that lead to increased ROP are essential. Utilizing microwave irradiation is one of the technologies practiced in the industry to optimize ROP (Hassani et al., 2016) and (Kahraman et al., 2020). Also, a study shows microwave heating has been used to analyze rock properties (Lu et al., 2019), (Zhao et al., 2020) and (Hong et al., 2020).

1.2 Research Objective

This research focuses on three main categories, drilling performance (D.P) analysis, a new method of rock strength estimation and an initial stage analysis of the effect of microwave irradiation on rock properties. The D.P study was conducted based on the mining field's full field trial (FFT), Baie Verte, located in the North of Newfoundland, Canada. Multiple influencing factors such as WOB, ROP, torque, RPM, chip size, penetrating lithology, strength, hardness, and rock mineral structure and composition have been analyzed to look into the cause of the variation of the ROP at shallow and deeper well depths. The objective was to determine the drilling performance for the next drilling phase to enhance the rate of penetration (ROP) and maximize drilling efficiency (DE).

The rock strength test was conducted using Granite rock at Drilling Technology Laboratory (DTL) at MUN to determine a new strength test known as Semi-PLSI, derived from the standard test of PLSI. This method aims to establish and simplify the testing procedures and correlations with other tests. This test estimates the strength quickly and minimizes possible errors by replacing the two conical platens of standard PLSI with one flat circular plate at the bottom and one conical platen at the top. A microwave irradiation study was utilized to analyze the heating's effect on the granite and sandstone rocks. The determination of the rock properties, including strength and ultrasonic wave velocities, is to observe the behavior of weakening the rock strength under the heating effect. This study aims to focus on methods of inducing fractures and reducing rock strength ahead of the penetrating tool, e.g., drill bit, to increase ROP and rock fragmentation.

1.3 Thesis Outline

This thesis consists of 7 chapters. The description of each chapter has mentioned as follows:

Chapter 1 is the introduction which describes the overview and a summary of this thesis. This chapter includes a background of the thesis content and the research objectives. Also, this chapter provides a summary of the chapter contents, including a literature review, methodology, technical paper publications, a quarterly report conducted at the DTL laboratory at MUN, and a conclusion of this study.

Chapter 2 is a detailed literature review that includes a broad concept of optimum rotary drilling, drilling performance analysis, methods, and technology for increasing ROP, e.g., the effect of applying microwave irradiation on a rock. Also, this chapter covers a comprehensive review of the methods of rock strength correlation based on laboratory mechanical tests.

Chapter 3 explains the methodology used to complete the research for chapters 4, 5, and 6. The methods include rock sample and test preparation, core logging, and types of experiments and performance. It also provides the field operation activities, equipment utilized, and data collection.

Chapter 4 represents the publication of a technical paper at GeoCalgary 2022. This chapter explains the investigation of abnormally low ROP observed at the time of full-field trial during LDH drilling in mining operations. It represents a detailed drilling performance by each lithology drilled. Also, this paper analyzes experimental laboratory tests correlated with drilling field data analysis and influencing factors for low ROP.

Chapter 5 is publication of the OMAE conference 2022. This paper provides a detailed approach to a new method, known as Semi-PLSI, to estimate the strength of the rock. Additionally, the correlation with other tests was developed for strength estimation.

Chapter 6 is another technical paper which was to OMAE 2023 proceedings. This which involves methods or technology to increase ROP. The chapter provided an initial analysis stage for investigating microwave irradiation (MI) for weakening the rock formation. Hence, determination of the influence of MI on a rock strength, rock properties (strength and V_P and V_S) and elastic constants of the rock were analyzed pre-and post-MI.

Chapter 7 provides a conclusion, summary, and recommendation for the study presented and future work related to drilling performance, strength tests, and methods of increasing ROP.

Chapter 2 : Literature Review

2.1 Optimum Rotary Drilling

2.1.1 LDH Technology

LDH drilling is the technology used to drill a hole that is considered greater than 50 cm in diameter. Such techniques are used for rock excavation using equipment such as Tunnel Boring Machines (TBMs), Raise Boring Machines (RBM), and Pile Drilling (Mafazy et al., 2022). Figure 2-1 shows a good example of LDH (TBM). Usually, TBM ranges from 1m (3.3ft) to 17.6m (58ft) in diameter. They applied in tunnel construction for traffic, hydropower, sewerage and water, underground storage, and mining. Different types of TBMs with different diameters are adapted to different formation conditions.

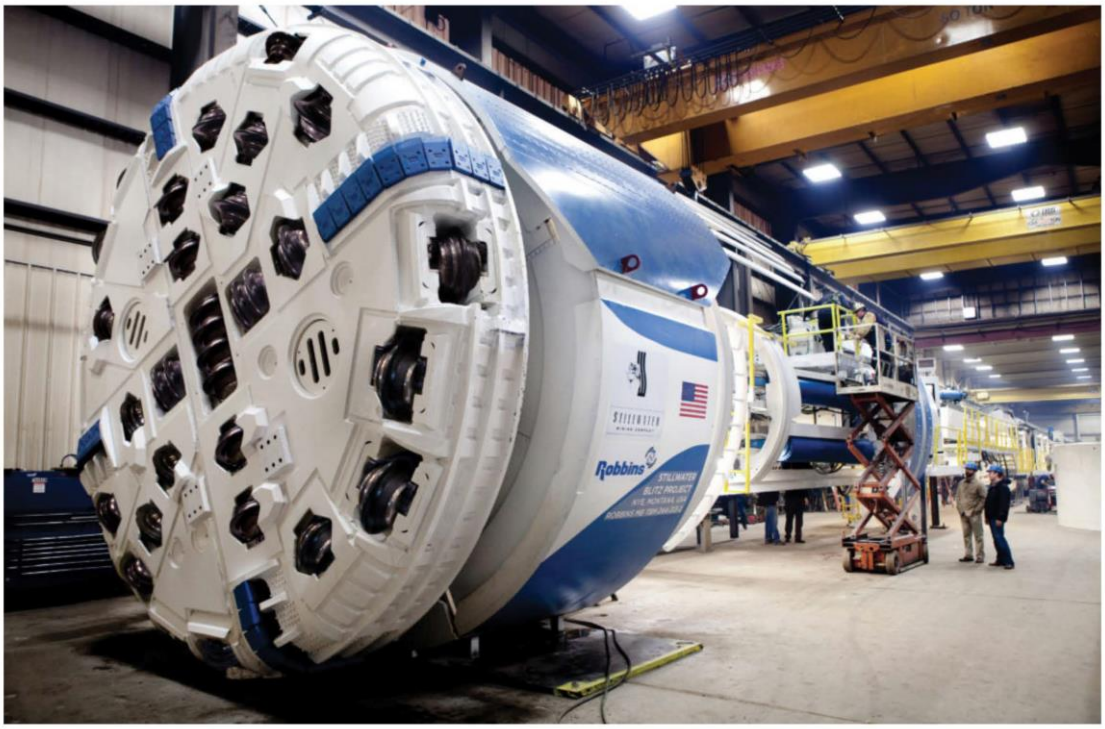

Figure 2–1. The mining head of James Robbins TBM
(Krzysztof & Piotr, 2019)

However, the main parameters of a TBM are thrust and torque, where a motor rotates the cutter head, and the thrust is provided by special cylinders that push the cutter head (De Moura, 2021). Allen, 1968 showed the advance of rotary drilling technology. He presented the development of large diameter holes in the mining industry where, up to 1967, large diameters of 72 in, 90 in, 108 in, 124 in, and 130 in were drilled to 2790 ft, 710 ft, 1435 ft, 935 ft, and 520 ft respectively.

2.1.2 Drilling Performance Evaluations

Drilling a wellbore in oil and gas and mining needs a lot of consideration to have better drilling performance and minimize drilling costs. An understanding of the geological formation being drilled is one of the essential factors to consider. Also, a limitation of drilling parameters is practiced when a geological condition is critical and inappropriate handling of running drilling. Thrust applied, the rotational speed of the bit, torque, ROP, and drilling fluid are among the parameters to be taken care of at the time of drilling. Drilling performance is measured from the beginning of drilling a wellbore to reach the target. Drilling engineers will have to optimize drilling to achieve the desired high ROP. It is the main parameter to analyze the performance of a wellbore. Other parameters like WOB, revolution per minute (RPM), and torque are also important. Maurer (1965) presented the concept of "perfect cleaning" and showed the relationship between ROP and other parameters, including WOB, in situ rock strength, bit diameter and rotary speed. His analysis shows that the higher WOB, the higher ROP until maximum weight is reached. Altindag (2003) estimated the ROP using particle size analysis and elaborated the relation of geometrical parameters, machine parameters and operating process to account for the drillability of rock, as shown in Figure 2-2.

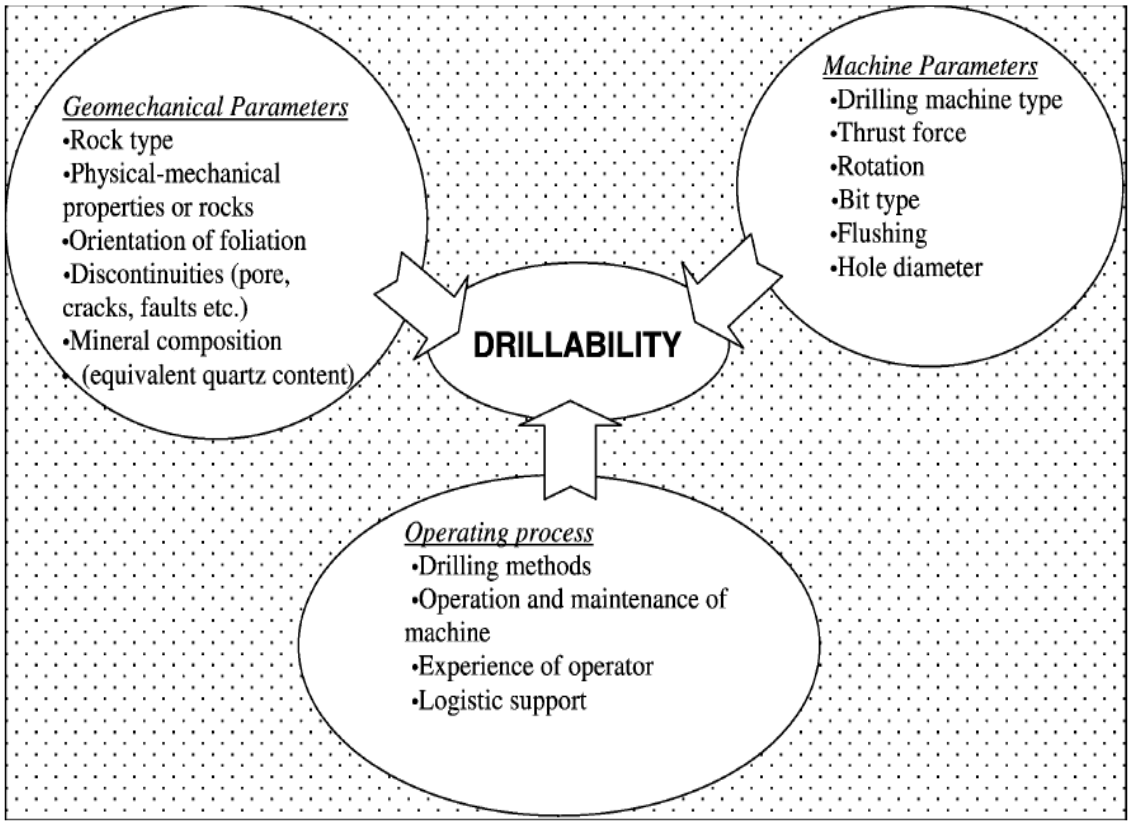

Figure 2–2. Factors affecting drill ability of a rock (Altindag, 2003)

Also, another study showed that drillability, which is the drilling efficiency of rock, depends on three main parameters rock characteristics, drill rig parameters, and operational parameters (Reyes et al., 2015). Butt (2016) provided a detailed explanation of the factors affecting drilling optimization, including drilling Efficiency (DE), which is the function of in situ or confined compressive strength of the formation (CCS) and mechanical specific energy (MSE). He also presented the Drill of Test (DOT) analysis to observe the relationship between ROP vs. WOB and the determination of the flounder point. A study showed a novel correlation to identifying inefficient drilling conditions by estimating the Drilling Specific Energy (DSE) and ROP from the field data (Armenta, 2008). DSE is the modified form of MSE, which include a hydraulic term. His results determine that the

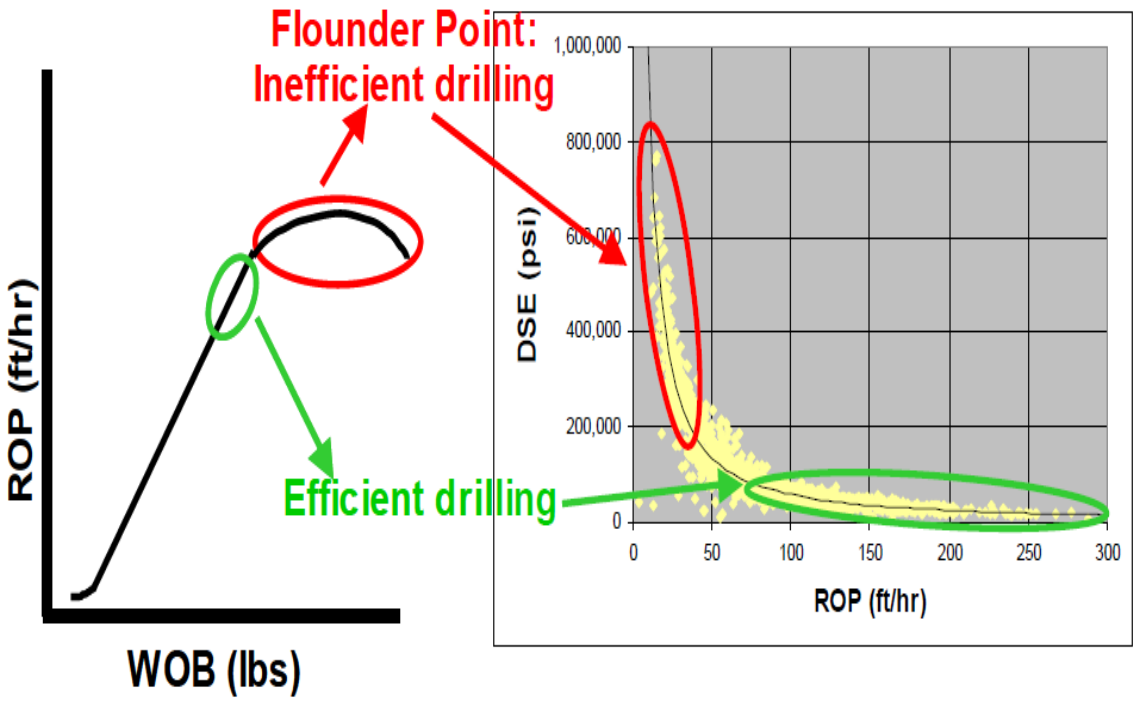

Figure 2–3. Determination of efficient and inefficient point for drilling optimization (Armenta, 2008)

efficient drilling zone with high ROP resulted in low DSE and a point of inefficient drilling known as a flounder point, which resulted in high DSE, as shown in Figure 2-3.

The application of drill cuttings for drilling performance analysis is essential. Geologists and reservoir engineers use cuttings to understand formation properties, such as porosity and permeability, waste management, real-time drilling operations, correct sampling, measurement, and interpretation of cuttings to prevent problems and improve drilling performance (Karimi, 2013). The common particle or grain size analysis (GSA) method is known as sieve analysis or test sieving (Ahmed et al., 2020). It is an analytical procedure to determine the particle size distribution of the coarse and finer aggregates. The method is followed by arranging several layers of sieves with different grades of sieve opening sizes (ASTM-D6913). Holtz and Kovacs (1981) presented detailed GSA methods and numerical

examples for grain size distribution and gradation theory that are applicable in geotechnical engineering. Reyes et al. (2015) analyzed the drill cuttings by generating a particle size distribution (PSD) and bar-PSD methods, where mean particle size (d) and coarseness index (CI) was computed to find the relationship with ROP and WOB. Ahmed et al., (2020) presented a study of drill cutting analysis to assist drilling performance in hard rock hole widening operation, where he compared the cuttings obtained using (a) coring bit/pilot hole (26.4 mm), (b) PDC bit-drilling (32,4mm) and (c) Hole Widening Drilling (HWD) with PDC bit (32.4mm) on the existing hole of (26.4 mm). His results showed cutting sizes were coarser for HWD operation from PSD diagrams which indicates high penetration. Ersoy and Waller (1997) showed that the particle size increased with increasing applied WOB for all the evaluated bit types. He noted that the percentage of regrinding decreased with increasing applied WOB. However, the percentage composition of fines increased with increasing rotary speed, possibly implying cuttings regrinding. He further showed the relationship between cutting size and the expended specific energy.

2.2 Rock Strength Estimation using Empirical Relations

The strength of the rock is one of the essential parameters for rock mechanical characterization in mining, oil and gas, and the construction industry. In-situ rock strength is usually estimated in the laboratory using mechanical tests, which include unconfined compressive strength (UCS), indirect tensile strength (ITS), and point load index (PLSI). These are known as destructive tests. On the other hand, tests like UCS can be estimated using non-destructive measurement tests known as ultrasonic wave measurements. For conducting the test, the procedures have been standardized by both the International Society

for Rock Mechanics (ISRM) and the American Society for Testing and Materials (ASTM) (Kahraman, 2001). UCS is usually used as a standard strength method for strength correlations. It is used in many mining companies for strength estimation. Additionally, UCS is required for building, producing, and validating rock mechanics and rock fracture numerical models. However, UCS consumes time for sample preparation and conducting tests and requires expensive equipment, and other rocks need a high load to break the Sample (Abugharara et al., 2022). Also, determining UCS in the laboratory would be challenging if the rock masses are weathered or fractured because preparing a core specimen for testing is difficult in this situation (Nazir et al., 2013). Empirical correlations and estimation of rock strength have been practiced by many researchers for suitable use of any strength methods. Implementing correlations of rock index tests has many advantages since simplifying saves time and does not require high load and economical reliability to practice (Asad, 2015). Sheorey (1997) presented a correlation between the ITS and UCS; his studies show that the compressive strength of the rock is approximately ten times the indirect tensile strength. Also, ASTM-D5731 shows that UCS can be estimated from PLSI. The analysis from standards shows that for NX. (54 mm) core, uniaxial strength is 24 times point load strength. Quan et al. (2021) developed detailed equations for UCS, BTS, and PLSI, between BTS and PLI, between P-wave and UCS, Young's modulus, and Poisson's. Also, Cargill et al. (1990) evaluated the methods for measuring the UCS of the rock. His results show a linear correlation between UCS vs. PLSI and Schmidt hammer tests. It was noted that the Schmidt hammer is dependent on the rock type. Some correlation shows better performance results than others; Farah (2011) studied and developed relations

between UCS and the physical properties of weathered Ocala limestone. He presented a better correlation of ITS with UCS than PLSI.

2.3 Methods and Technology for Increasing ROP

2.3.1 Friction Reduction to Increase Thrust and Torque at the Bit

2.3.1.1 Drilling Fluid Additives (Polymers, Flocculants, Lubricants)

A drilling fluid is one of the critical indicators of hole cleaning in drilling operations. It is also known as drilling mud. The mud is circulated from the surface into the drill string to the bottom of the well and returns to the surface through the annulus. The fluid in rock drilling is categorized into simple compressed air through foams of at least 70% gas (usually nitrogen, carbon dioxide, or air), water-based muds (WBMs) and oil-based muds (OBMs), or synthetic-based muds (SBMs). OBMs contain 50% mixture of diesel, mineral oils, or linear paraffin (L.P.s) with water. However, SBMs are pseudo-oil-based muds with liquid materials like ethylene, such as olefins, esters, and synthetic L.P.s (ASME, 2005). The primary purpose of drilling fluid is to cool and lubricate the drill string and bit, suspend and circulate the cuttings from bit-rock interaction to the surface. In addition, drilling fluid transmits hydraulic energy to the tools and the bit, seals permeable formation by forming mud cake and provides wellbore stability by preventing the fluid from entering the wellbore formation**.** The mud is used to maintain high drilling efficiency by circulating drill cuttings once the bit cuts the rock to avoid a significant quantity of energy to regrind the rock's chips, causing drill bit wear and decreasing ROP (Carlos et al., 2017). Also, drilling fluids have been used to reduce torque and friction to increase ROP in the drilling industries (Rao et al., 2002). He investigated the drilling performance on various rocks and compared the

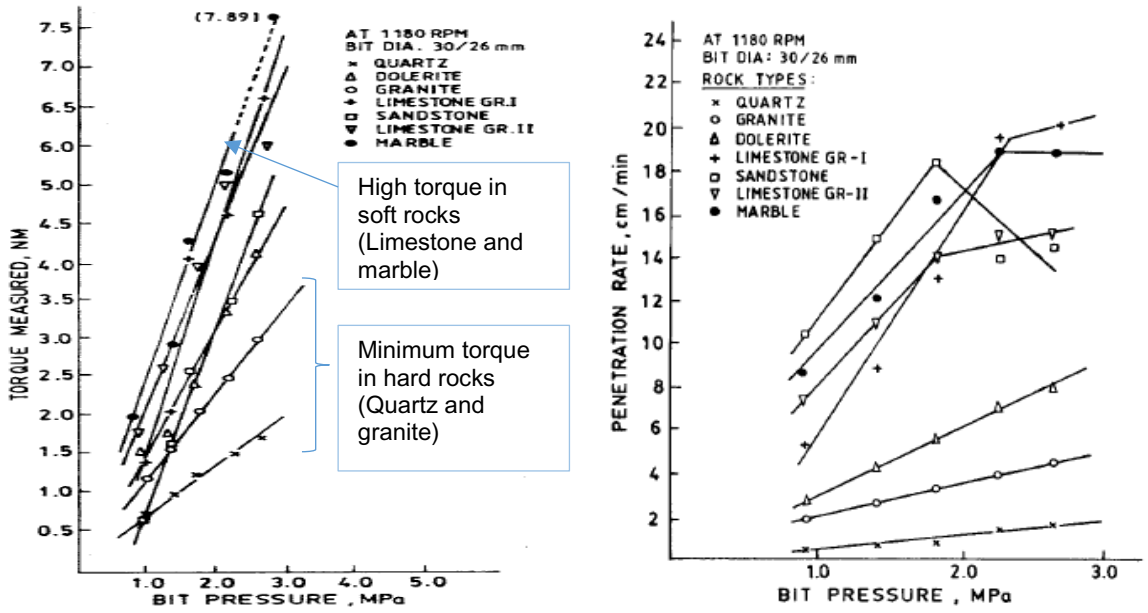

Figure 2–4. Left: The effect of bit pressure and the torque developed and Right: penetration rate with bit pressure (Rao et al. 2002)

effect between the mixture of polyethylene-oxide (PEO) added to the drilling water and plain water as drilling fluids. The study showed substantially increased ROP and reduced torque developed at the bit-rock interface. Also, the torque effect due to bit pressure on different rocks indicates that the magnitude of the torque is minimum in hard rocks like granite and quartz while maximum in softer rocks like limestone and marble (Figure 2-4). However, when the bit pressure exceeds its maximum, the frictional resistance at the bit-rock increase; hence, ROP tends to decrease. In rotary drilling, indentation is regarded as the action of cutting edges of the bit, which are continuously pushed into the rock to establish a bite 'cutting' by which the bit is given a lateral movement to break out fragments of rock (Teale, 1965). Also, in the field, polymers are added to the drilling fluids to control viscosity and filtration properties and reduce friction, heat generated (in the rock-cutting process), and drag developed in the drilling operation consequence of bit wear reduction.

Rawal et al. (2021) presented the laboratory investigation of a bit-wear of the diamond core drilling on sandstone rock samples by optimizing the drilling fluid (water) with polymeric drilling fluid additives. The study uses a 10-ppm concentration of each drilling fluid, and the result showed that carboxymethyl cellulose (CMC) showed high wear reduction compared to guar gum (G.G.) and polyacrylamide (PAM) and water without drilling fluid additives.

2.3.1.2 Axial Oscillation Tools (Downhole Agitator)

The agitator system is a gentle oscillation tool that helps reduce friction and improves weight transfer with no impact force to downhole devices. It is compatible with all measuring while drilling (MWD) systems. The agitator comprises a power section, a valve and bearing section, and a Shock section (Figure 2-5).

The functions of main parts of the agitator tool are:

- The power section: generates a pressure pulse in the system by driving the valve
- Then, the shock tool is activated after receiving pulses from the power section.
- The shock tool converts pulses to axial movement to overcome friction. The energy is delivered through the valve and bearing section, where the pumped fluid produces. The valve sections open and close, which makes the total flow area (TFA) change, resulting in high and low pressure at a minimum and maximum TFA, respectively (Figure 2-5).

Toasudjai et al. (2022) used an extreme temperature elastomer (X.T.) motor paired with an agitator system to reduce friction and facilitate the weight transfer to the BHA while sliding in long tangents or curves for great depths. His research compared the first agitator run's

ROP and the standard motor's average ROP with non-agitator runs in the same field area (Figure 2-6). X.T. motor with agitator-system BHA showed high performance when penetrating TVD in hard formation. The average ROP with a non-agitator was 27.3 m/hr, while using an agitator rose to 40.6 m/hr, and the on-bottom ROP was higher than the standard motor without agitator wells, around 30%.

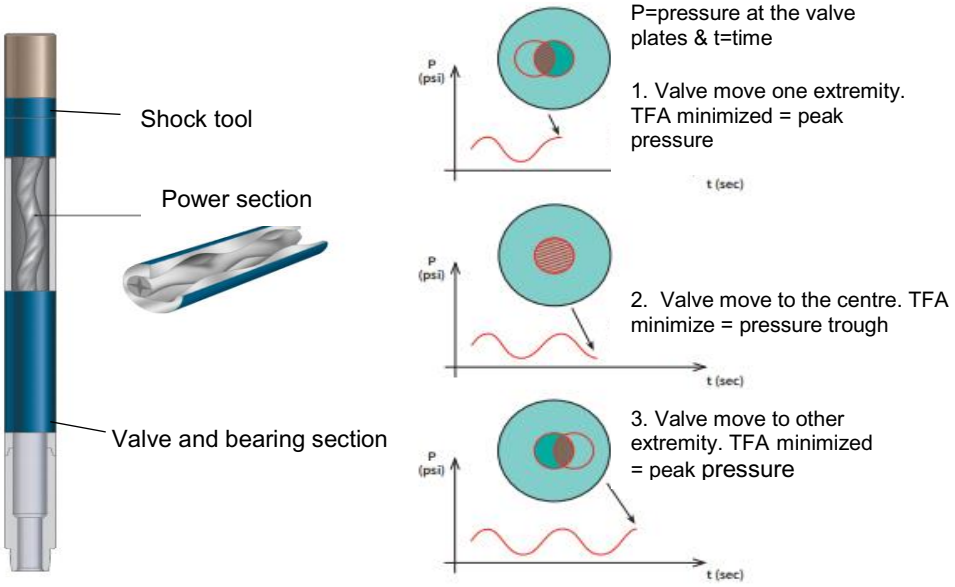

Figure 2–5. Left: Agitator system, and Right: position of the valve when the agitator operates (NOV Inc, 2016)

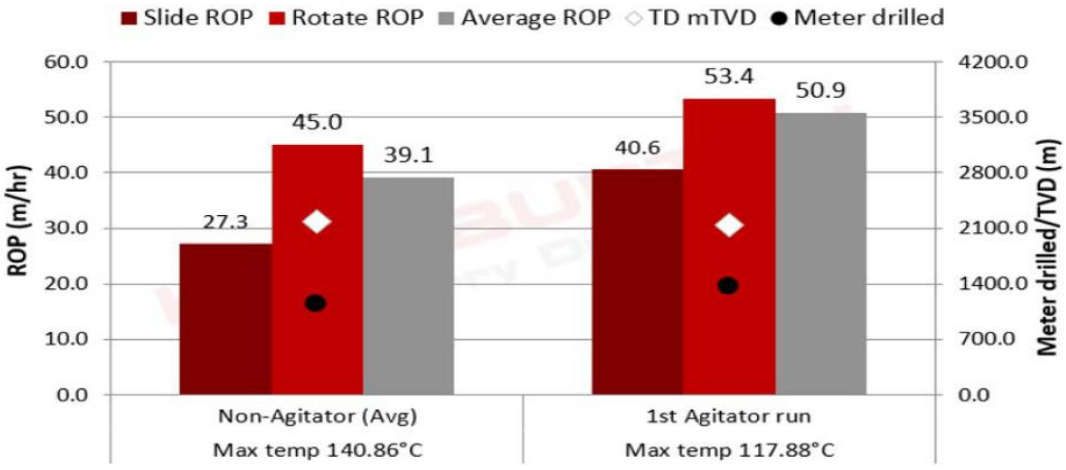

Figure 2–6. ROP comparison (Toasudjai et al., 2022)

2.3.1.3 Other Methods to Reduce Torque and Drag

Understanding the basic concepts of the torque developed when the drill bit penetrates the rock is essential. The drilling ROP and torque at the bit-rock interface depend on the thrust, rotary speed, and rock properties. In drilling, the torque has two main components. One is the power generated by the rotational speed. The other is frictional resistance based on the thrust applied and rock resistance to rotation. The drilling technique with low or desired torque will reduce drag and specific energy, which may minimize bit wear and increase ROP. Torque and drag (T&D) is the frictional resisting on drill string rotation and advancing forward (Aston et al., 1998). The theory of T&D is a common challenge in deviated well drilling, such as directional, horizontal, and extended wells in oil and gas drilling (Johancsik et al., 1984). In deviated wells, the drill string undergoes the sliding process, which increases the friction between the drill string and the borehole wall, which affects the WOB to be different from the thrust applied. Other technology and methods of reducing friction by reducing T&D have been applied to improve ROP. McCormick et al. (2012) presented a detailed practice and evolution of T&D reduction using normal force and coefficient of friction:

1. Reducing the normal forces,
2. Reducing coefficient of friction,
3. Methods of increasing dynamic friction from Static friction.

The drag (Eq.2-1) depends on the normal force, the coefficient of friction, and the tubular, and Eq.2-2 shows the relationship for torque which depends on the normal force, torque radius, the coefficient of friction, and the tubular movement. The normal force acts on each section of the drill string shown in Figure 2-7 below.

$$F_{drag}=F_N*\mu*\frac{|T|}{|V|} \qquad [2\text{-}1]$$

$$\tau = F_N*r_{torque}*\mu*\frac{|A|}{|V|} \qquad [2\text{-}2]$$

F_{drag} = force due to drag; F_N = normal force; τ = torque; T = trip speed;

V = resultant speed = $\sqrt{(T^2 + A^2)}$; A = angular speed = $\pi * D * RPM/60$;

r_{torque} = torque radius; μ = coefficient of friction.

The normal force is an opposing force acting perpendicular direction against weight string in the borehole. The normal force is increasing from vertical, inclined to lateral section of the well (Figure 2-7). Reducing or using possible lower weight of the string would reduce the normal force as well as T&D force and enhance ROP, e.g. the use of aluminum alloy of an average of 175 lb/ft3 is less than the density of still, 490 lb/ft3, which may reduce T&D effectively to transmit the WOB (McCormick et al., 2012). Hence, minimizing the normal force will result in less drag and more efficient weight transfer to the bit, which will lead an increase in penetration rate. Coefficient of friction measures the degree of resistance to motion of two elements sliding against each other. McCormick et al. (2012) mentioned that for a standard drilling operation, the modeled cased hole coefficient of friction with a water-based mud (WBM) may be 0.25, while the modeled open hole coefficient of friction maybe 0.35. However, several methods have been applied to minimize the coefficient of friction to allow affordable torque and drag to transmit the required thrust force to the drill bit including lubricants e.g., ultra Lube II, efficient hole cleaning and the use of co-polymer beads.

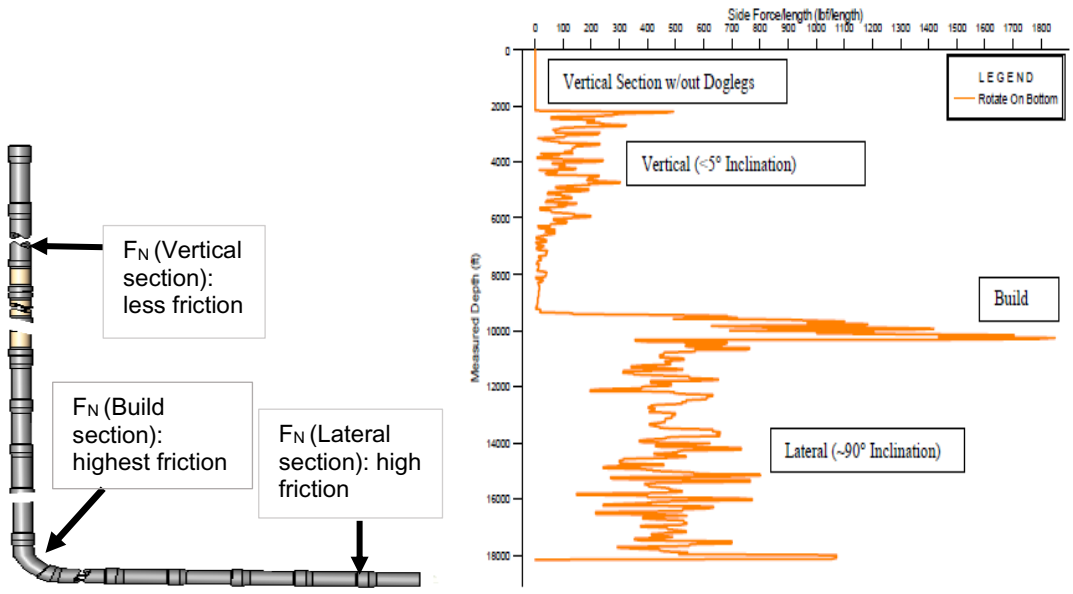

Figure 2–7. Typical slide force distribution for each section (McCormick et al., 2012)

2.3.2 Downhole Thruster

Downhole vibration is a problem that occurs in drilling, which reduces ROP, twists off the string, and contributes to the downhole failure of the motors, measurement while drilling (MWD) systems, and the bits (Schmalhorst, 1999). Therefore, to overcome the cost of drilling, a reduction of vibration of the drill string is needed, and among them is applying thrust force directly to the bit. A downhole thruster is a tool that applies direct thrust or torque at the bit. They are installed in the BHA assembly to increase direct WOB at the bit by generating WOB using drilling fluid hydraulics. The main pump working principle is to disengage the lower part of BHA and drill string. Hence, it provides a constant, controllable WOB that reduces axial vibrations and shocks related problems. The technique of using a thruster has shown a dramatic increase in ROP, bit lives, less downhole failures (Reich et al., 1995). Figure 2-8 is one of the examples of a simple thruster.

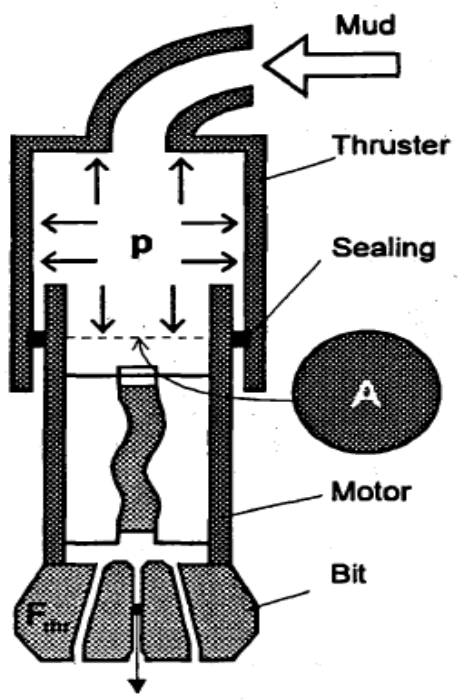

Figure 2–8. Simple Thruster BHA (Reich et al., 1995)

2.3.3 Methods of Weakening the Rock Formation

2.3.3.1 Application of Microwaves Irradiation (MWI)

The use of microwaves increased dramatically after World War II. Various applications include communications, medical purposes, domestic services, and industrial applications. Gwarek et al. (2004) identified microwaves applications in food processing (heating, thawing, biological deactivation, quality control), Industrial material drying (paper, wood, explosive wood drying), chemical reaction enhancement (micro-reaction control, fluidized beds), melting of industrial materials (glass, rubber, sludge), sintering (ceramics, metal powders), plasma generation, plasma generation, mineral processing (rock crushing, comminution) and waste treatment and recycling. Pre-treating rock using microwave radiation is widely used in the mining industry for rock crushing and comminution.

Different Researchers analyze the use of MWI to assist rock breakage. Lin et al. (2021) studied the effects of electrical conductivity on natural ores (Hongtoushan copper ore, Sishanling iron ore, and Dandong gold ore) by conducting microwave heating, and test results showed that under microwave irradiation, the stronger the electrical conductivity of the metal minerals, the smaller the penetration depth. Lu et al. (2019) analyzed the effect of the strength of basalt rock on the microwave at different exposure power levels.

It carried out X-ray diffraction and scanning electron microscopy/energy-dispersive X-ray spectroscopy for mineral composition and distribution analyses.

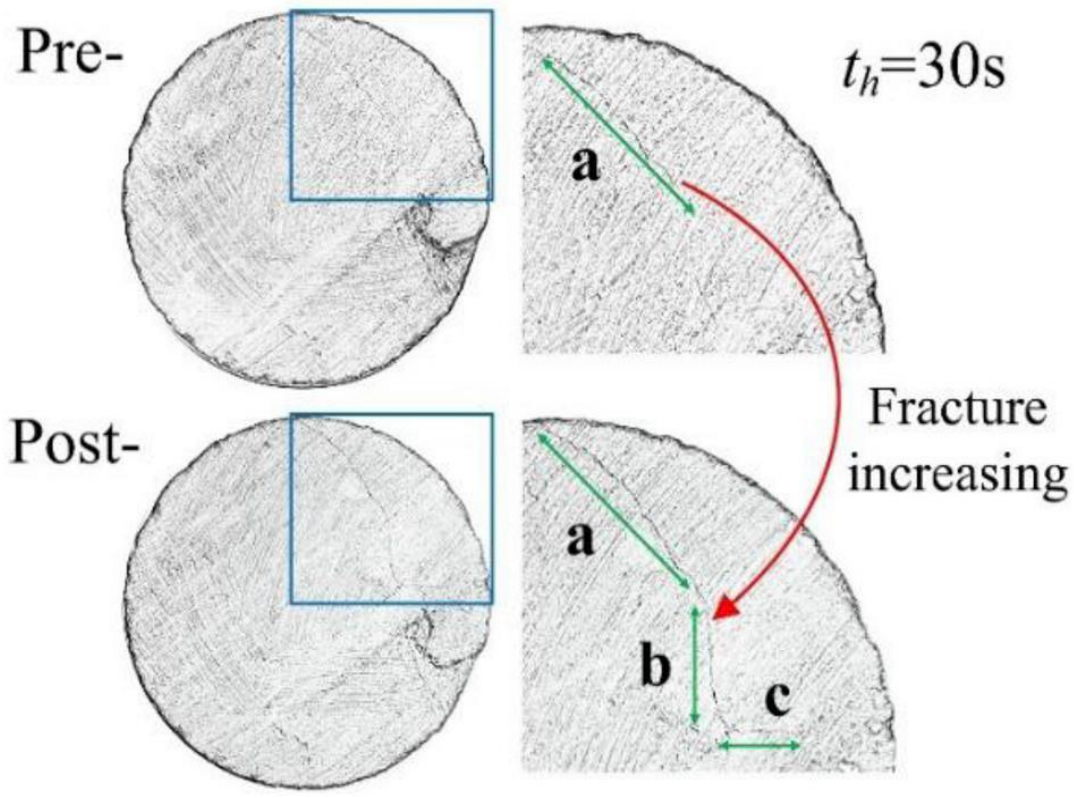

Figure 2–9 Crack propagation on the surface of the coal sample
(Hong et al. 2020)

Zhao et al. (2020) analyzed the influence of microwave power and water saturation on the rocks and mineral analyses. The mineral groups are the most significant influence on microwave sensitivity, followed by crystal structure and iron content. Also, the effect of water depends on how much water saturation is on the heating mineral. Moreover, the microwave is applicable for degassing coalbed methane (Hong et al., 2020). He uses coal cores to evaluate fracture initiation and propagation. The fractures increased as the microwave temperature rose, and the ultrasound wave velocities (P&S- wave) decreased as the tested samples induced new fractures. Figure 2-9 above shows the fracture propagation after the coal sample is heated for the 30s. Also, in rock breakage applications, there is a challenge of abnormal disc cutter wear of a TBM and unstable borehole caused by complex geology. Pre-treatment of rock by microwave heating can reduce high rock mass strength to a certain extent (Wei et al., 2019). Hassani et al. (2015) proved that ROP can be increased on the pre-weakened rock surface by applying the same thrust.

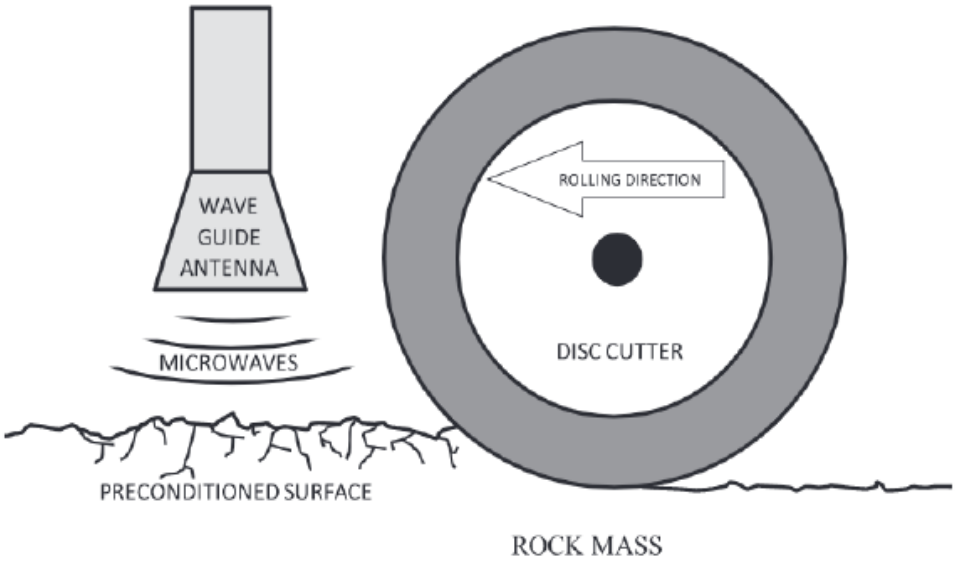

Figure 2–10. Schematic diagram of microwave assisted disc cutter of continuous TBM (Hassani et al., 2015)

He demonstrated the concept of attaching a microwave antenna to a continuous TBM's cutter head. ROP was observed to increase as the microwave power increased. Figure 2-10 shows the microwave antenna for pre-treating rock.

2.3.3.2 Fundamentals of Microwaves Heating and Mechanisms

Microwave irradiation represents the mechanisms of transfer of electromagnetic to thermal energy. Hence, microwave irradiations are electromagnetic radiation with electric and magnetic forces traveling perpendicular to each other, converting to a new form of energy, thermal energy. Microwave energy reacts differently based on the material's nature and responses, and they are classified as Conductors, insulators (transparent), and absorbers (Figure 2-11). Usually, conductors such as copper and aluminum reflect Microwaves. Insulators will allow microwaves to pass through. Absorbers soak up some part of the microwave energy and produce heat, known as dielectric materials (Kahraman et al., 2020).

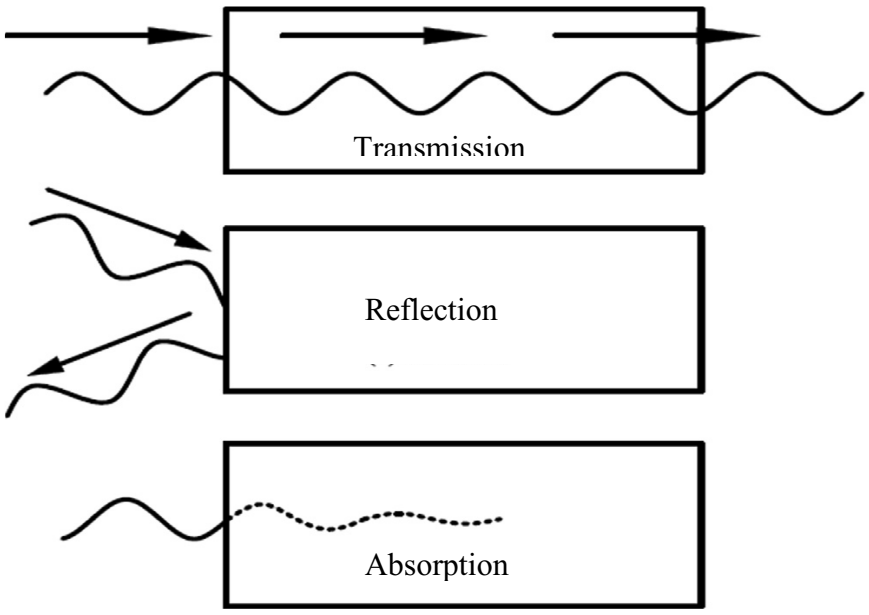

Figure 2–11. Different materials under microwave irradiation (Huang et al., 2020)

A loss occurs when electromagnetic waves pass through a material consisting of a field of an electromagnetic field and the temperature. The complex relative permittivity of the materials introduced is equal to the dielectric constant and dielectric loss factor, as shown in equation [2-3] (Xu et al., 2020). Dielectric constants define the ability of a material to store microwave energy and depend on many factors, including molecular structures, moisture, heating temperature, and frequencies of the wave (Wei et al., 2019).

The dielectric loss factor on the imaginary part represents the degree of energy loss (under an electric field) being converted to heat (Horikoshi et al., 2018).

$$\varepsilon_r = \varepsilon' - j\varepsilon'' \qquad [2\text{-}3]$$

ε_r = Complex relative permittivity of the material or (relative dielectric constant);

ε' = Dielectric constant;

ε'' = Dielectric loss factor;

i and j are $\sqrt{-1}$

A microwave system consists of three main parts: a wave generator (magnetron), waveguide and heating cavity. A magnetron produces microwave energy and is transmitted to the cavity by a waveguide. Specification of the microwave is related to microwave frequency (Hassani et al., 2015). Each material has an optimal frequency that may determine. In practice, however, the nearest possible permissible frequency used in the industry for interference considerations, such as 0.915 and 2.45 GHz (Marland et al., 2001). Also, most laboratory experiments were conducted using commercial microwave ovens with a fixed frequency of 2.45 GHz since high frequencies are unsafe (Huang et al., 2020). Microwave frequency affects heating performance by determining its penetration depth and

electromagnetic field distribution and influences the dielectric property of the material. The energy mode can be categorized as a single-mode cavity, the only mode applied in the system, and has the exact dimensions as a waveguide. A multimode cavity is a closed metallic box with dimensions several times the wavelength, and this mode have high energy than the single mode (Hassani et al., 2016).

2.3.3.3 Microwave Energy (Power) and Exposure Time;

The absorption of microwave energy is associated with the electric strength within the material, and a higher heating rate may result in a more significant formation of cracks within a rock. High irradiation power or electric field strengths have better microwave heating effects on materials. Based on the specification, microwaves can be utilized by their power, commercial microwave ovens, power (up to 3 kW), and industrial microwave system (3-200 kW). A lot of researchers used microwaves that have different intensities for experiment purposes. Some researchers use low power less than kitchen microwaves, such as (Znamenackova et al., 2003) analysis of the effect of microwaves on andesite samples. The samples were exposed to 900 W microwave power at a frequency of 2.45 GHz for 30 min in a multimode cavity and the measured temperature reached 1260-1280 °C. Satish et al. 2006 used a low-power microwave (150 W) to investigate the effect of microwaves on basalt in a multimode cavity. It was observed the temperature reached 115 °C after being treated for 360s. Motlagh (2009) analyses different rock's mechanical properties and abrasivity. The core samples were treated in different power levels (800, 1250, and 3000 W) for 0, 15, 30, 60 and 120, and 240 s time of exposure. The observation showed decreased UCS values and cerchar abrasivity index after microwave treatment.

2.3.3.4 Effect of MWI on the Mineral of the Rock

Each mineral has a dielectric constant (D.C), which determines the heating capacity of the microwave energy. Therefore, rock-forming minerals have different capabilities to absorb microwave energy, which may lead to differences in thermal expansion when exposed to microwaves and result in the internal stresses of the rock structure inducing internal fractures. Hence, expansion of the rock on heating's mineral constituents creates stress along grain boundaries and causes inter-and trans-granular cracks, weakening the rock.

Metallic minerals, such as magnetite and pyrite, absorb microwave energy. Mafic minerals are good microwave absorbers as they heat and expand faster such as amphibole and pyroxene. On the other hand, silicate minerals like quartz and feldspar are weak microwave absorbers (Kahraman et al., 2020). Chen et al. (1984) found rocks containing more minerals like silicate, carbonate, and sulfates are transparent to microwaves. Hassani et al. (2016) investigated the influence of microwave heating for three different rocks with exposure times 1.2, 3, and 5 kW for 10, 65, and 120 s, in which the norite (mafic intrusive) rock and granite were fractured and basalt observed surface spalling. Therefore, he concluded that not only the minerals affect temperature distribution on the rock but also the microwave power and size of the Sample exposed to microwave irradiation.

2.3.3.5 Effect of Water Content on a Rock Sample

Hartlieb et al. (2018) explain how water saturation in the rock plays a significant role in microwave irradiation and the effect of rock mineralogy and chemical composition. The results showed water content in either rock (mafic or sandstone) porous volume or mineral structure increases the heating effect. However, sandstone and granite have lower ranges of microwave absorbers compared to basalt and mafic, which absorb microwaves faster.

The more water content in concrete aggregate can significantly increase the microwave heating rate and alter thermal stress (Wei et al., 2019).

2.3.4 Drill Bits Re-configurations and Micro-fractures Initiation

Using different bits configuration is one of the methods of optimizing drilling ROP. A Drill of Test (DOT) is needed to conduct the analysis. DOT is an important test to obtain a set of drilling data for a given formation for performance analysis. It is conducted while drilling by varying WOB and rotary speed. Then ROP results are presented as a function of WOB and rotary speed (Butt, 2016), (Brooks, 1963) and (Dupriest, 2005). Many researchers have used DOT for drilling performance prediction. One advantage of DOT is that drilling ROP vs. WOB curve can be obtained over a short interval of the hole. Hence, it decreases the possibility of a change in formation during the test period (Warren, 1963). A study has been conducted using physics-based and data-driven prediction models; the physics-based models are empirical correlations designed to model drilling performance. Usually, the parameters are calibrated by DOTs. (De Moura, 2021). Recently, one of the methods conducted using DOTs is the application of drill bits re-configurations to predict drilling ROP performance. Abugharara et al. (2022) presented a drilling performance evaluation through drill bits re-configurations and micro-fracture initiations. He showed the performance of three bits a flat bottom or flat base (FB) bit, a drill hole opener (DHO) bit, and a core hole opener (CHO) (Figure 2-12). His results showed ROP increases using DHO and CHO over the FB bit, where the ROP of DHO increased by 37.5 % at 5kN and 47.1 % at 10kN. Similarly, the ROP of CHO increased by 12.5% at 5kN and 11.8 % at 10kN, indicating that the initiation of micro-fractures could enhance the ROP. Another study of DOT was conducted to analyze the performance of the hole widening operation involving

drilling cutting analysis and drilling parameters (Ahmed et al., 2020). He uses a different bit configuration; (a) coring bit/pilot hole (26.4 mm), (c) hole widening drilling (HWD) on (a) using PDC (32.4 mm) and (b) PDC hole drilling - (32.4 mm), (Figure 2-13). He observed that HWD achieves a higher ROP in the same type of rock and the same drilling input parameters.

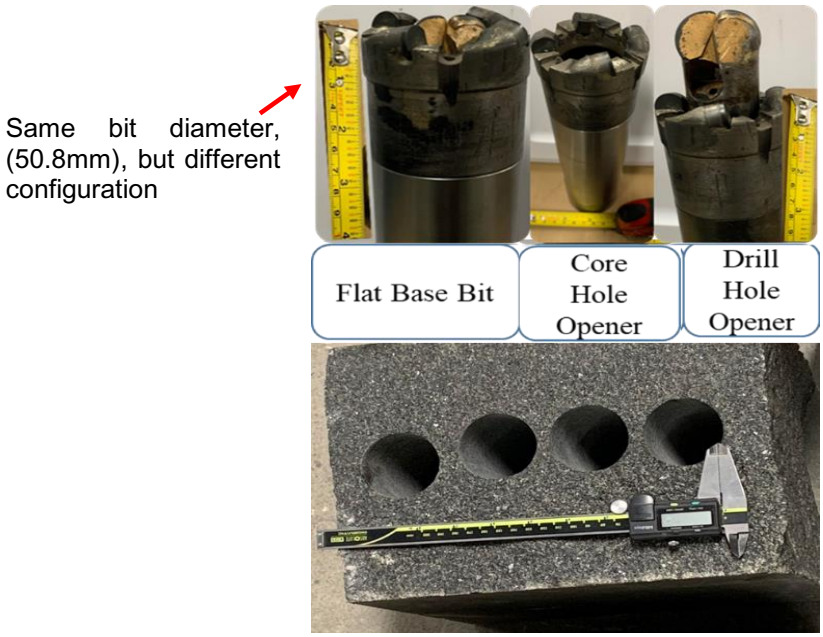

Figure 2–12. Three different bit configurations used for drilling (top) and granite block (bottom) (Abugharara et al., 2022)

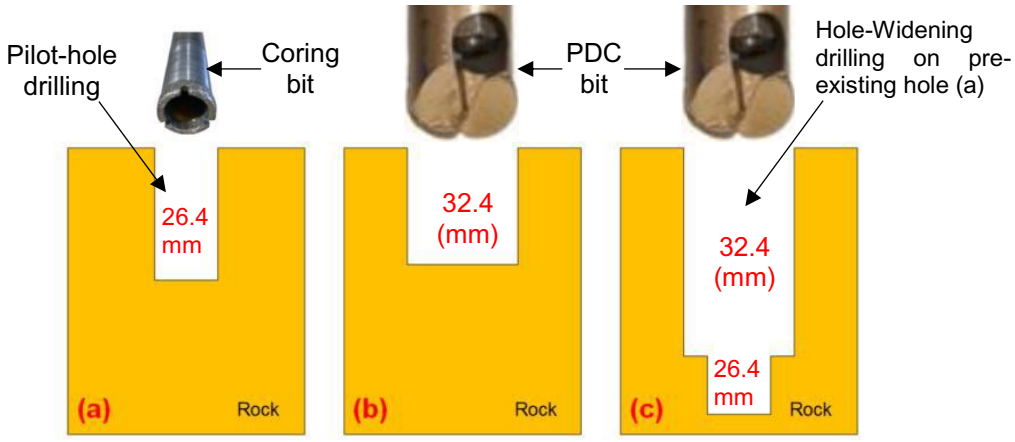

Figure 2–13. Drill cuttings collected for each bit configuration for Drilling Performance analysis (Ahmed et al., 2020)

Chapter 3 : Research Methodology

3.1 Field Drilling Application and Logging Data

In this research, field drilling and logging data have been utilized to analyze the drilling performance. Experimental laboratory analysis has shown different factors influencing drilling performance ahead of the bit to penetrate the rock. In this work, literature reviews explained in the previous chapter have been practiced and real-time data obtained from the field to help to accomplish the data analysis.

3.1.1 Boreholes Drilling Operations

In the field operation, two boreholes were drilled: a diamond drilling hole (DDH) and a large diameter hole (LDH). The drilling of DDH was to obtain the core for understanding the formation's geology, such as lithology and rock quality designation (RQD). Also, LDH was drilled for rock excavation of an ore (mine) body.

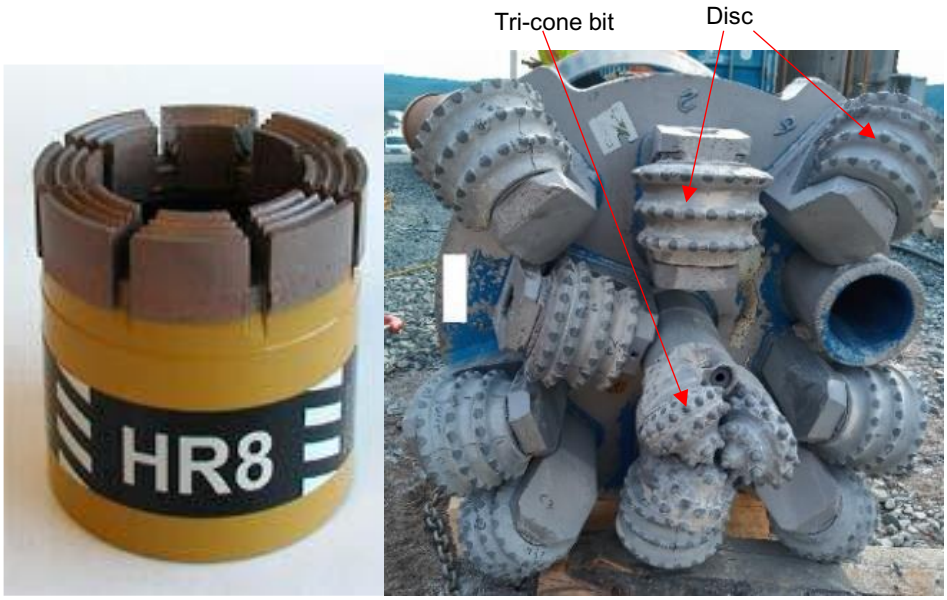

Figure 3–1. Left: Diamond coring Bit and Right: 1m-LDH cutter head (Mafazy et al., 2022)

Figure 3-1 shows the example of a bit used for coring the subsurface rock and a 1m-size cutter head of LDH used for a mining operation in the field. The cutter head is an LDH bit which includes several disc cutters and a tri-cone bit in the middle.

3.1.2 Drilling String Configuration of an LDH

Drilling an LDH was the main focus due to the primary purpose of ore (mines) extracting from underground rock formations. The wellbore was drilled at approximately a measured depth of 90 m with an inclination of 30 degrees to the vertical (Mafazy et al. 2022). The drill string configuration includes an LDH cutter head (the drill bit), drill collar stabilizer, cross-over, standard drill pipe, and non-rotating stabilizer pipe. Some of the functions of drill string like drill collar stabilizer were used to transmit enough weight to the bit (cutter head). A non-rotating stabilizer pipe was also included to control the direction tendency of

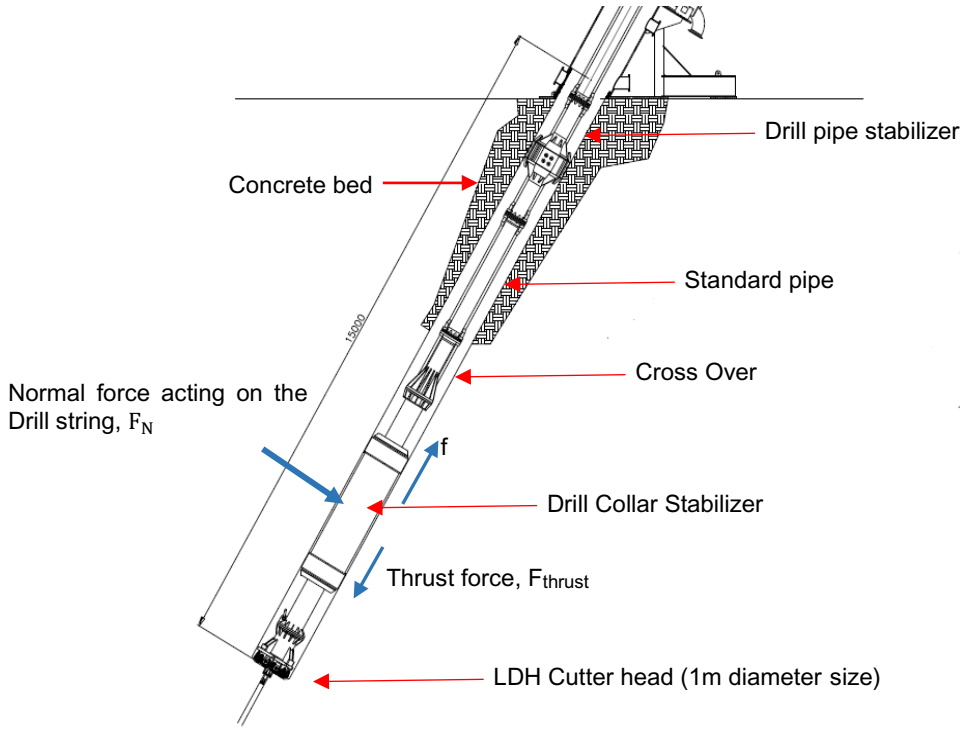

Figure 3–2 Drill string configuration and the forces acting on it (Novamera, 2021)

the well. Also, a Standard pipe is used to transmit rotary motion from the surface to the bit. Figure 3-2 is the LDH profile that was drilled during FFT.

3.1.3 Correlation of Formation Lithology, Rock Properties, and Drilling Parameters

The correlation was conducted between rock formation lithology, drilling data (ROP and WOB), drill cutting analysis, drilling fluid circulation (a direct flash (DF) and reverse flush (RF)), and mechanical rock properties of the formation (rock strength, hardness, and P&S-

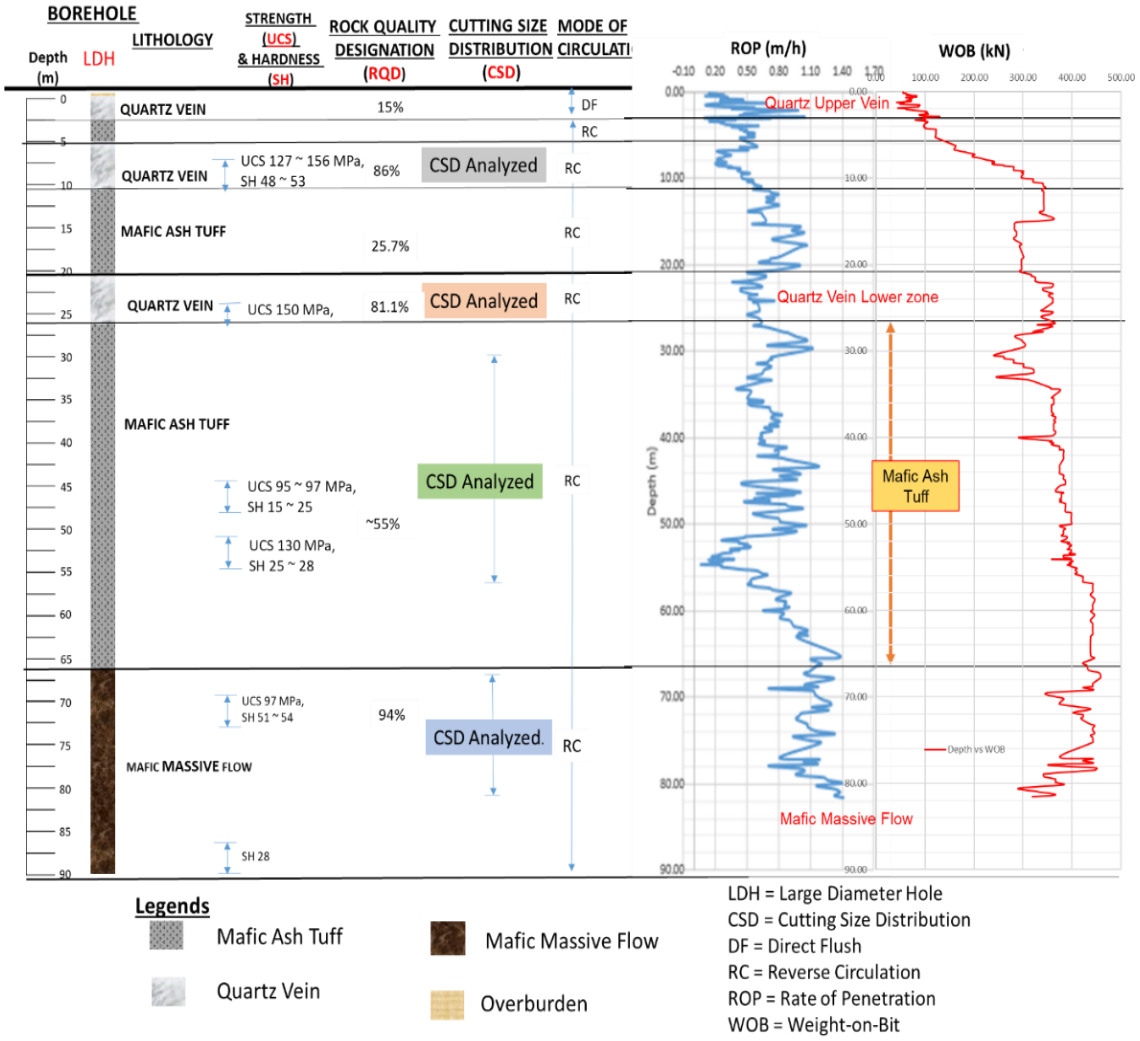

Figure.3–3. Correlation of lithology, rock properties, drilling data and drill cuttings (Mafazy et al., 2022)

wave velocities). Figure 3-3 shows the performance analysis correlations of the wellbore. The detailed research work of this analysis is presented in chapter 4.

The formation geology is a body of rock several meters below the earth's surface, containing lithologies that differ from adjacent rock bodies. A lithology is formed by a rock layer with various mineral and physical characteristics such as rock strength, hardness, color, shape, etc. The relations of different parameters helps to provide a clear understanding of wellbore performance, which enables the identification of the intervals with high variations of critical parameters such as ROP and WOB applied and provide further step to perform analysis to determine the causes of the problem that occurred.

3.2 Rock Material Characterization

3.2.1 Rock Core Logging

Core logging is the method of observing, analyzing, and documenting the physical properties and parameters of the rock core (Abzalov, 2016). The NQ (Diameter = 47.6mm) core size was recovered from DDH as a pilot hole before drilling an LDH.

The core run length is 4.5m, stored in the (1.5m × 0.17m) wooden box in dimensions arranged in three rows. The core analysis was used to identify the lithology, mainly quartz and mafic, along the core run, and each core run counted the depth intervals of the borehole. Also, other characteristics were noted, like highly fractured intervals, RQD, and potential minerals like hematite at the broken rock surfaces. Figure 3-4 shows the core logging process, including labeling, RQD measurements, and samples selected for the other tests in the laboratory.

Figure 3–4. Core logging and sample selection for Laboratory test at MUN (Mafazy et al., 2022)

3.2.2 Rock Mechanical Properties and Laboratory Experimental Apparatus

Mechanical properties of the rock refer to the stress-strain characteristic of the rock under stress and failure, mainly including strength, stability, and deformation characteristics. The rock's properties were required to understand this behavior on how the rock can easily break and change its shape under natural stress or external force. The laboratory mechanical test is one method used to determine the properties of the rock. The tests include rock strength tests, which are unconfined compressive strength (UCS), indirect tensile strength (ITS), and point load strength index (PLSI). Also, the Schmidt hammer (SH) test was used to

determine the rock's hardness. The mechanical test was conducted at the MUN-DTL laboratory. The equipment used for the strength test is a geomechanics frame, SH-test is a Schmidt hammer device, and an ultrasonic wave measurements device.

3.2.2.1 Geomechanics Frame

The geomechanics loading frame is the experimental equipment that has the capability of performing different strength tests, including compressive strength (both UCS and CCS) test, indirect tensile strength (ITS) test, and point load index (PLI). The frame has a loading frame that can provide a maximum of 450 KN, and it includes multi-sensor data management systems, and the analysis requires data to be coordinated in time. It contains two primary sensors, a linear variable displacement transducer (LVDT), and a load cell.

Figure 3–5. Geomechanics frame at Drilling Technology Laboratory (DTL), MUN (Mafazy et al., 2021)

Also, a data acquisition (DAQ) system is connected to perform multitasking, including analog to digital conversion. The physical design of the apparatus coordinates a load cell for measuring maximum axial and tri-axial force (stress=force/area) reached and LVDT for measuring linear displacement due to axial compression of the tested specimen. Figure 3-5 shows several main parts of the geomechanics frame; 1-the axial compression pressure piston, 2- bottom and top compression plate, 3- manual compression hydraulic pump, 4-control valves, 5- safety bypass valve, 6-hydraulic fluid reservoir, 7-Data Acquisition System (DAQ-Sys).

3.2.2.2 Schmidt Hammer (SH) Device

The SH device is the apparatus for measuring the surface hardness of the rock, as shown in (Fig. 3-6). It consists of spring-loaded steel, which releases a certain amount of energy on the tip of the metal plunger in contact with a core/rock specimen (ASTM-D5872, 2021). There are digital and manual SH devices, and they are made into two standard types, L- and N-type, based on their impact energies of 0.735 and 2.207 Nm, respectively.

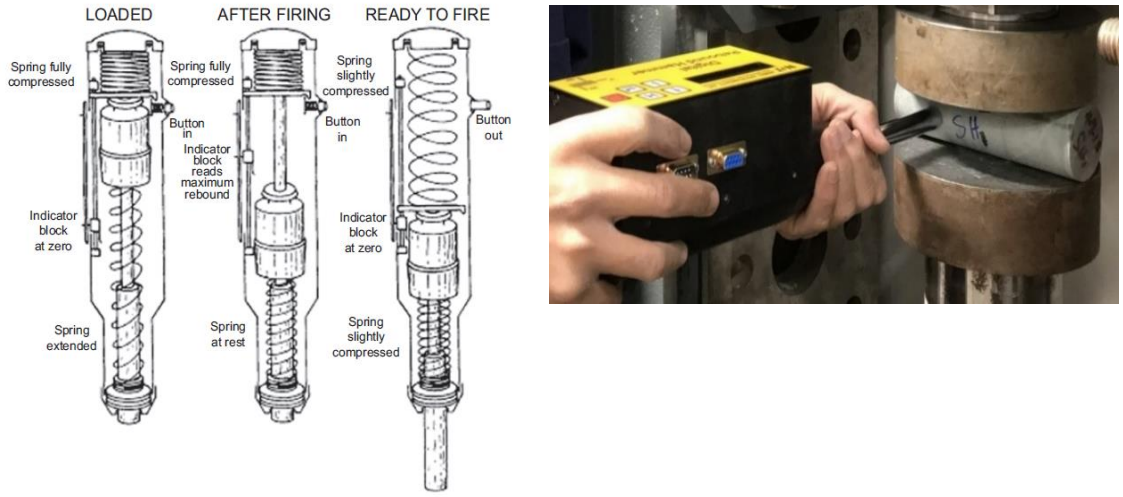

Figure 3–6. Left: Working principle of SH-device and
Right: SH-test on the rock specimen (Mafazy et al., 2021)

The significance of the SH device is a non-destructive test provides a rapid and inexpensive measure of the hardness of the surface of the rock, the rebound values applicable in a variety of engineering work involving rock characterization, e.g., prediction of the rate of penetration in tunnel boring machines, underground mines, rock quality constructions and grouping of the test specimen.

3.2.2.3 Grain Size Analysis (GSA)

Grain/Particle Size Analysis (GSA/PSA) is the method used to generate quantitative data about the size of the particles and distribution of the particle size. In this research, GSA was presented and applied in chapter 4 to analyze drilling performance at a specific depth of low ROP. The grain Size Distribution (GSD) curve was plotted to a logarithmic scale on the x-axis versus the percentage passing by weight (finer or coarser) on the y-axis. Figure 3-7 shows an example of the GSD curve of the particle from finer to coarser. Fig 3-7 represent the sorted grain size as *well-graded* grain, which has a good representation of the grain size over a wide range. Also, a *poorly graded* grain has a deficiency or same-size particles, e.g., a gap-graded or skipped graded and uniform gradation (Holtz and Kovacs, 1981). The parameters D50, D90, D60, D30, and D10, coefficient of uniformity (Cu), and coefficient of curvature (Cc) were determined using the GSD curve generated. D90 represents the 90 percentile by volume of the total particles smaller than the D90 value, while D50 represents the mean size of the particles. Also, D60, D30, and D10 represent 60%, 30%, and 10% of the sample passing by weight, respectively. These parameters are primary components for calculating Cu and Cc. Cu describes how the particle size is sorted well or poorly graded, and Cc describes the shapes of the particles (represented by the shape of the curve), whether the curve is steeper coarser, or finer.

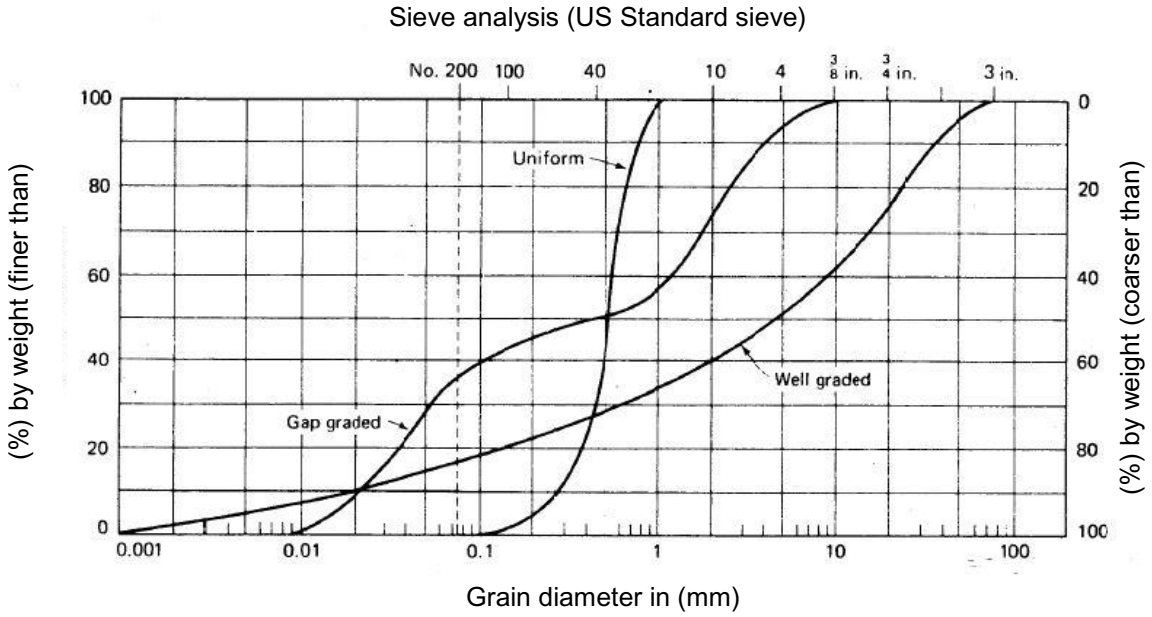

Figure 3–7. Typical Grain Size Distribution (GSD) curve (Holtz and Kovacs, 1981)

Cu and Cc are defined by equations 3-1 and 3-2, respectively.

$$C_u = \frac{D_{60}}{D_{10}} \qquad [3\text{-}1]$$

$$C_c = \frac{(D_{30})^2}{(D_{10})(D_{60})} \qquad [3\text{-}2]$$

The main apparatus used to perform GSA is known as a mechanical sieve shaker. It is used to hold the sieve stack. The shaker applies sufficient motion to the sieves to achieve the desired separation within the shaking period of 10 to 20 minutes. The particle settled by size within each sieve. The sieve sizes range from 0.075mm to 38.1mm. They are categorized as finer sieves (0.075 mm to 4.75 mm) and courser sieves (4.75 mm to 38.1 mm) sizes. Figure 3-8 shows a complete set of the set device for GSA analysis used in this research, specifically in chapter 4, for determining particle size behavior with drilling data analysis.

Figure 3–8. Left: Sieve set for finer and courser and Right: Mechanical sieve shaker

3.2.2.4 Mineral Liberation Analysis (MLA) Technology

The MLA is the automated process of mineral analysis that can visualize and identify different minerals in a rock core sample. Usually, the surface of a sample specimen is scanned by a beam of electrons which and then reflected to form an image called a Scanning Electron Microscope (SEM) (Sylvester, 2012). SEM produces a beam of incident electrons that react with the Sample to form three signals; backscattered electrons (BSE), which is the maximum energy produced after the collision of incident electrons with the specimen. Another signal is secondary electrons (SE), which are emitted with low-energy electrons after the interaction. Also, energy dispersive X-ray (EDX) is another signal emitted when an electron beam exchanges electrons from the inner to outer shell electron (PSzonka & Sala, 2018). Hence, using special software, the MLA device integrates backscattered

electrons (BSE) and X-ray data to sort out minerals and map their distribution in the scanned specimen. Figures 3-9 and 3-10 below show sample preparation and the device used in this work

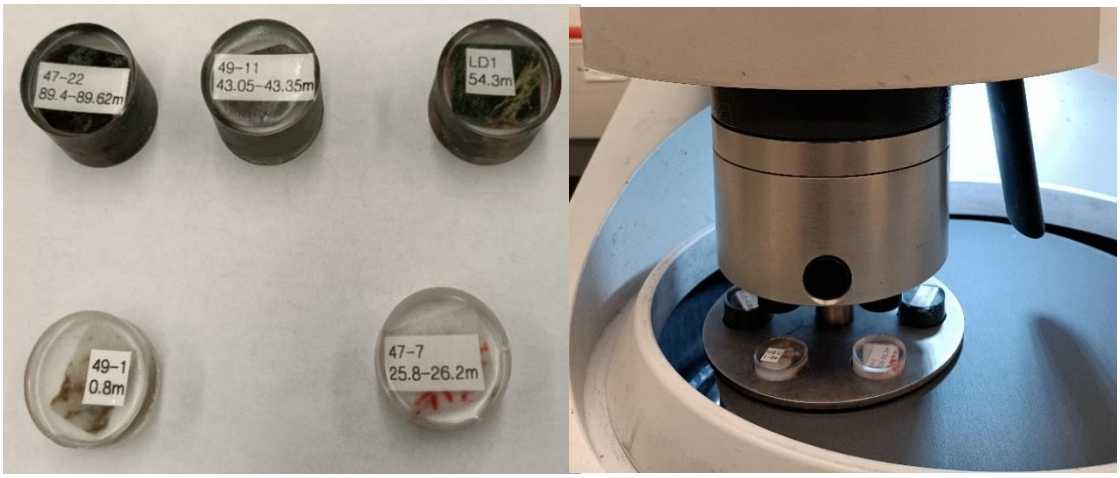

Figure 3–9. Left: Sample prepared for MLA, and Right: Samples in the MLA device at MUN (Mafazy et al., 2022)

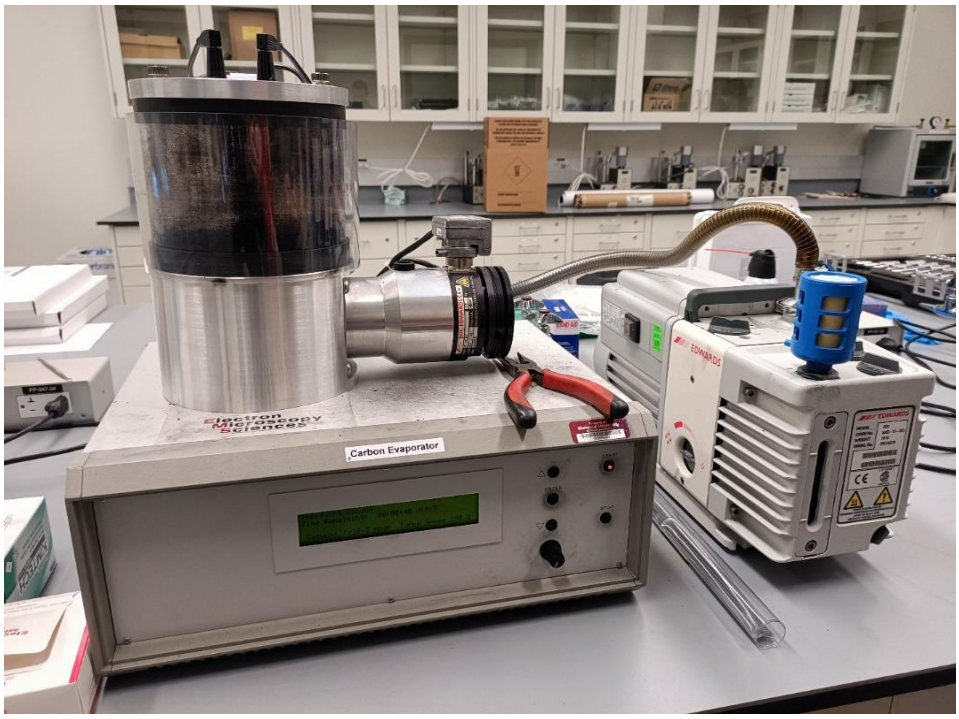

Figure 3–10. MLA device (MLA 650) at MUN (Mafazy et al., 2022)

MLA technology acquires valuable mineralogical information for analysis, such as BSE providing distribution of the material in the scanned Sample and S.E. producing sample surface quality image or resolution. It is a computer-automated system, reducing human errors and many manual analyses. The more sample analyses, the more productivity increases with a better statistical representation. It can analyze fine material at the scale of micrometers (Sylvester, 2012).

Chapter 4 : Influence of Rock Microstructure on Rock Strength and Drilling ROP

This chapter discusses the published technical paper titled "Influence of Rock Microstructure on Rock Strength and Drilling Rate of Penetration (ROP)". The authors of this paper are Salum Mafazy, Michael Marsh, Zijian Li, and Dr. Stephen Butt. The paper was published through the proceedings of GeoCalgary 2022 on October 2 - 5, 2022 - At the 75th Canadian Geotechnical Conference (CGS), Calgary, Alberta, Canada. The author's dedicated contributions are described as follows:

- Salum Mafazy: Research topic proposal, experimental plan and performance, literature review, data analysis, and manuscript preparation.
- Michael Marsh and Zijiani Li: Mineral Liberation Analysis (MLA) test performance and manuscript review
- Dr. Stephen Butt: Research and experimental support. Supervision and manuscript review step by step and approval of the paper.

4.1 Abstract

During recent near-surface drilling operations to a measured depth of 90 m using both diamond core drilling and large diameter drilling, there was a marked decrease in drilling ROP over the depth interval of 50 - 55 m. A laboratory investigation was conducted, which included detailed core logging, rock mechanical tests, cuttings size analysis, and Mineral Liberation Analysis (MLA). Theoretical models were utilized and compared with field drilling performance metrics. It was observed that high rock strength in the mentioned interval, and it is proposed that this caused the reduction in ROP. MLA application showed

that the mineral composition remained constant, but the rock microstructure differed in that interval. Hence, the alteration of microstructure may be the contributing factor that leads to increased rock strength and reduced ROP.

4.2 Introduction

Large Diameter Hole (LDH) drilling is the method for drilling holes that can be considered greater than 50 cm in diameter for mining extraction. Such techniques are used for Tunnel Boring, Raise Boring, and Pile Drilling. Understanding the geometry, geological characteristics and properties of underground rock, such as lithology variation, Rock Quality Designation (RQD), etc., is essential for optimizing drilling performance and ultimately reducing drilling operation costs. The geological properties are typically obtained via core analysis prior to mining extraction (if desired). The analysis is needed to identify additional geological information and to determine the strength and hardness of the rock. Drilling performance for most drilling operations is evaluated using the ROP metrics. Additionally, drilling parameters such as Revolution per Minute (RPM), Weight-on-Bit (WOB), and torque are also essential for the drilling performance of a well. Drilling optimization depends on these drilling performance parameters and hole cleaning efficiency. The higher the cleaning/drilling efficiency of a well, the higher the performance. Drilling efficiency depends on the specific energy required to penetrate the rock formation (Butt, 2016). This study utilizes field trial LDH drilling (1 m) performance metrics and data. A notable reduction in ROP across a specific measured depth interval of 50 m to 55 m was observed. At the same time, no notable variation in above and/or below geological lithology was logged, and any variation in drilling operating parameters was accounted for.

The well was drilled through a mineral vein deposit (and host rock), inclined 30 degrees to the vertical, and reached a measured depth of 90 m. This work aims to investigate the cause(s) of such abnormal drilling performance behavior. Laboratory experiments were performed for rock characterization, including core logging, rock strength testing, grain size distribution analysis, and Mineral Liberation Analysis (MLA).

4.2.1 Application of TBM and Large Diameter Bit using Disc Cutters

In the study of mechanical rock crushing, several cutting methods are applied to mining equipment. The primary cutting methods can be categorized as drag bit cutting, point-attack bit cutting, disc cutting, button cutting, and roller cutting (Breeds & Conway, 1992). Disc cutters are used in drilling equipment like TBMs. TBMs were applied in mining in the late 1950s to 1970s. In recent years, there have been improvements in TBM design due to advancements in new technology and computer system development (Cigla et al., 2001).

Figure 4–1. Large Diameter Bit (1m)

For the field trial LDH drilling, a disc cutter bit arrangement was utilized. The disc cutters are mounted on a cutter head via independent bearing assemblies where the disc cutters are free to roll with respect to the thrust and drag force applied. Figure 4-1 shows a large diameter bit.

4.2.2 Application of Core Logging

Diamond Drilling (D.D.) uses drill bits impregnated with fine to micro-fine industrial diamond crystals (Cumming & Smit, 1980). The drill bit is combined with the core barrel and attached to the drill string. The diamond bit cuts the rock column into a cylindrical shape known as the drill core. Usually, the core moves into the drill pipe while the bit penetrates the rock (Abzalov, 2016). Once the drill core is recovered, it is placed in the core tray and stored in the core boxes. The application of drill core is widely used in engineering drilling, exploration of mineral deposits, geological boreholes, hydrogeological wells, and other underground drilling operations.

Core logging is the process of documenting critical geological information to determine the lithology, mineralogy, geologic history, and other geological parameters of a drilled location. Also, core logs include wellbore logistic information such as the well location, wellbore number, etc. RQD can be calculated from information recorded and obtained from the logged core data (Eq. 4-1). RQD is developed to provide an estimation of the quality of a rock mass for the drilled core. It is calculated as a percentage of intact core pieces longer than 10 cm in the total length of the core. It is a quick method applied in core logging applications, and regardless, it is limited to determining the rock mass quality for the core pieces less than ten centimeters (Palmstrom, 2005). Equation 4-1 defines the expression for calculating RQD, and Table 4-1 expresses the grading of the RQD values.

$$RQD = \frac{\sum \text{Length (L) of core pieces} > 10 \text{ cm length}}{\text{Total length of the core run}} \quad [4\text{-}1]$$

Table 4-1. Rock quality designation (RQD) percentage and grading (Palmstrom, 2005).

RQD (%)	Grade
0 – 25%	Very poor
25 – 50%	Poor
50 – 75%	Fair
75 – 90%	Good
90 – 100%	Excellent

4.2.3 Mechanical Tests for Rock Characterization

Rock mechanical tests are used to obtain the mechanical parameters of a rock mass and help researchers/engineers studying on different rock characteristics. For example, various mechanical tests are utilized to determine Unconfined Compressive Strength (UCS), Indirect Tensile Strength (ITS), Point Load Strength Index (PLSI), Elastic Modulus, Poisson's Ratio, etc. Additionally, the determination of stress and strain of the rock under failure conditions will determine the strength, deformation, and stability characteristics of the tested rock.

In the area of rock characterization, researchers have conducted a tremendous amount of research and high achievements. Quan et al. (2021) conducted strength tests on Granite and Rock-Like Materials (RLM) as concrete (isotropic rocks) and developed empirical correlations that describe the relationship between the UCS, ITS, and PLSI, between PLSI and ITS, and between P-wave and UCS, Young's modulus, and Poisson's ratio. According

to Quan et al. (2021) evaluated tensile and shear fractures on the sandstone samples to optimize drilling performance using a roller cone bit and Polycrystalline Diamond Compact (PDC) Bit. Also, Zhao et al. (2018) performed several laboratory mechanical tests to determine the damage characteristic of the rocks and presented FLAC3D numerical simulation analyses to optimize the rock mechanical parameters obtained.

4.2.4 The Relationship between Cutting Size and Drilling Performance

Drill cuttings have been used in many applications involving mining and oil and gas drilling to determine the subsurface information. Mud loggers use drill cuttings to obtain information on lithology, and geological engineers need cuttings to understand rock properties such as porosity and permeability. Furthermore, cutting size distribution helps drilling operations improve drilling performance and prevent problems while drilling since they are associated with the drill bit, rock formation, and fluid interaction (Karimi, 2013). Grain Size Analyses (GSA) is generally conducted to analyze drill-cutting size parameters. The cuttings contain a variation in size ranges, and there is a need to sort them from fine to coarse by using a standardized grain size distribution curve, representing the particle size and weight composition. The detailed procedures and analysis followed (ASTM D6913/6913M, 2017).

4.2.5 Specific Energy and ROP Prediction Models

In rock excavation methods, the penetration of the drilling tool into the rock can be achieved by two main actions, 'indentation' in which the tooth of the bit is pushed into the rock to establish a bite; 'cutting' by which the bit gives lateral direction for breaking the rock into small pieces (Teale, 1965). Generally, drilling energy is a key parameter for penetration by cutting the rock into small fragments. Hence, drilling energy is used to characterize the

drilling penetration and cuttings transportation process, known as Drilling Efficiency (DE). DE is defined as the energy consumed by the drilling process. Work done per unit volume excavated is known as specific drilling energy. The Mechanical Specific Energy (MSE) model is used to analyze drilling efficiency.

Equation 4-2 presents the model for calculating MSE (Teale, 1965). Then according to Butt (2016), the relation between D.E., the strength of the rock penetrated, and MSE is shown in Eq. 4-3.

$$MSE = \frac{WOB}{A_B} + \frac{60*2\pi*NT}{A_B*ROP} \qquad [4\text{-}2]$$

Where: MSE = mechanical specific energy, Pa; N = rotary speed, rpm; A_B = bit area, m^2; ROP = rate of penetration, m/h; T = torque, Nm; WOB = weight-on-bit, N

$$DE = \frac{CCS}{MSE} 100\% \qquad [4\text{-}3]$$

Where; CCS = in situ or confined compressive strength of the formation.

ROP is a result of the different drilling parameters such as rock strength variation, WOB applied, fluid circulation, etc. ROP models are used to predict the maximum WOB at any bit rotation and to observe the ROP variation for a given bit condition. The concept of the *'perfect cleaning*' in rotary drilling is one of the earlier invented ROP models, which means the tooth of the bit removes all the rock cuttings completely under the conditions presented in Equation 4-4 (Maurer, 1962):

$$R = \frac{k}{S^2}\left[\frac{W - W_o}{d_b}\right]^2 N \qquad [4\text{-}4]$$

Where: R = rate of penetration, m/h; k = constant; S = in situ strength, MPa; W = weight on bit, kN; W_o = threshold weight on bit, kN; d_b = bit diameter, m; N= rotary speed, rpm

4.2.6 Mineral Liberation Analysis (MLA) Technology

MLA is the automated process that allows quantitative evaluation of mineral abundance, associations, sizes and shapes of minerals in a drill core sample in an automated systematic fashion. The advantage of using MLA is that it is a computer-automated system. It increases productivity with a better statistical representation when more samples are analyzed. MLA can analyze fine material at the scale of micrometers. Also, it gives a clear mapping of the mineral grain microstructure of the rock sample. However, MLA has difficulties distinguishing similar mineral compositions and polymorphs (Pszonka & Sala, 2018). The MLA technology has been applied in many applications, such as in the mineralogy and metallurgical processing industry, different studies of sediments and sedimentary rock, microstructure in mine tailings, etc. (Sylvester, 2012).

4.3 Background

This paper utilizes field trial LDH drilling performance metrics and data. The field trial drilling occurred in a geological zone involving mainly quartz and mafic rock lithology. Drilling research was conducted throughout the vein (quartz) and host (mafic) lithology. A Diamond Diameter Hole (DDH) of NQ (47.6 mm) size was drilled before an LDH for geological evaluation. An investigation was conducted for the specified interval to analyze the cause of low ROP. It includes an analysis of the core extracted from DDH. Also, the elastic property, rock strength, and hardness tests were performed. The rock's mineral composition was conducted using MLA technology. Additionally, grain size analyses of the drill cuttings from the LDH were conducted. Then the cuttings size distribution parameters such as D10, D30, D50, D60, D90, Cu, and Cc correlated with drilling

parameters to analyze the occurred phenomena. Also, the ROP from the LDH was validated with the Maurer model, MSE, and the D.E. within the specified drilling interval.

4.3.1 Core Logging

Before the laboratory mechanical tests were performed, the drill cores from the DDH (intervals of 46.47 m to 55.3 m) were analyzed to identify lithology and RQD. Fig. 4-2 and Fig. 4-3 show the core boxes with their respective depth intervals. Table 4-2. Illustrates the relationship between interval depth, lithology type, and corresponding RQD.

Table 4-2. Core analysis for RQD and lithology

Depth (m)	Identified Lithology	RQD	Grade
46.5 m to 51 m	Mafic ash tuff with greyish- white color	55.8%	Fair
51 m to 55.3 m	Mafic ash tuff green-greyish color	56.6%	Fair

Figure 4–2. Core depth; 46.47 m to 51 m

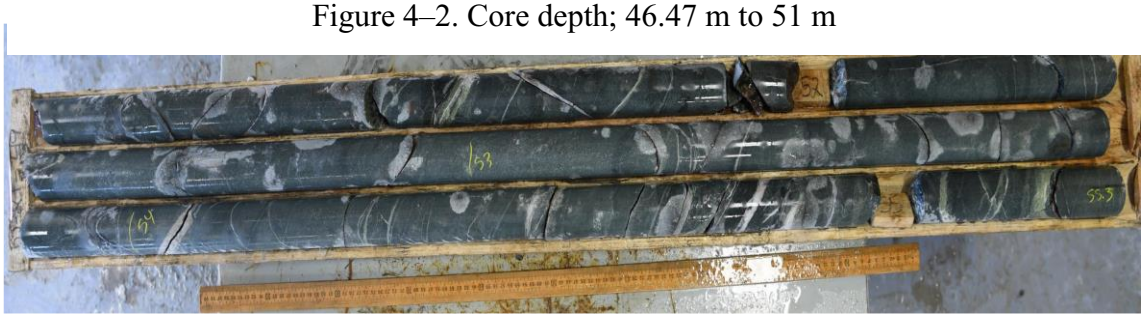

Figure 4–3. Core depth; 51 m to 55.3 m

4.3.2 Sample Preparation

Core samples were prepared for each of the selected mechanical tests. The sample preparation procedure started with the section of intact cores from each respective interval of interest. Then each sample was cut to a specified dimension as dictated by the ASTM standards.

4.3.3 Mechanical Tests

4.3.3.1 Strength Tests

In this study, UCS, PLSI, and ITS tests were performed on all test samples via the geomechanics loading frame. The frame has a maximum design load of 450 kN and is equipped with a Multi-sensor Data Management System, including a Linear Variable Displacement Transducer (LVDT) and load cell. The LVDT measures the linear displacement of the tested Sample. Also, a data acquisition (DAQ) is connected for the analog signal to digital conversion. The experimental procedures, sample preparation, and calculations for the UCS, PLSI, and ITS follow ASTM D7012, ASTM D5731, and ASTM D3967 standards, respectively. The set up shown in Figure 4-4.

Figure 4–4. Left: UCS, Middle: ITS, and Right: PLSI; experimental setup on the geomechanics frame at Drilling Technology Laboratory (DTL), MUN

The UCS and ITS test were performed using a setup of a flattened circular plate of geomechanics frame, while PLSI was placed between a set up of conical plates (Fig 4-4).

4.3.3.2 Hardness Test

A digital Schmidt hammer device was used to test rock hardness. The sample preparation and procedures follow ASTM D5873. For a digital device, the rebound hammer values are automatically normalized to the horizontal direction by setting up an angle, $\theta = 0°$ (Basu & Aydin, 2004). The test was performed at ten different positions on the rock core sample, and the rebound values were recorded automatically.

4.4 Results and Analysis

4.4.1 Drilling Parameters and ROP Models Analysis

Drilling parameter data from the LDH drilling field trials was recorded. The data was analyzed to determine the correlation between drilling parameters and varying lithology. More specifically, the variation between quartz, mafic ash tuff, and mafic-massive flow. An unexpected low ROP can be observed in the mafic ash tuff interval between 50 m to 55 m. Figure 4-5 illustrates the correlation of WOB, ROP, and measured depth. Later, the ROP was normalized using 20 rpm to remove the effect of rotary speed on the ROP. Normalized ROP was obtained from the actual ROP multiplied by the ratio of the rated rotary speed over the actual one (Xiao et al., 2015). The relationship between actual ROP, normalized ROP with depth, and WOB is shown in Fig. 4-6 and Fig. 4-7. Also, in this work, the Maurer model was used to validate the results. Figure 4-8 shows Maurer ROP with WOB. It is observed that ROP increases with increasing WOB until abnormal low ROP behavior is observed between 50-55 m. Also, MSE and DE were analyzed, as illustrated in Figure 4-9.

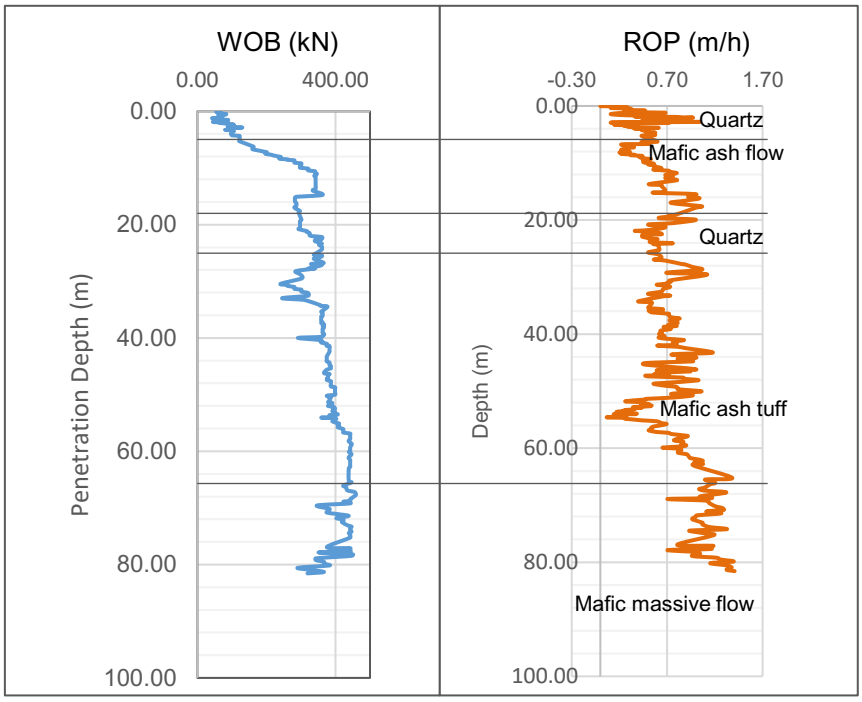

Figure 4–5. Left: WOB and Right: ROP with depth

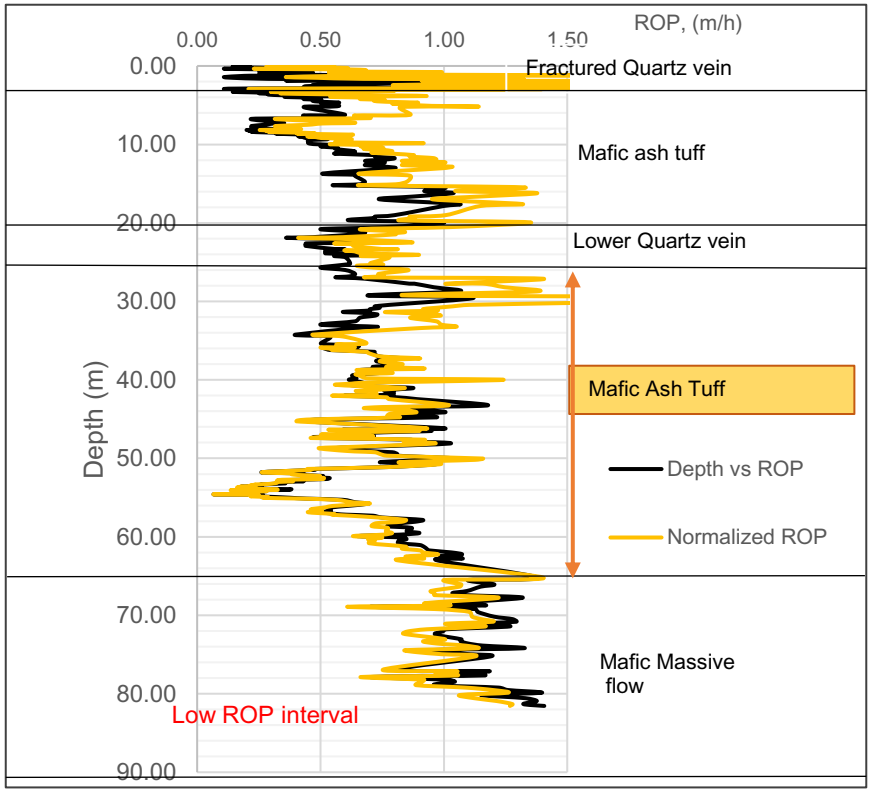

Figure 4–6. Actual ROP vs Normalized ROP with penetrated depth

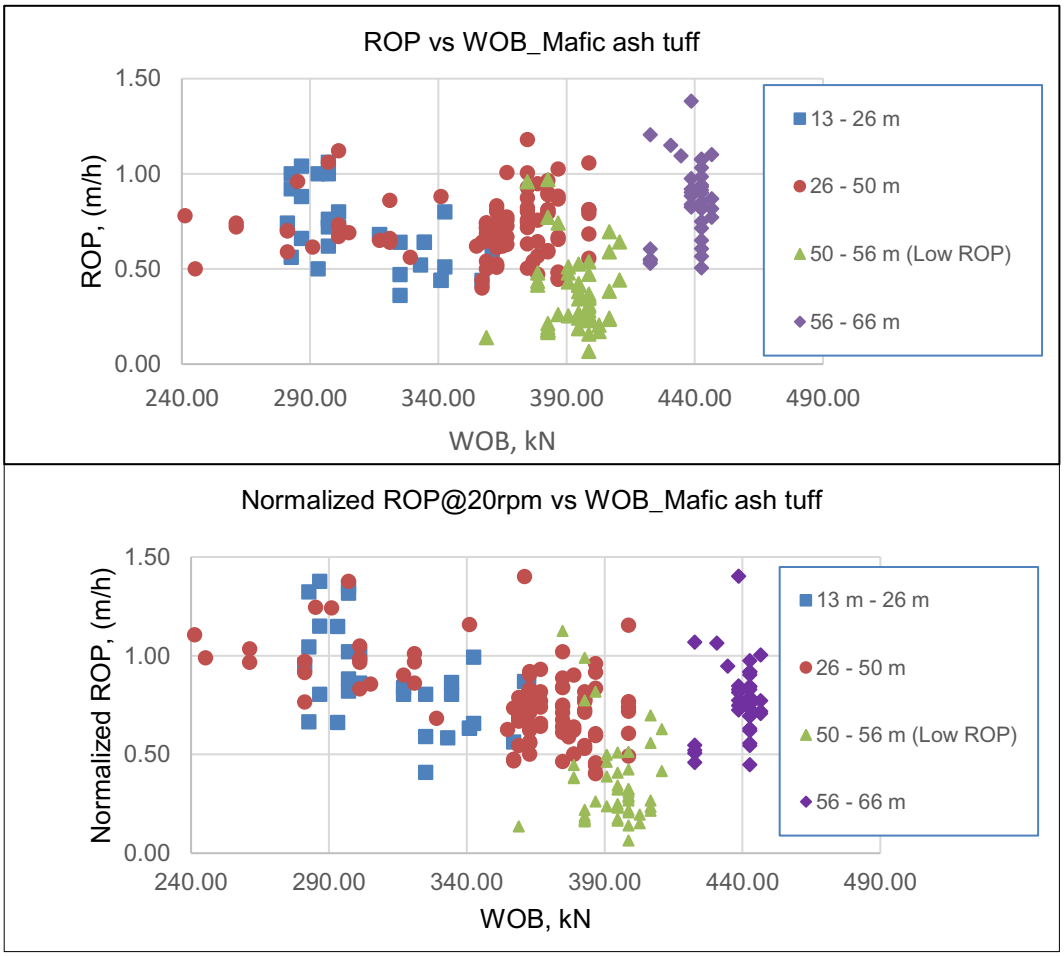

Figure 4–7. Top: Actual ROP and Bottom: Normalized ROP

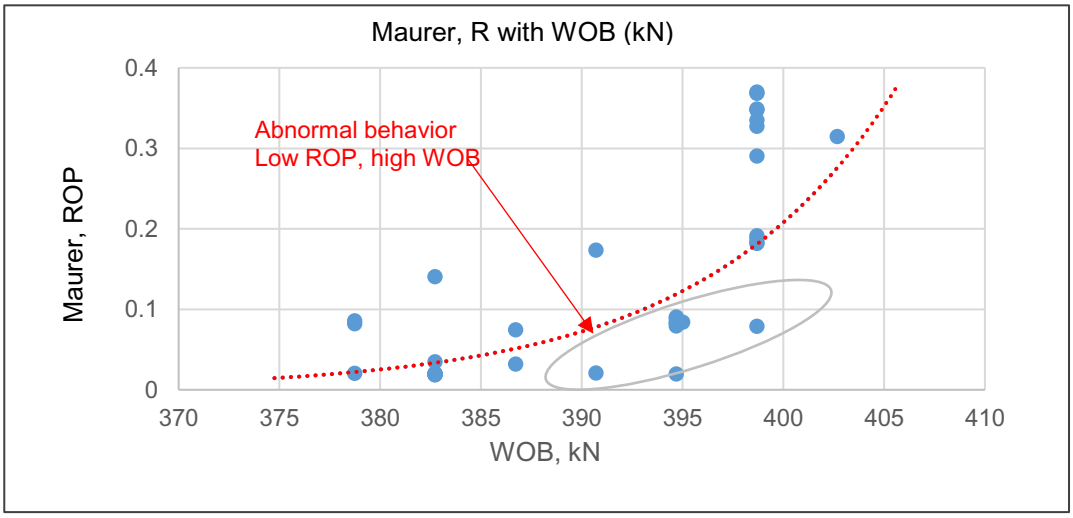

Figure 4–8. Maurer ROP with WOB the interval between 47m to 60m

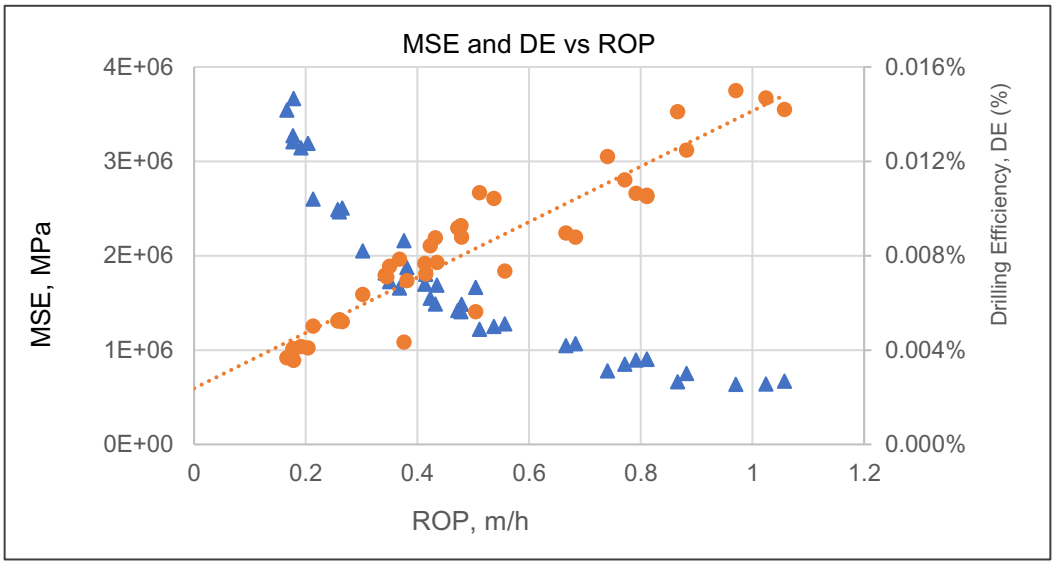

Figure 4–9. MSE and DE with ROP

4.4.2 Strength and Hardness

4.4.2.1 Unconfined Compressive Strength (UCS)

UCS results were obtained at varying depths within the interval of interest (same lithology of mafic ash tuff). Trends shows UCS values increase as the depth increases (Fig. 4-10).

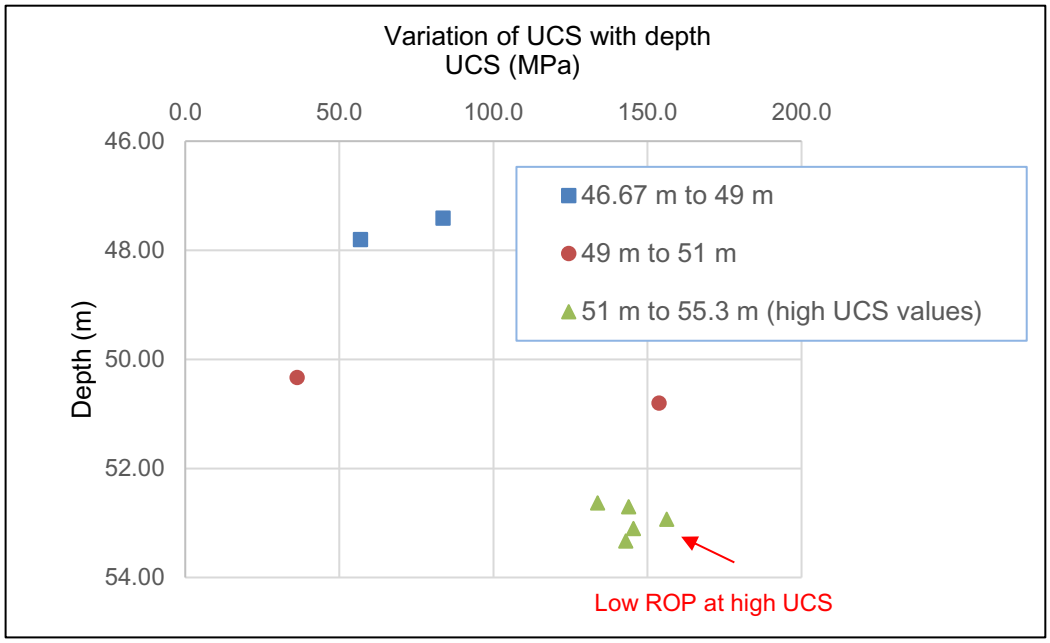

Figure 4–10. UCS values with penetration depth

High UCS around 150 MPa is observed between depths of 52 m to 55.3 m, which is the depth interval where lower than expected ROP was observed.

4.4.2.2 Point Load Strength Index (PLSI)

The PLSI represents the strength of the intact rock core. Corrected PLSI ($I_{s(50)}$) was calculated from uncorrected (I_s) PLSI data and as illustrated (top) in Figure 4-11, the comparison between both index values is slightly different.

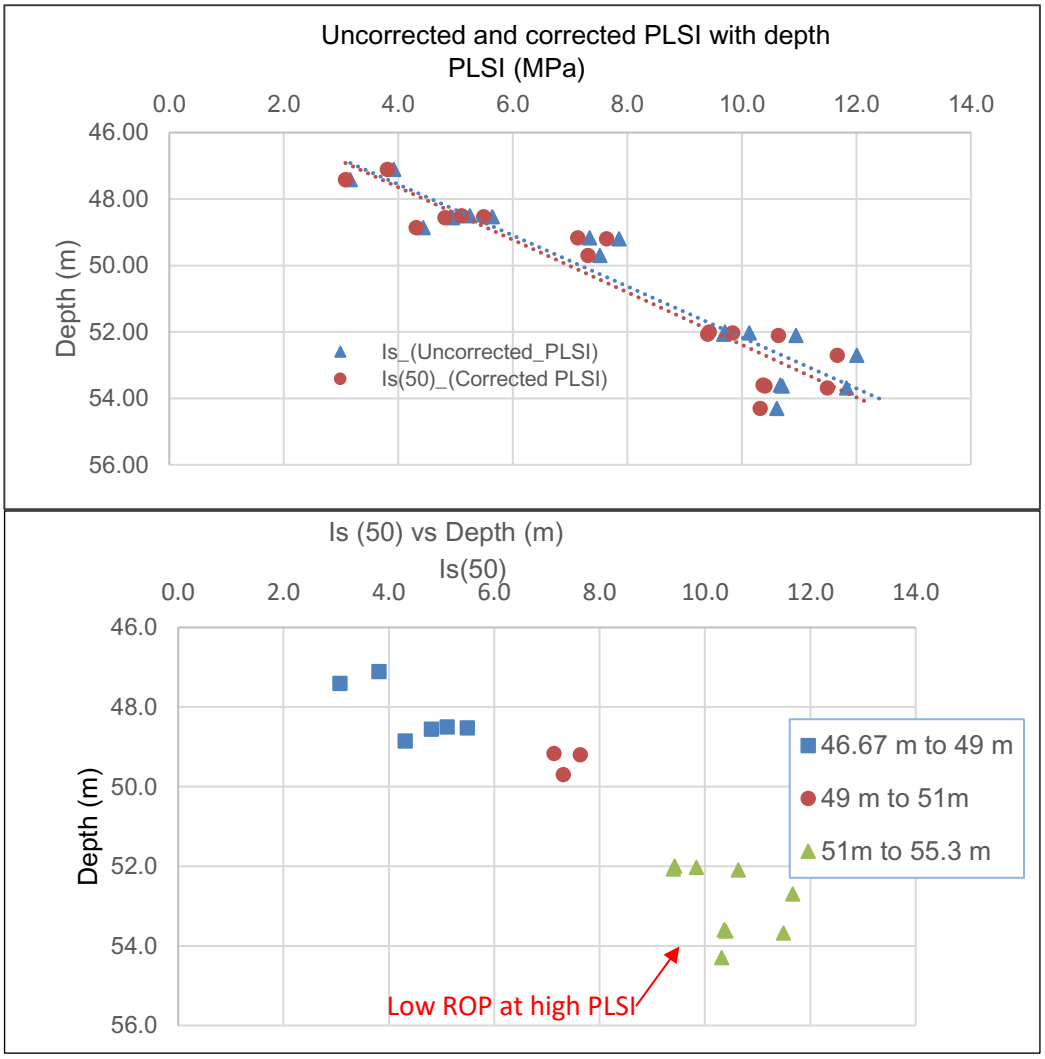

Figure 4–11. Top: Uncorrected and corrected PLSI and Bottom: corrected PLSI with penetration depth

Also, Figure 4-11 (bottom) shows the relationship between corrected PLSI and penetration depth. It is observed that corrected PLSI increases with an increase in depth. Hence, the maximum corrected PLSI in the 52 m to 55.3 m interval is 13 MPa.

4.4.2.3 Indirect Tensile Strength (IT)

ITS results with depth were observed to increase with depth. Maximum ITS strength was between 20 - 24 MPa, at a depth of 54 m, as shown in Figure 4-12.

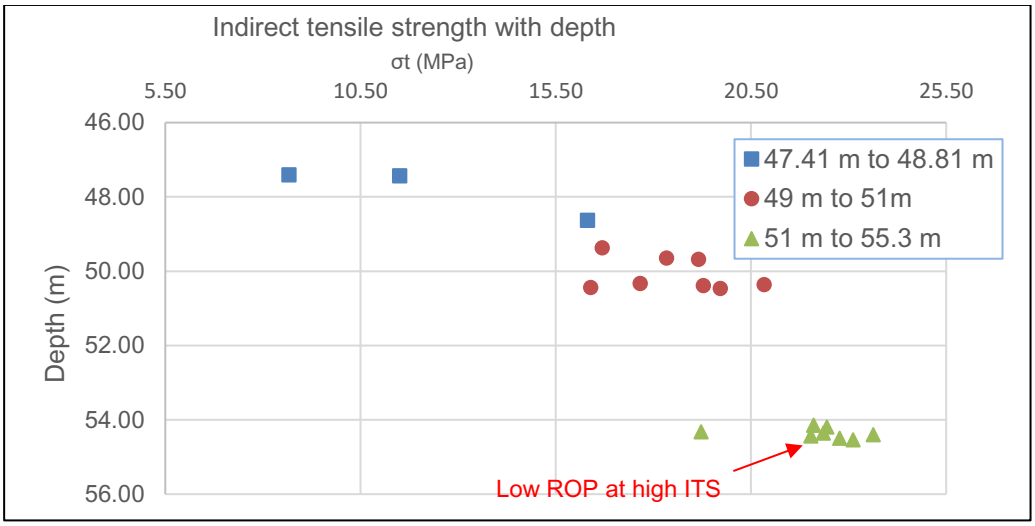

Figure 4–12. Indirect tensile strength (ITS) with penetration depth

4.4.2.4 Schmidt Hammer (SH)

Table 4-3. Schmidt hammer values with depth penetration

Lithology	Depth (m)	Schmidt Hammer
M.A.T - greyish-white color	47.41	20.7
	50.13	22.7
M.A.T - green-greyish color	52	25.1
	53.19	28

The above table 4-3 represents the hardness of the rock, which is observed to increase with increased penetration depth (20.7 to 28.0 at 47.41 m to 53.19 m, respectively. Furthermore, the hardness of the rock is observed to be high, with a low ROP (53.2 m).

4.4.3 Grain Size Analysis (GSA)

The grain size distribution (GSD) curves for cuttings representing the mafic ash tuff lithology were plotted. The interval between 37.6 m - 52.7 m shows the mean size of the particles (D50 values) is between 4 mm and 7.2 mm, as shown in Fig. 4-13. However, from 53.6 m - 55.6 m, D50 values increased between 6 mm and 10 mm as indicated in Fig. 4-14. Grain size parameters were determined, including D90, D60, D50, D30, and D10, Coefficient of Curvature (Cc), and Uniformity Coefficient (Cu). Figure 4-15 shows that the D50 values increased slightly with an increase of WOB. This observation was to be

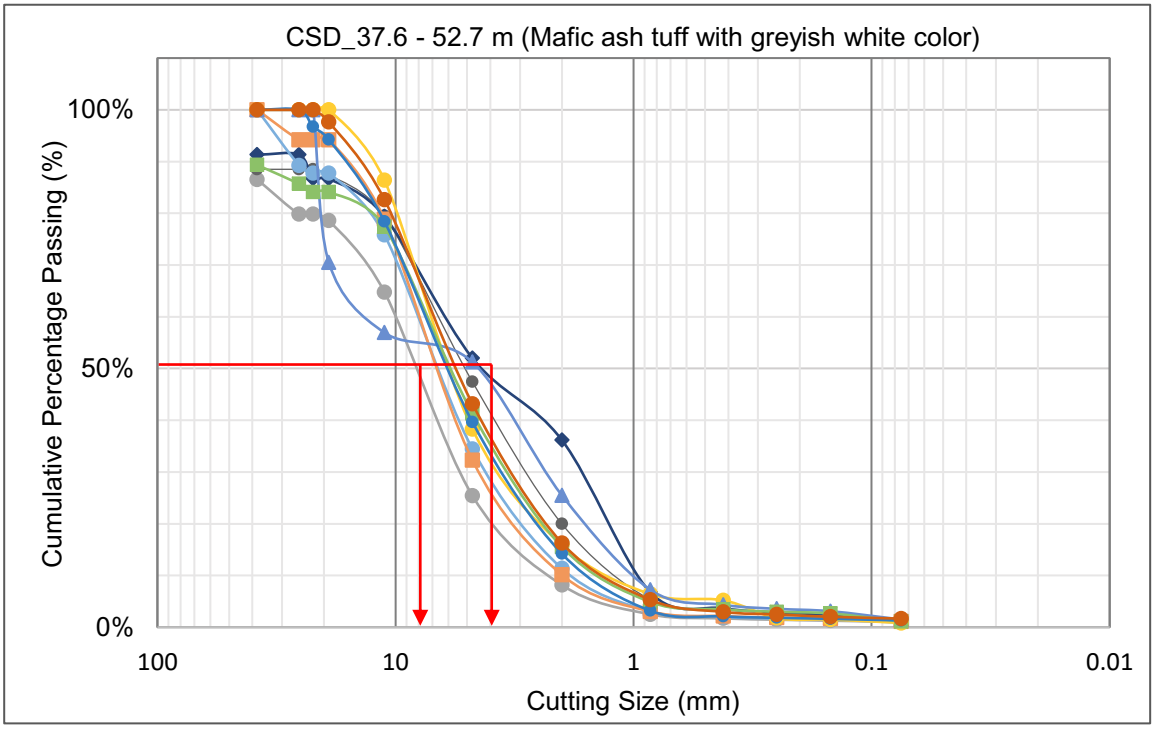

Figure 4–13. Grain size distribution for the cuttings from 37.6 m to 52.7 m

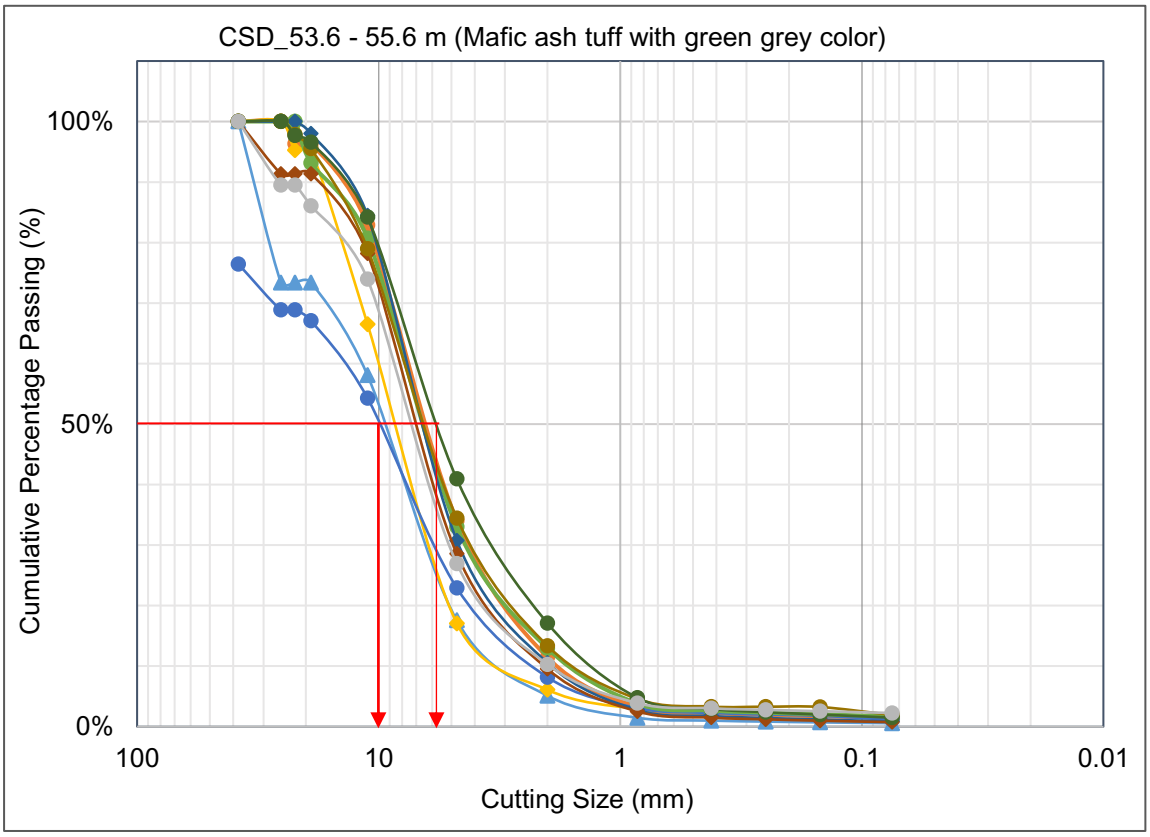

Figure 4–14. Grain size distribution within low ROP intervals 50 m to 55 m

expected because the particle size of cuttings is getting bigger. However, D90, which represents the 90 percentile by volume of the total particles that is smaller than D90 value, was observed to decrease (abnormality at specified interval) at the lower than expected ROP interval and at approximately 400 kN WOB.

The Cu and Cc were also analyzed. Figure 4-16 shows the values of Cu and Cc are between 4 to 7 and 0.5 to1, respectively. According to gradation theory, the results indicate the cuttings are well-graded grain size (Holtz & Kovacs, 1981). However, as seen in Figure 4-16, the curves are steeper between 53.6 m to 55.6 m when compared to the lower interval, which means particles are getting larger with increasing measured depth.

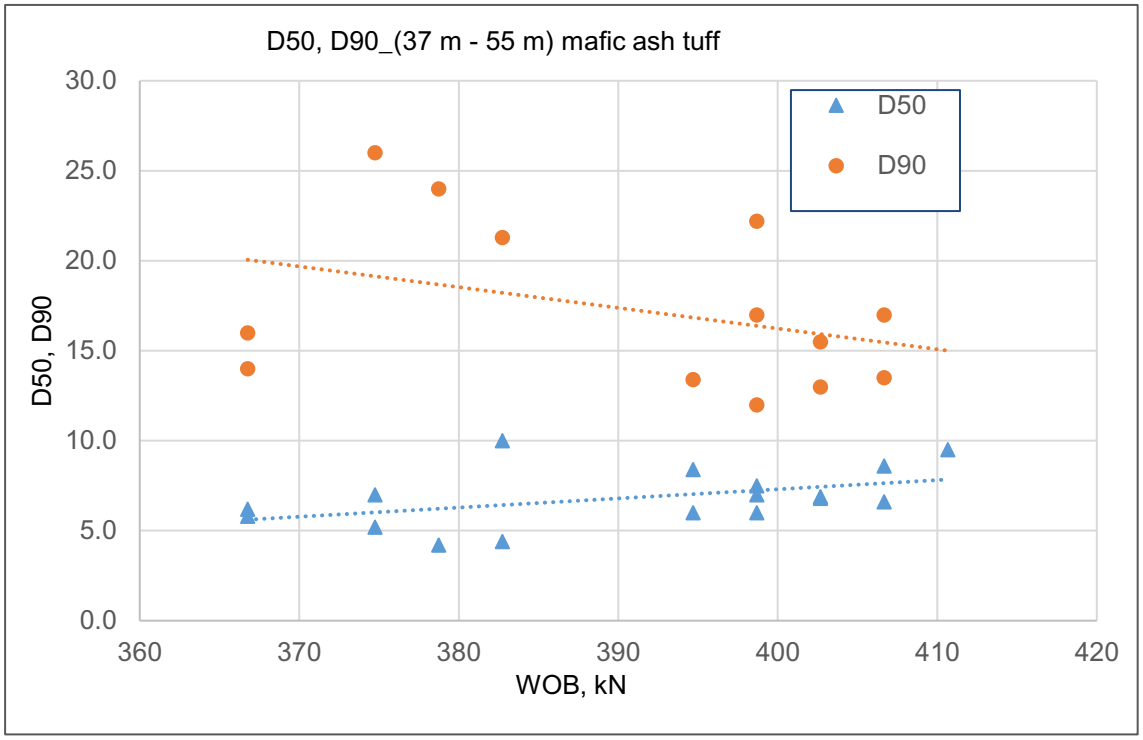

Figure 4–15. D50 and D90 of the grain size between 37 m to 55 m

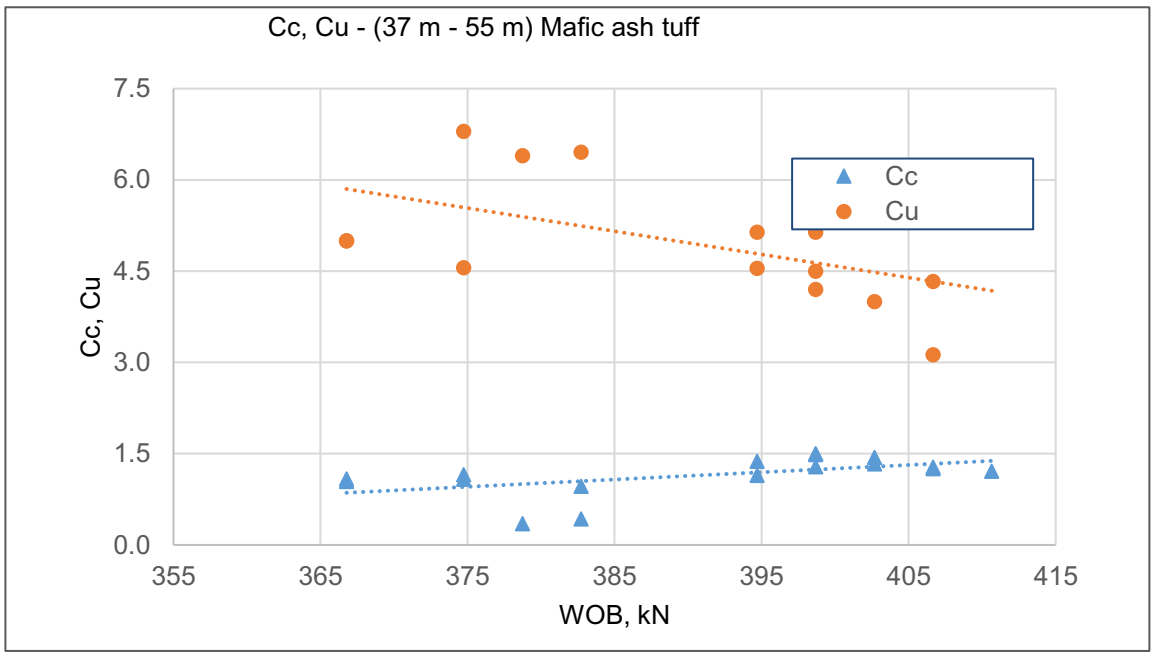

Figure 4–16. Cc and Cu of the grain size for the interval 37 m to 55 m

4.4.4 Mineral Liberation Analysis (MLA)

MLA tests were conducted on two samples of mafic rock (mafic ash tuff) in (Figure 4-17). One sample at a measured depth of 43.05 m (above the zone of interest) with a corresponding expected ROP of 1.09 m/h and another at a depth of 54.3 m (at the zone of interest) with a corresponding abnormally low ROP of 0.17 m/h. From Table 4-4, it can be observed that both samples contain a similar overall composition (material balance). However, the grain microstructure varies when comparing the tested samples, as observed in Figure 4-18, representing mineral composition and grain distribution map. Additionally, the grain structure at 54.03 m (low ROP) shows the presence of accumulated alteration of epidote minerals (see Figure 4-18). Both of these may influence the increasing strength of the rock and reduced ROP at the interval of interest.

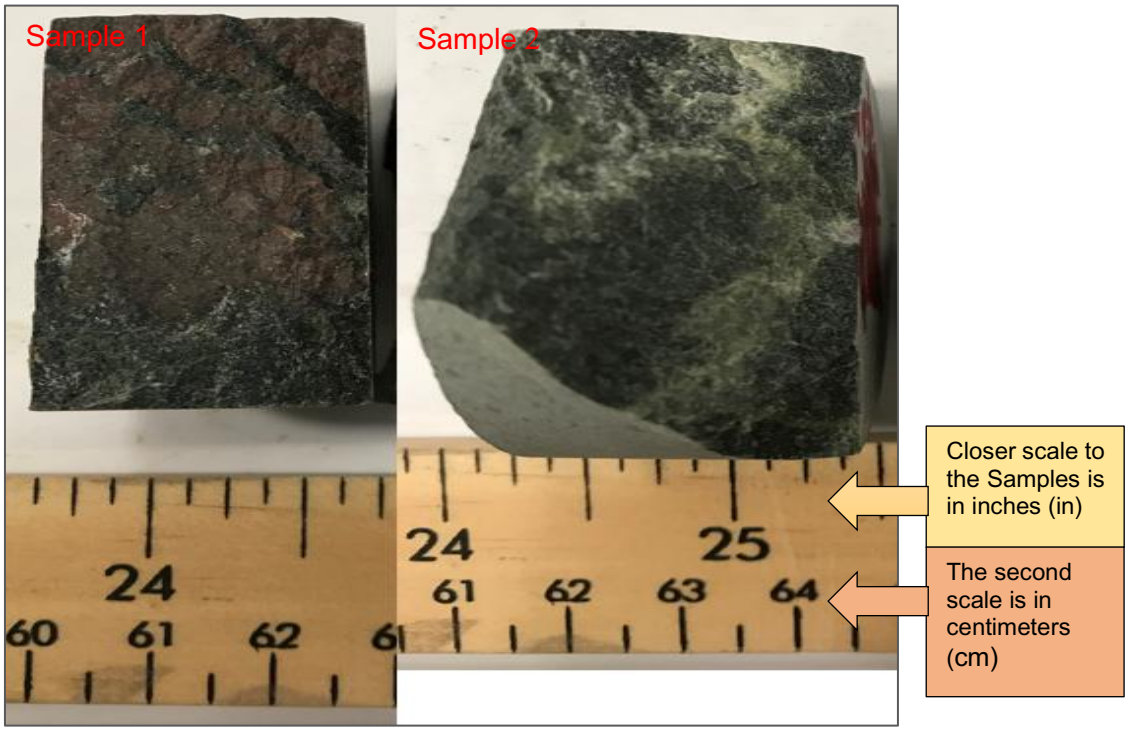

Figure 4–17. Samples 1 and 2 at 43.05 m and 54.3 m, respectively

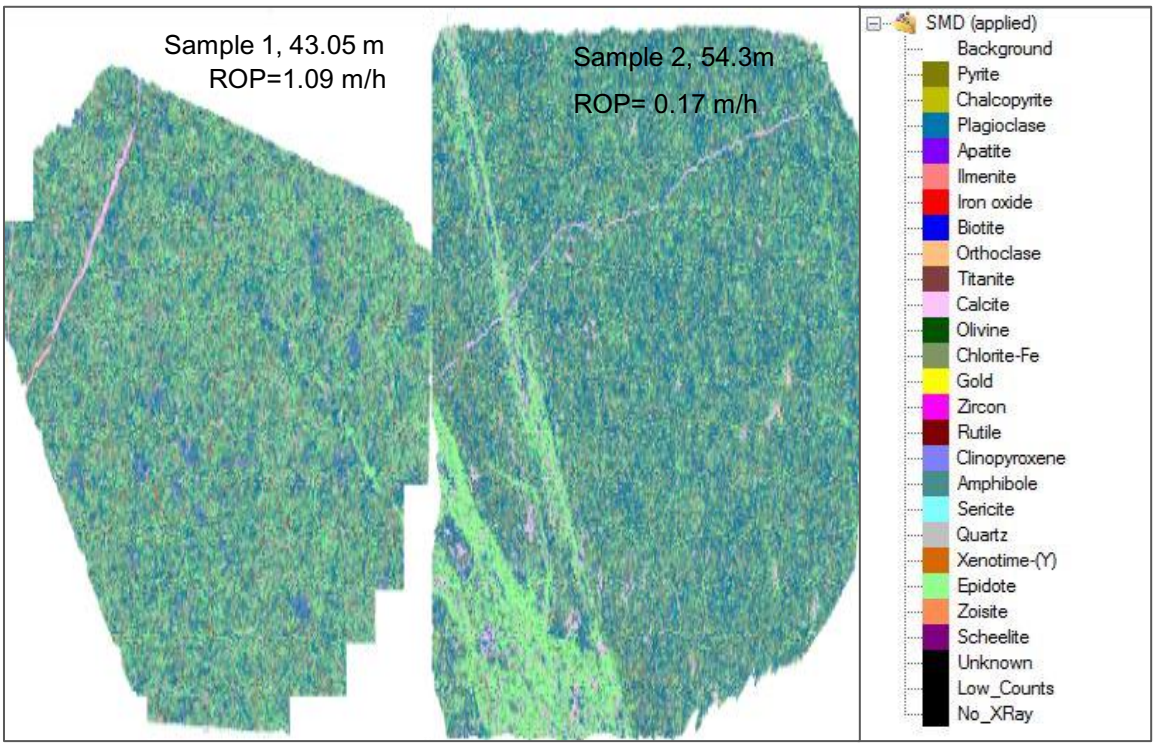

Figure 4–18. Left: MLA map for samples 1 and 2, and Right: legends

Table 4-4. The MLA Weight and Area Composition for each Analyzed Sample

Minerals	Sample 1 (D = 4 3.05 m)		Sample 2 (D = 54.3 m)	
	Weight%	Area%	Weight%	Area%
Total	100.00	100.00	100.00	100.00
Plagioclase	21.77	24.20	23.92	26.55
Epidote	27.62	23.89	26.07	22.52
Chlorite-Fe	18.52	18.42	17.30	17.19
Quartz	12.39	14.08	13.21	12.90
Amphibole	9.75	9.54	8.51	9.66
Orthoclase	3.85	4.49	3.40	3.96
Titanite	2.26	1.94	2.67	2.93
Clinopyroxene	1.97	1.73	2.38	2.04
Calcite	0.99	1.09	2.17	1.90
Biotite	0.33	0.32	0.21	0.21
Iron oxide	0.53	0.30	0.04	0.04
Apatite	0.01	0.01	0.00	0.00

4.5 Conclusions

This study presents different tests and analyses to investigate the cause of an unexpectedly low ROP from an LDH field trial. A notable reduction in ROP across a specific measured depth interval of 50 m to 55 m was observed, while at the same time, no notable variation in above and/or below geological lithology was logged, and any variation in drilling operation parameters was accounted for. The summary of the study findings are:

- The RQD for low ROP interval was found similar as just before the interval. Hence, RQD did not give a reasonable conclusion for the occurrence of low ROP at the specified interval.
- The ROP was observed below 0.5 m/h despite an increase of WOB within the interval specified. Actual ROP and normalized ROP are plotted against penetration depth. A decrease in ROP was observed for both cases. The Maurer ROP was plotted and clearly shows the trend of increased ROP when WOB increases, except at a depth of 54 m when WOB is between 390 to 400 kN. Also, it was observed that when MSE increases, both ROP and DE decrease.
- The rock strength for the low ROP interval was higher than just before the interval by 150 MPa, 13 MPa, and 24 MPa for the UCS, PLSI, and ITS, respectively. Also, rock hardness increased to 28. Hence, the increase in rock strength and hardness in the low ROP interval is a contributing factor to a decrease in ROP.
- A marginal increase in particle size was observed for the low ROP interval due to the rise in WOB. Also, according to gradation theory, the cuttings are well-graded

grain size. However, the D90 values show a decrease (abnormality trend) with the increase of WOB (400 kN), in the low ROP interval.

- MLA showed that variation of mineral grain microstructure may have caused an increase in rock strength and ROP at the depth interval of interest.

Chapter 5 : Rock Strength Estimation through a Semi-Point Load Strength Index

The chapter is another paper manuscript describing the rock strength estimation. This paper's title is "A new Approach for Rock Strength Estimation through a Semi-Point Load Strength Index and Correlation with Destructive and Non-Destructive Tests". This paper was published on the proceedings of the ASME 2022 held on June 5-10, 2022 - The 41st International Conference of Ocean, Offshore and Artic Engineering, OMAE 2022, in Hamburg, Germany. This paper is authored by Abdelsalam abugharara, Salum Mafazy, and Dr. Stephen Butt.

The author's efforts and contributions are described below:

- Abdelsalam Abugharara: Literature review, data analysis, and manuscript preparation.
- Salum Mafazy: Conducted experimental plan, sample coring, preparation, implementation, and performance of the mechanical tests, data analysis, and preparation and review. He also modifies some sentences and figures in this chapter.
- Dr. Stephen Butt: Supervision and approved the experiment plan and manuscript review and approval.

5.1 Abstract

Multi-scale civil, mining, and oil and gas drilling projects require determining rock strength as the main property of surface and subsurface rocks for safe structures, economic mining operations, and drilling performance optimizations. The Unconfined Compressive Strength (UCS) is a primary rock strength test. It has been considered a time-consuming test for

sample preparation, costly, and unaffordable. However, it is required for correlations for rock strength obtained from other tests. A semi-Point Load Strength Index (Semi-PLSI) is proposed in this research as a new approach to estimating rock strength. The objectives of this research include reducing testing costs, simplifying sample preparation and testing procedure, precisely stabilizing specimens while testing, and improving accuracy and repeatability. Various sample dimensions and (length to diameter) ratios are prepared from granite blocks for this test. A 400 (kN) Geomechanics Loading Frame (GLF) is used for testing. The GLF is equipped with an advanced data acquisition system for data recording. Results correlations are conducted. The correlations include Semi-PLSI, UCS representing the shear fracture strength, and indirect tensile strength (IT) representing the tensile fracture strength. The correlations also involve the Semi-PLSI and the primary and secondary ultrasound wave velocities, which represent Non-destructive measurements. As an initial stage of evaluation, the correlations present good agreements. Also, the different rock strength tests that are conducted for estimating rock strength enrich this new approach of the Semi-PLSI proposed for UCS estimation and demand for deeper investigation

5.2 Introduction

Rock strength is fundamental in understanding rocks and formations as one aspect of mechanical rock properties and rock characterization. Determining rock strength is essential, and it is required for establishing safe structures (civil and mining) and evaluating drilling performance (geotechnical and petroleum industries) (Fjaer et al., 2008) and (Jaeger et al., 2009). Various strength methods, indices, and techniques have been used to determine rock strengths. These methods are categorized as either Non-Destructive

Strength Methods (NDSM) or Destructive Strength Methods (DSM). Some of the NDSM include ultrasound measurement and Schmidt/Rebound Hammer. Some of the DSM include Confined and Unconfined Compressive Strength (CCS and UCS, respectively), Indirect Tensile Strength (IT), and Point Load Strength Index (PLSI).

UCS and CCS are the rock strength methods that consume the most time in sample preparation and conducting the tests. They also are unaffordable for small-scale projects to provide expensive equipment. They also require expensive apparatus, a pressurized cell (Hoek's cell) with confinement for determining the confining pressure of burden formation, as well as they need high loads for breaking samples (Palchik, 2007) and (Mishra & Basu, 2012). However, because of the importance of that (i) UCS is always used as a standard strength method that all researchers need for strength correlations, (ii) some industries, such as mining companies, mostly require UCS data more than any other strength data, and (iii) UCS is required for building, producing, and validating rock mechanics and rock fracture numerical models (Jaeger et al., 2009) and (Hoek et al., 2002), attention towards the rock strength data produced from conventional and innovative strength methods and their correlations with UCS gained more focus (Mishra & Basu, 2012), (Ghosh & Srivastava, 1991), (Chau & Wong, 1996), (Tuğrul & Gurpinar, 1997) and (Sulukcu & Ulusay, 2001). In addition to building numerical models for rock mechanics, empirical procedures have also been developed to estimate rock strength and to examine the isotropy of rocks, including the granite rock used for this research and other rock types through direct physical, mechanical, and drilling tests (Abugharara et al., 2016; Abugharara et al., 2017; Abugharara et al., 2019 and Rasul et al., 2021).

As a continuation of offering simple, practiced, and reliable rock strength estimation methods, this research proposes a new approach for rock strength estimation through the Semi-Point Load Strength Index (Semi-PLSI). The purpose of this approach is to propose a testing setup that allows samples in the axial test of the PLSI that (i) provides more stability and balance to samples before and during testing and (ii) a safer testing environment that prevents scattering and flying broken samples.

5.3 Materials and Methods

Materials used for this research consists of three main groups materials from which the core was obtained, equipment used for sample preparation, and equipment used for sample testing. For coring three granite blocks (~30 cm long, ~30 cm wide, ~ 15 cm thick), a coring rig with a core barrel (47.6 mm) was used to obtain cores at about 30 cm long. The coring parameters applied include moderate tab water flow rate, constant WOB, and with 600 rpm to ensure a smooth and effective coring process. Following coring the samples, a diamond blade saw table was used to cut the samples at pre-determined lengths and dimensions per strength testing types. After samples were cut and labeled, flat, smooth, and parallel ends of all samples were checked using the grinder, mainly for UCS samples. Final measurements of lengths, diameters, and weights were taken. A coring bit of 47.6 mm diameter was used for coring granite blocks using a coring rig set up to obtain cores, from which samples for all tests were prepared.

Figures from 5-1 to 5-3 show samples for all tests before and after performing the tests, which included Semi-PLSI, PLSI, I.T., V.P., VS, and UCS.

Figure 5–1. Samples for Semi-PLSI and PLSI tests (Group A and B), respectively before and after testing

Figure 5–2. Samples for semi-PLSI (group C, and D) and
PLSI (groups E, and F) before and after testing.

Figure 5–3. Left : (top and middle): samples for IT - before and after testing. Left : (bottom): VP, VS, and UCS samples before testing. Right: UCS sample after tests

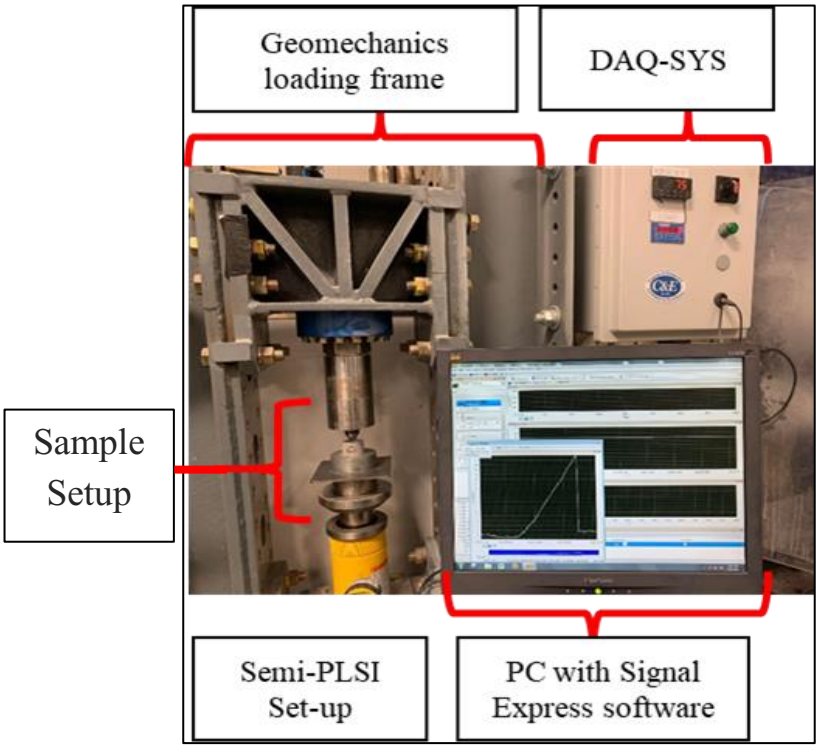

Figure 5–4. Fully instrumented geomechanics loading

Figure 5-4 shows the Geomechanics loading frame employed for testing. The frame was instrumented with a DAQ-SYS that utilized a LabVIEW-signal express software is capable of multiple range sampling rate measurements. The frame can also use various piston types per the desired intended test. Figure 5-5 shows drawings of different sample dimensions on top and four main testing set-ups that were installed on the Geomechanics loading frame for the Semi-PLSI test, PLSI test, and I.T. test, and UCS on the bottom.

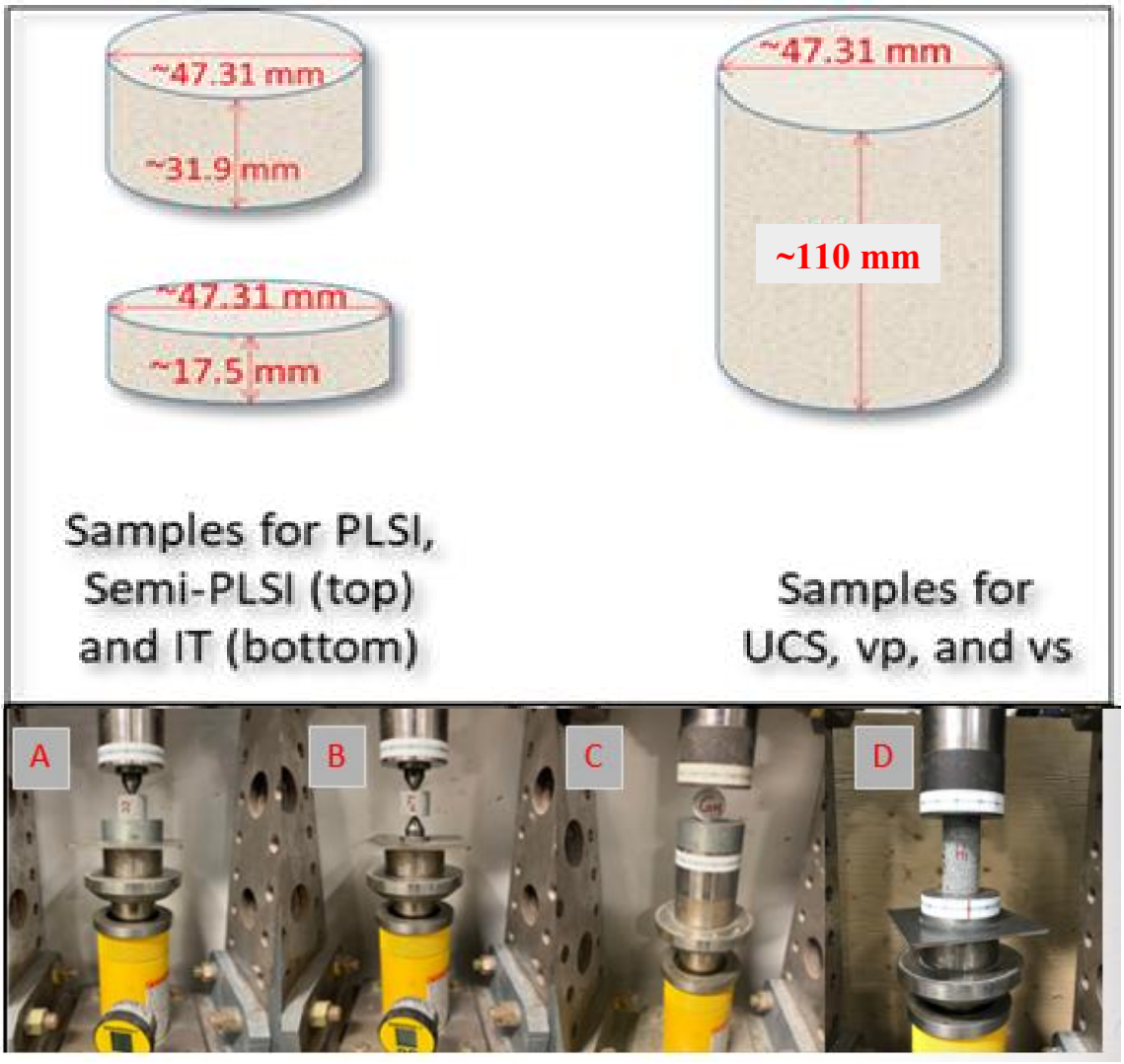

Figure 5–5. Top: Sample dimensions. Bottom: set-up tests for (a); semi-PLSI, (b); PLSI, (c); IT, and (d); UCS

5.4 Results and Discussion

This section contains results obtained from tests, which include (i) ultrasound-testing method that provided primary and shear wave velocities (V_P and V_S, respectively). This test was performed on the samples prepared for the Unconfined Compressive Strength (UCS) shown in Figure 5-3 (bottom). (ii) Indirect Tensile Strength (I.T.) test, whose samples are shown in Figure 5-3 top. (iii) Point Load Strength Index and Semi-Point Load Index tests (PLSI and Semi-PLSI, respectively), whose samples are shown in Figures 5-1 and 5-2. (iv) UCS test, whose samples are shown in Figure 5-3 bottom. All samples were prepared and tested according to the ASTM standards, including (ASTM D4543-19 for sample preparation, ASTM-D5731-16 for PLSI, ASTM-D3967-16 for IT, ASTM D2845-08 for vp and vs, and ASTM D 2938 – 95 for UCS). The Semi-PLSI sample dimensions were made to be in the range of PLSI sample criteria as per the ASTM D5731-16.

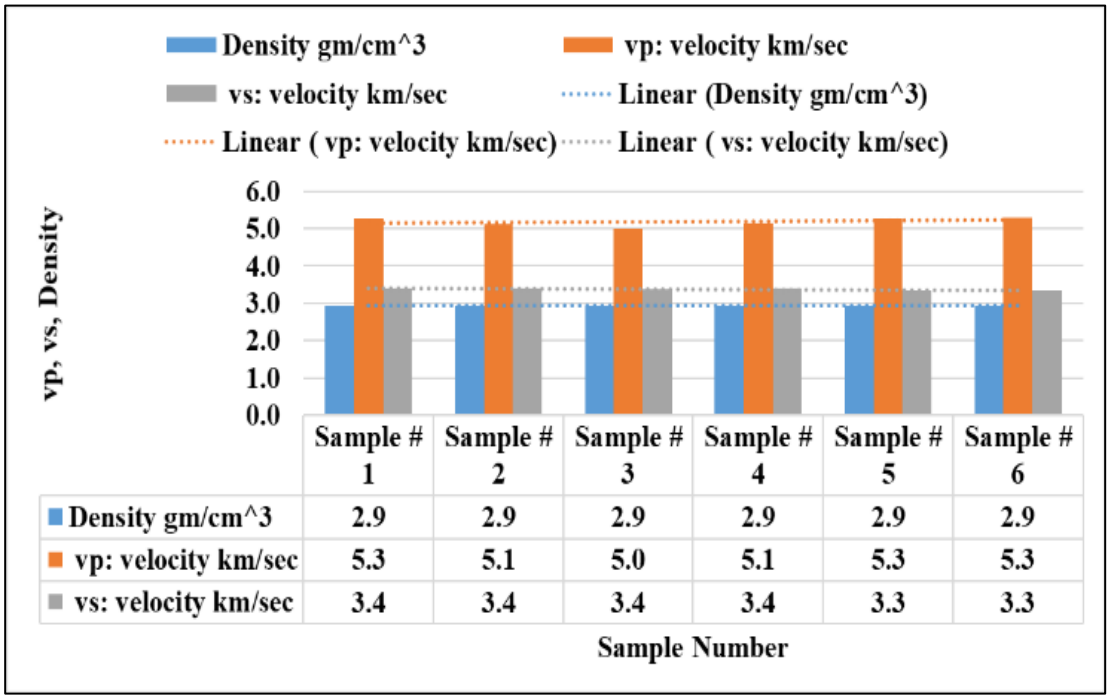

Figure 5–6. V_P, V_S, and density of UCS samples

Figure 5-6 shows density, V_P, and V_S results from UCS samples. Density was the same for all samples, including those prepared for the other tests. However, V_P and V_S were measured only from samples prepared for UCS as per the ASTM D2845-08.

5.4.1 Mono Correlation Analysis

For a complete range of correlations, Semi-PLSI was planned to be correlated with $V_{.P.}$, V_S, IT, PLSI, and UCS. At first, the indenter used for Semi-PLSI was similar to the pair indenters used for PLSI.

The diameter of the indenter head was 5mm. All samples tested by PLSI and Semi-PLSI were broken when reaching the failure point, as shown in Figure 5-2, which differentiates it from the indentation test that breaks the samples in the multi-fracture process. Figure 5-7 shows strength results correlations between IT and UCS (top), PLSI and UCS (middle), and Semi-PLSI and UCS (bottom).

Correlations between IT and UCS were conducted to show confidence in results, whereas a rule of thumb in IT and UCS correlations indicates UCS is about ten times greater than IT. After that, the correlations showed confidence in the results obtained for IT and UCS. Correlations were then carried on to include UCS and PLSI and UCS and Semi-PLSI. Correlations also involved V_P and V_S as Non-destructive measurements. Moreover, correlations showed good agreement as per the generated correlation models summarized in Table 5-1.

Figure 5-8 shows correlations between PLSI and Semi-PLSI with IT. The correlation followed a zero-insect linear relationship. The correlation showed good agreement between Semi-PLSI and PLSI with IT as all three strength types follow tensile fractures.

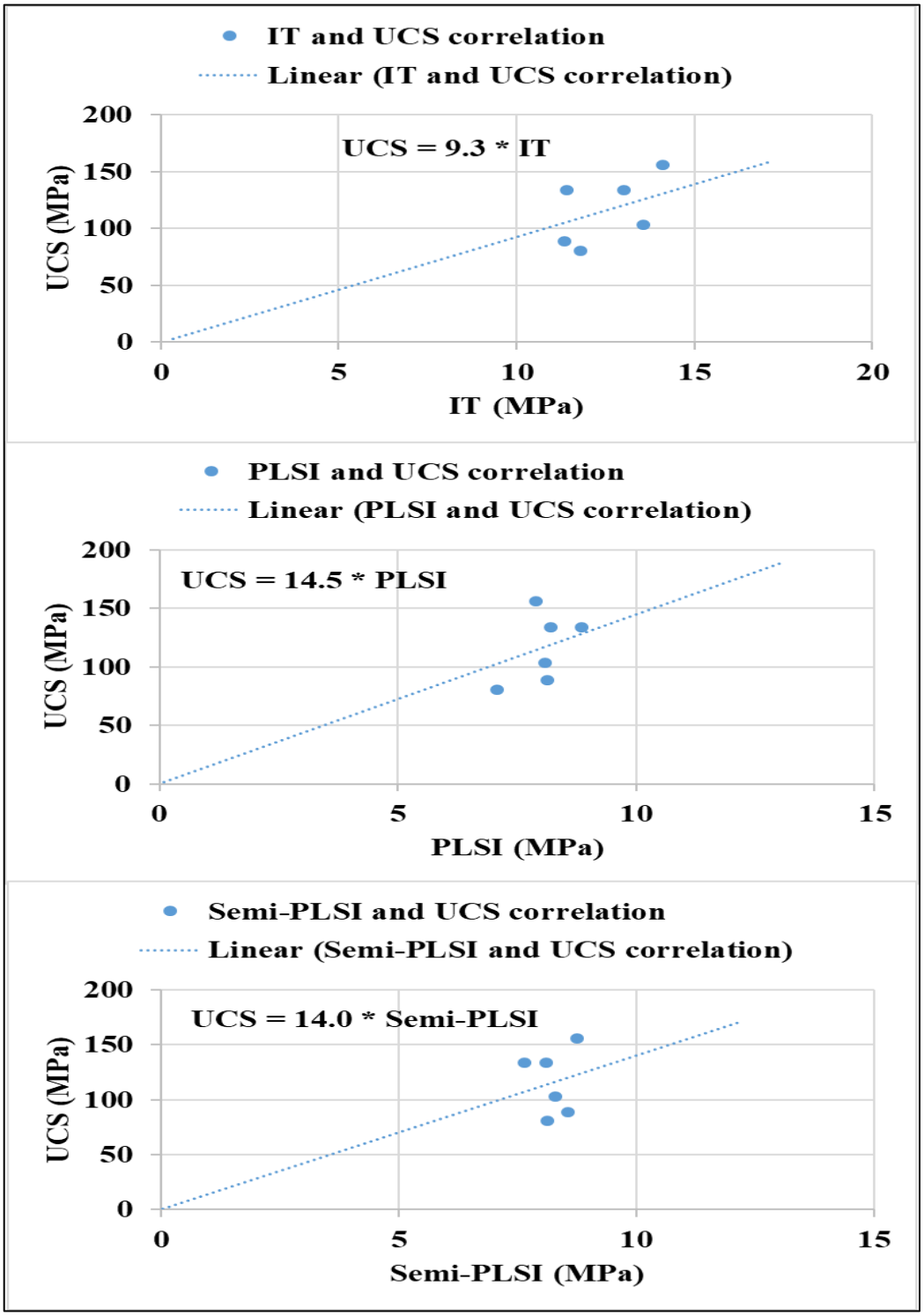

Figure 5–7. Correlations between UCS and IT, PLSI, semi-PLSI from top to bottom, respectively.

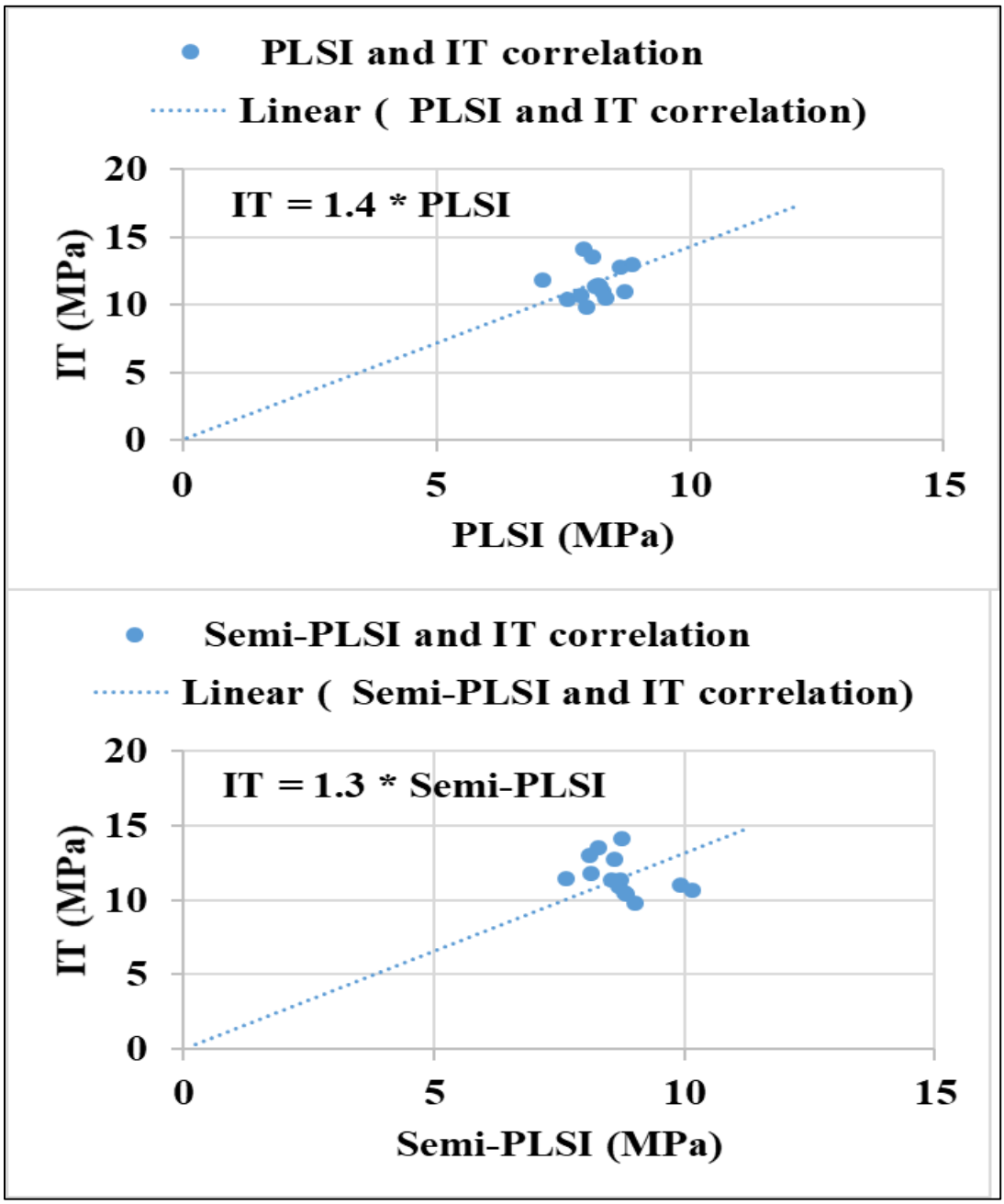

Figure 5–8. Top: Correlations between IT and PLSI and Bottom: IT and semi-PLSI

Figures 5-9 and 5-10 show another set of correlations. This correlation is between results obtained from destructive tests (Semi-PLSI in Figure 5-9 and PLSI in Figure 5-10) with results from Non-destructive tests (V_P, in Figure 5-9 and V_S in Figure 5-10). Having various

data types and results abstained from different strength methods enriches and supports the

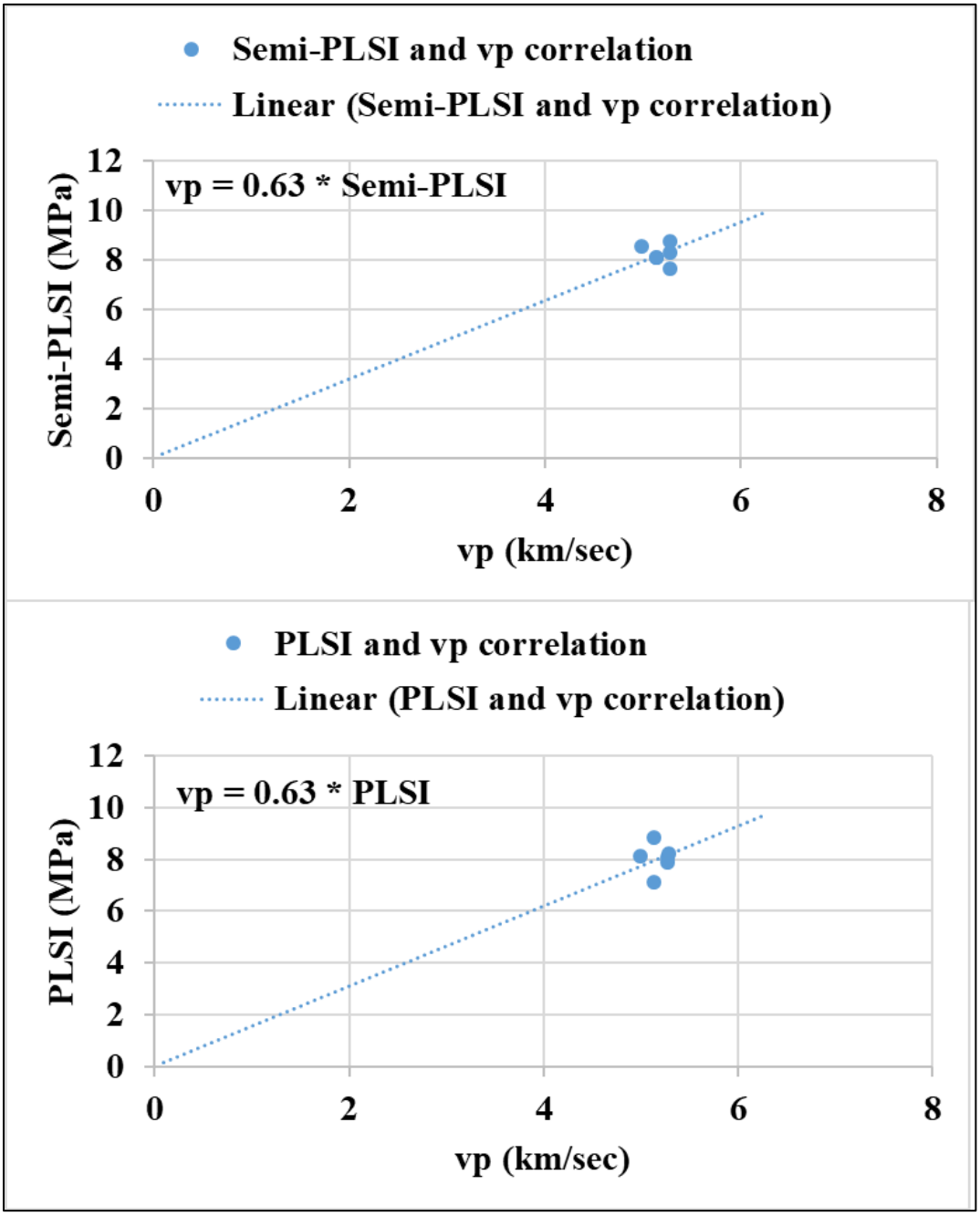

Figure 5–9. Top: Correlations between V_P and semi-PLSI and Bottom: V_P and PLSI

data quality and provides more confidence in data analysis and results.

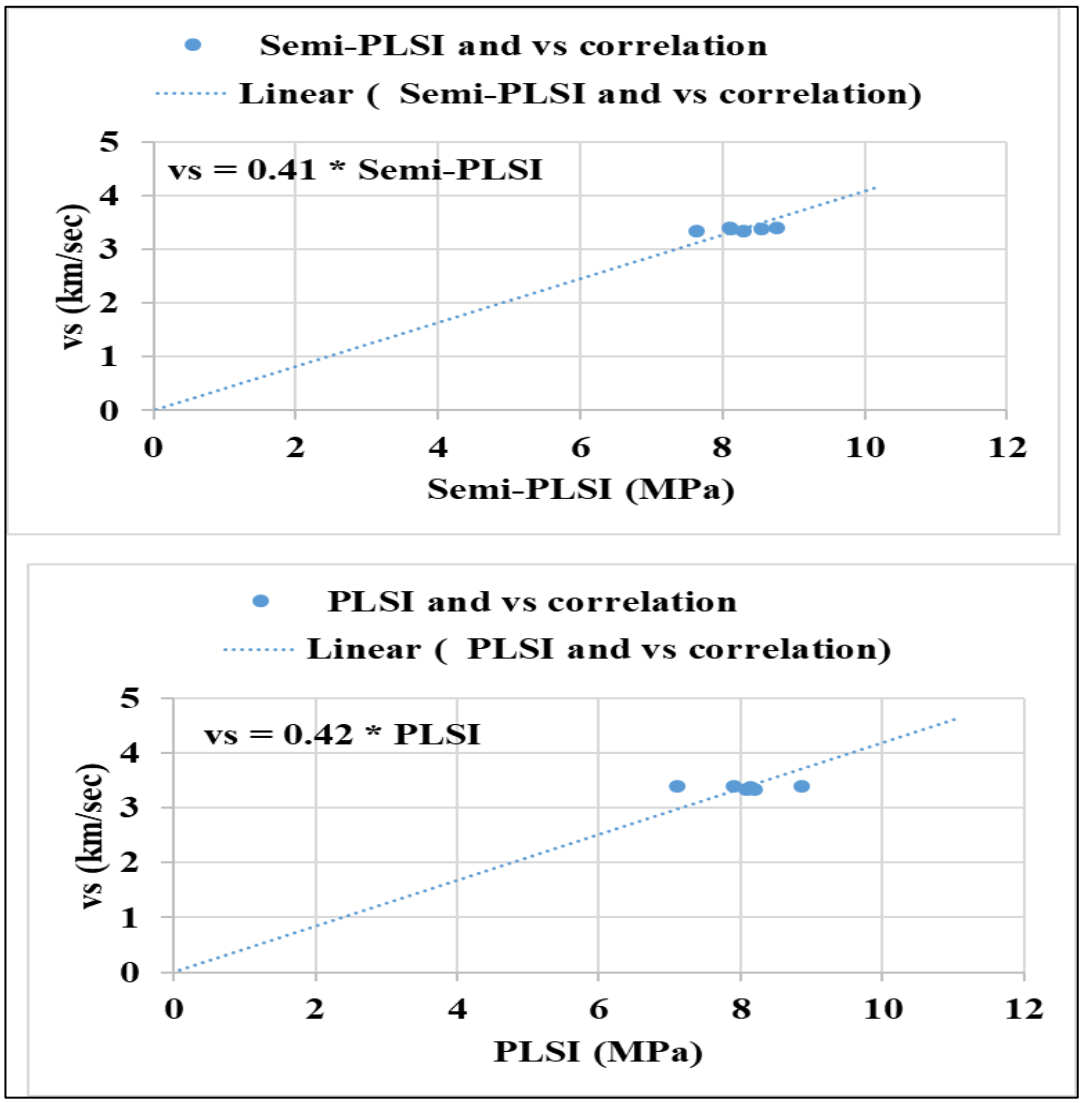

Figure 5–10. Top: Correlations between V_S and semi-PLSI,and Bottom: V_S and PLSI

5.4.2 Dual Correlation Analysis

The dual correlation analysis shown in Figures 5-11 to 5-14 display the results of interest in combination for a more comprehensive comparative study. The mono correlations include (i) UCS versus Semi-PLSI and PLSI (Figure 5-11), (ii) V_P versus Semi-PLSI and PLSI (Figure 5-12), (iii) V_S versus Semi-PLSI and PLSI (Figure 5-13), and UCS versus $V_{.P.}$ and V_S (Figure 5-14). Figure 5-11 shows the correlation between UCS and both Semi-

PLSI and PLSI in a dual correlation analysis using the zero intersect linear relationship. This Figure also shows the correlation between destructive strength tests, where UCS is estimated from Semi-PLSI and PLSI.

Figure 5-12 and 5-13 show correlations between V_P and V_S with both Semi-PLSI and PLSI in a dual correlation analysis using the zero intersect linear relationship. These figures also shows the correlation between measurements from Non-destructive strength (V_P and V_S) and destructive strength tests (Semi-PLSI and PLSI), where the Semi-PLSI is estimated from V_P and V_S. Also, the estimated Semi-PLSI can be used to estimate UCS as a second way of USC estimation using the correlations presented in Figure 5-11.

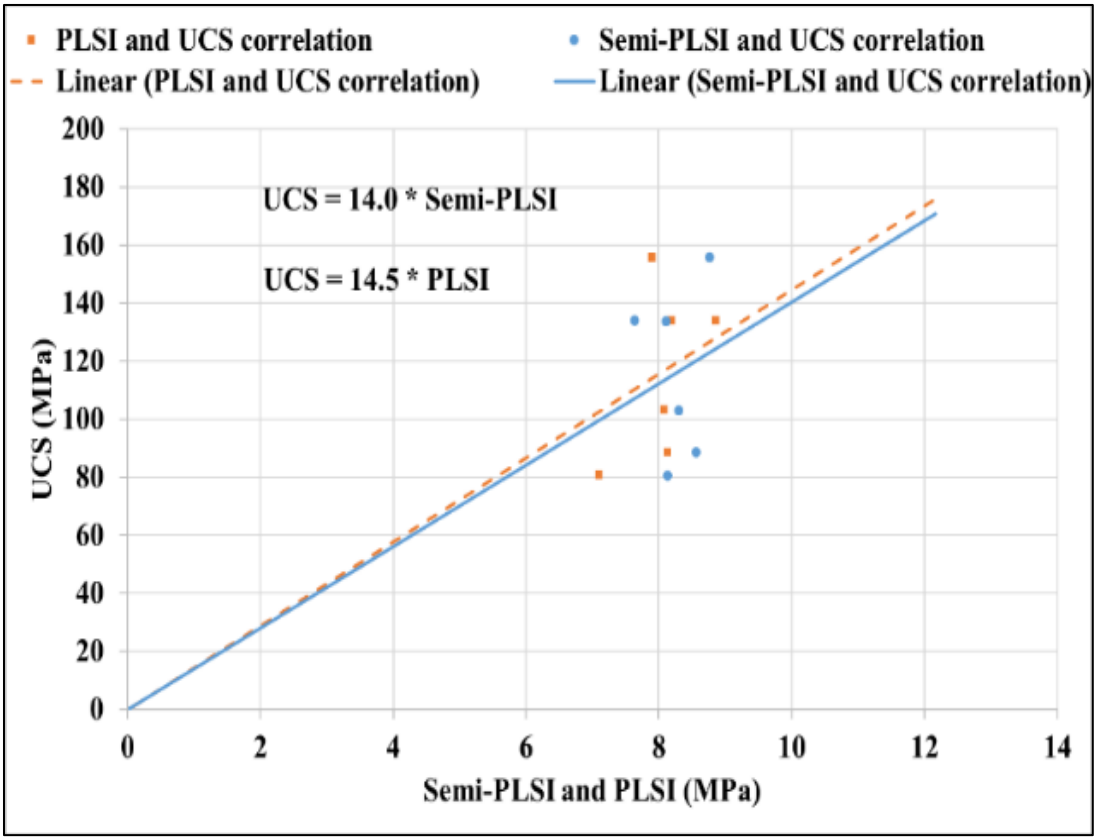

Figure 5–11. Correlations between UCS, semi-PLSI, and PLSI.

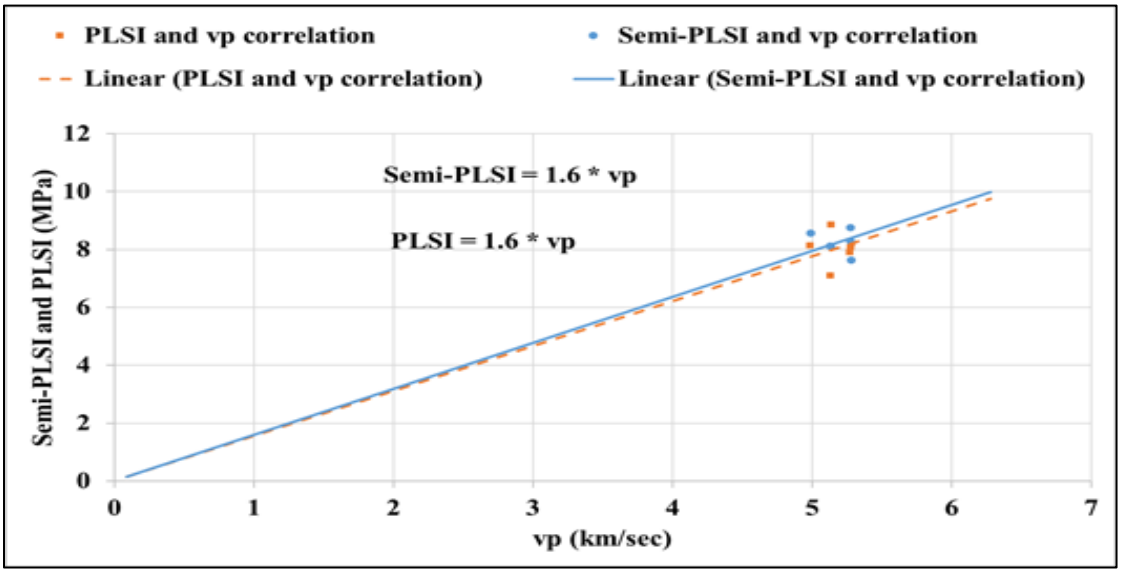

Figure 5–12. Correlations between V_P, semi-PLSI, and PLSI.

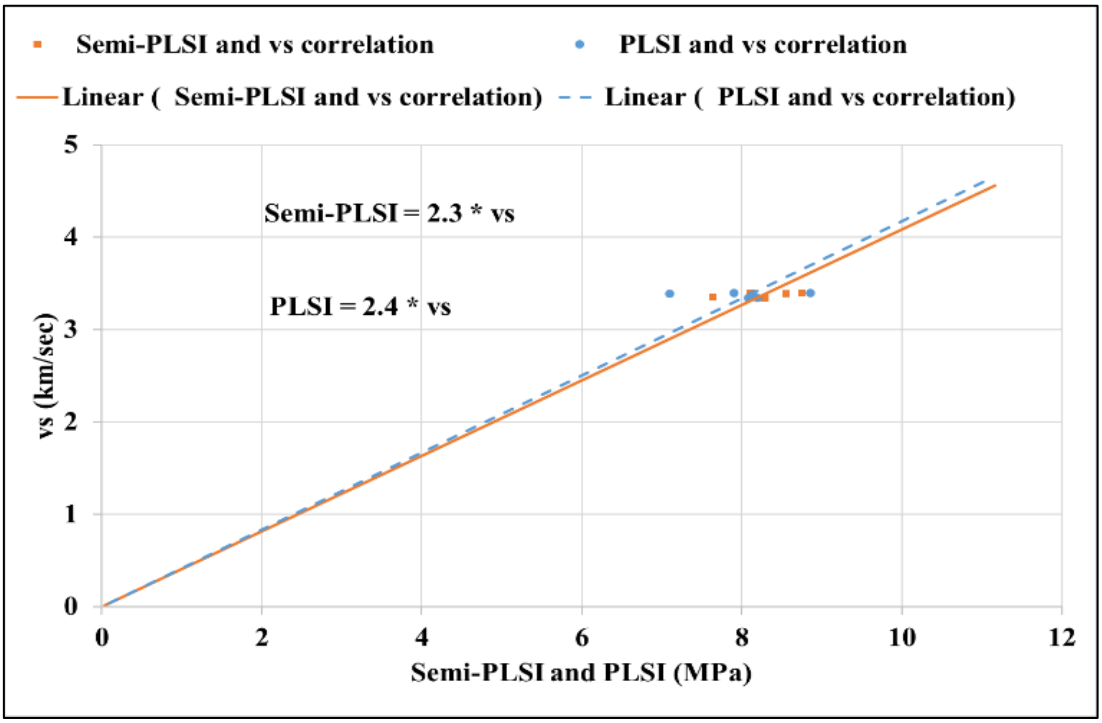

Figure 5–13. Correlations between V_S, semi-PLSI, and PLSI.

Figure 5-14 shows the correlation between V_P and V_S with UCS. These correlations can be used to validate the UCS values that are obtained from V_P and V_S (Figure 5-14) and the UCS values that are obtained from Semi-PLSI (Figure 5-11) as the new approach of UCS estimation proposed through this research.

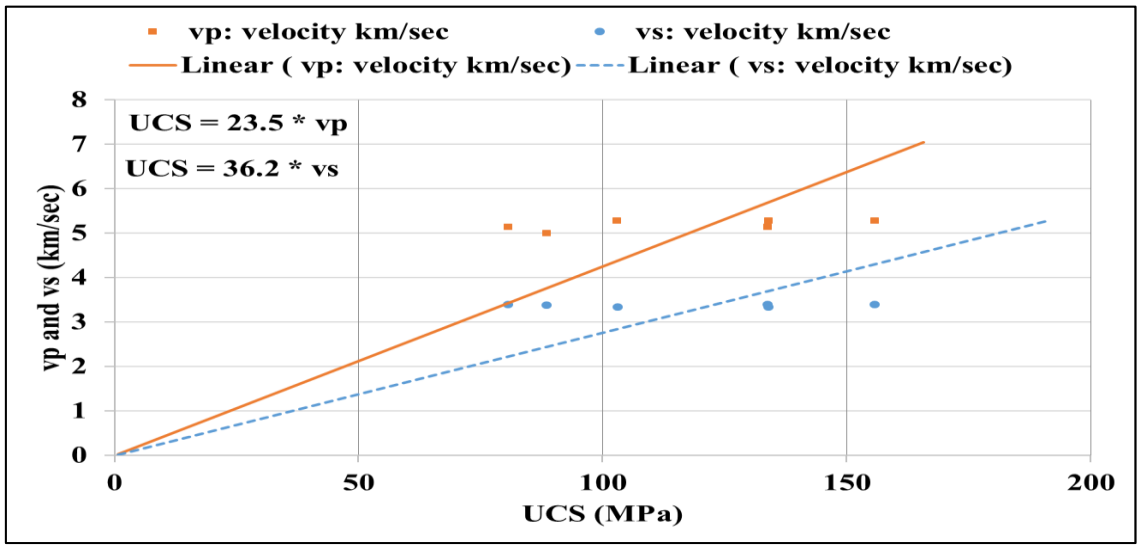

Figure 5–14. Correlations between V_P and V_S with UCS.

Table 5-1. Summary of correlations

Ref.	Correlation	Equation
1	UCS, IT	UCS = 9.3 * IT
2	UCS, PLSI	UCS = 14.5 * PLSI
3	UCS, Semi-PLSI	UCS = 14 * Semi-PLSI
4	UCS, vp	UCS = 23.5 * vp
5	UCS, vs	UCS = 36.2 * vs
6	IT, PLSI	IT = 1.4 * PLSI
7	IT, Semi-PLSI	IT = 1.3 * Semi-PLSI
8	PLSI, vp	PLSI = 1.6 * vp
9	PLSI, vs	PLSI = 2.4 * vs
10	Semi-PLSI, vp	Semi-PLSI = 1.6 * vp
11	Semi-PLSI, vs	Semi-PLSI = 2.4 * vs

This new testing approach provides various ways for estimating results using data correlations between data obtained from different testing types. For example, UCS can be calculated in three different ways, including (i) direct measurements through conducting the test on UCS samples shown in Figure 5-3, (ii) correlation with IT, Semi-PLSI, and PLSI as shown in Figures 5-7 and 5-11, and (iii) correlation with V_P and V_S as shown in Figure 5-14.

5.5 Conclusions

This baseline development of UCS estimation through the proposed new approach of Semi-PLSI provides a start of more investigation into this method for research expansion, support, and validation.

This research invented a new technique of rock strength estimation and correlated it with other strength tests destructive tests (UCS, IT, and PLS), and non-destructive tests (ultrasonic measurements) i.e P-wave and S-wave velocities.

The correlation results presented were very good for both tests and gives a positive results of Semi-PLSI comparable with standard PLSI. This increase the level of confidence using Semi-PLSI as a testing technique for strength determination.

Chapter 6 : Evaluation of Microwave Irradiations on Rock Properties and Drilling Performance

This chapter represents the OMAE conference paper with the same tittle. The paper has submitted on the proceedings of the ASME 2023 which will be conducted on June 11-16, 2023 - The 42nd International Conference of Ocean, Offshore and Artic Engineering, OMAE 2023, in Melbourne, Australia. This paper is authored by Salum Mafazy, Abdelsalam abugharara, and Dr. Stephen Butt.. The authors are:

- Salum Mafazy: proposed the test matrix and experimental plan, sample preparation and test performance, data analysis, and manuscript preparation.
- Dr. Abdelsalam Abugharara: assisted with the literature review, experimental plan, and manuscript review.
- Dr. Stephen Butt supervised, gave complete support, and provided technical assistance and a final review of the manuscript report.

6.1 Abstract

Enhancing the Drilling Rate of Penetration (D-ROP) is a target for lowering the ultimate cost in reaching hydrocarbon reservoirs, evaluating reservoir formation, and extracting minerals and reducing rock crushing consumed energy through mining operations. It has been reported that ROP can be positively influenced depending on optimization of several factors such as drilling parameters alteration and rock fragmentation process. In this research, D-ROP is evaluated by altering the status of the formations being drilled by the use of Microwave Irradiation (MI) while all other applied parameters are kept constant. Unlike published works, this research collectively investigates the influence of MI on D-

ROP of hard formation providing confirmation on rock property alteration through non-destructive tests including ultrasonic wave velocities measurement and destructive tests including Indirect Tensile Strength (ITS). Results show gradual alteration in rock properties as per MI exposure time including a reduction in P-wave and S-wave velocity, a decrease in Young's Modulus of elasticity (E) as well as Poisson's ratio (v). Also, an outcomes shows a formation of the fractures when the rocks exposed to MI which led to a decrease in rock strength and influences a weakening of the rocks and ultimately led to increase in D-ROP.

6.2 Introduction

An optimal mechanical technology and pre-treating rock by microwave irradiation to break and causes rock fragmentation could bring advantages in terms of large-scale production drilling or rock removal process. The main application, including drilling and blasting or mechanical miners, is one of the methods used to excavate rocks (Kahraman et al., 2020). Therefore, some limitations hinder drilling ROP on hard rock, such as low cleaning efficiency and excessive cutter wear for different reasons, including high rock strength.

A mechanical test determination has been used to analyze rock properties and correlate with drilling log data to optimize drilling performance. Mafazy et al. (2022) presented a detailed investigation of mafic and quartz rocks to analyze rock properties. His results noted that rock microstructures decreased rock strength and caused a reduction in ROP. Also, Kolapo (2021) proved the ROP decreases when rock strength increases.

This work applied a microwave test to determine the heating effects on rock properties. The ultrasound wave measurements (V_P and V_S) and indirect tensile strength (IT) tests were

conducted before and after the rock samples specimen was exposed to microwave. The observation showed that with an increase in heating time, both rock properties decreased, which was caused by fracture initiation and propagation on the rock.

6.3 Materials and Methods

6.3.1 Samples Material Preparation

This study analyzes two types of rocks, Granite (GR) and sandstone (SS). The samples were obtained by coring process from Small Scale Drilling Simulator (SDS) in the DTL Lab at MUN. The coring bit used is NQ size, 47.33 mm in diameter. Then, the samples were cut into different sizes for strength tests (IT) and ultrasonic wave measurements. Figure 6-1 and 6-2 show a prepared rock sample for the IT test to observe the effect before and after heating microwaves. IT samples for SS and GR were prepared by following

Figure 6–1. Heated Samples, Left: Before IT test and Right: After IT test

dimensions, thickness, t = 16mm, and diameter, D = 46.7 mm, for the ratio t/D = 0.34 (ASTM-D3967). Also, the ultrasonic measurements sample was prepared with t = 100 mm/ 4 in and D = 46.7 mm.

Figure 6–2. Left and Middle: Unheated-IT Samples and Right: Heated samples for Ultrasonic wave Test

Figure 6–3. Granite sample after DOT-Test On SDS.

Also, Drill-off-Test (DOT) as shown in Fig. 6-4 was conducted on Small-scale Drilling Simulator (SDS) at the Laboratory. The main parts of SDS for this specified drilling

experiment was including a dual Polycrystalline Diamond Compacts (PDC) bit of a diameter 35 (mm) and applying varying Weight-On-Bit (WOB) ranging between 113.48 to 226.8 (Kg). Samples was prepared for the drilling and coring tests. This research report only the drilling results of granite rocks shown in Fig. 6-3 above.

Figure 6–4. DOT Set-up on Small-Scale Drilling Simulator
for the granite rock sample before and after MI.

6.3.2 Tests and Experimental Set-up

Figure 6-5 shows the experimental setup for all three tests at the DTL Laboratory at MUN; including a geomechanics frame, ultrasonic wave device, microwave of 1200 Watts, and infrared gun for IT-strength determination, P and S wave measurements, microwave heating, and temperature recording, respectively.

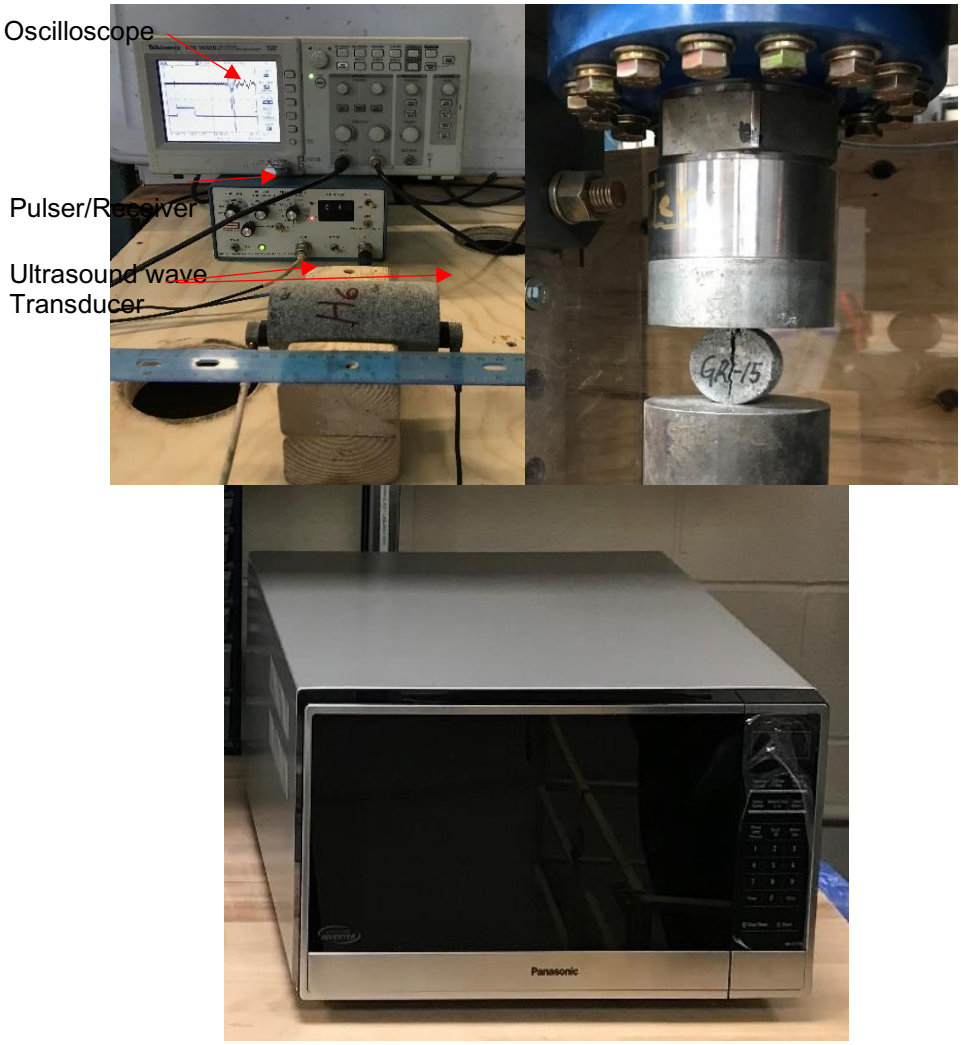

Figure 6–5. Top: Left: Ultrasonic wave device and Right: IT-test on the Geomechanics frame. Bottom: 1200 Watts – Microwave

6.3.3 Developed Testing Matrix and Procedures for MWI-Test

After the sample preparation, the experiment was the following procedures prepared. For an ultrasonic wave measurement, the text matrix is:

The test was designed for two heating cycles. 1st cycle followed exposure time from 1 min to 5 min with an increment of 1 min. After cooling, the 2nd cycle re-heated the same Sample from 2 min to 6 min in 1 min increments.

- Ultrasound wave was measured before and after each cycle

An IT test follows the procedures below:

- There were six sets of samples; each group of an IT test had eight samples. One set of IT tests was conducted without being heated to a microwave to obtain the IT strength of GR before microwave irradiation effects.
- Then, the remaining five sets of an IT test were tested with an increment of 30 seconds for each group from 10 sec to 120 sec. After the samples completed microwave heating, the pieces were let to be cooled down, and the IT test was conducted.

Figure 6-6 shows a device and method used for recording the temperature of the specimen after being exposed to microwave irradiation.

Figure 6–6. Recording temperature of the specimen by using infrared gun

6.4 Results and Discussion

This report represents the 1st stage of the microwave test to be conducted at DTL Lab. Two proposed tests were carried out for precise data determination and analysis, destructive and non-destructive tests. Also, relating the experimental laboratory work to the practical operation in the field is essential for finding solutions for enhancing ROP. The focus of the field drilling application is to optimize or increase ROP for the cost reduction of the project. The strength test was chosen because of its direct effect on ROP and ultrasonic wave velocity to support the strength analysis and avoid destroying the Sample for future laboratory experiments.

6.4.1 Ultrasound Wave Velocities Results

6.4.1.1 Effect of Heating Temperature on the Rock Samples

The results from the two groups are shown in Figures 6-7 and 6-8 for Ultrasonic measurement and IT test, respectively. Both samples show a direct proportional heating temperature with an increase in heating time. In Fig 6-7, two heating cycles were conducted for the GR sample (for an ultrasound measurements). GR-1 and G-2, after MWI temperature at 2^{nd} cycle heating, were nearly the same as GR-3 and GR-4 of 1^{st} cycle heating, respectively.

Also, the heating temperature for the 2^{nd} cycle was observed to increase more due to the microfracture created due to the 1^{st} cycle heating, which allows the samples to absorb more heat in samples. The crack formation was observed for samples GR-3, GR-4, and GR-5, as shown in figure 6-9 below.

After a microwave heating of the IT sample, the average temperature was taken for each group set of IT-test. An increasing temperature trend was observed. The GR samples have higher temperatures at the early exposure time than the SS samples. Hence, as time increased, the samples were observed to have similar temperatures, as shown below in figures 6-8.

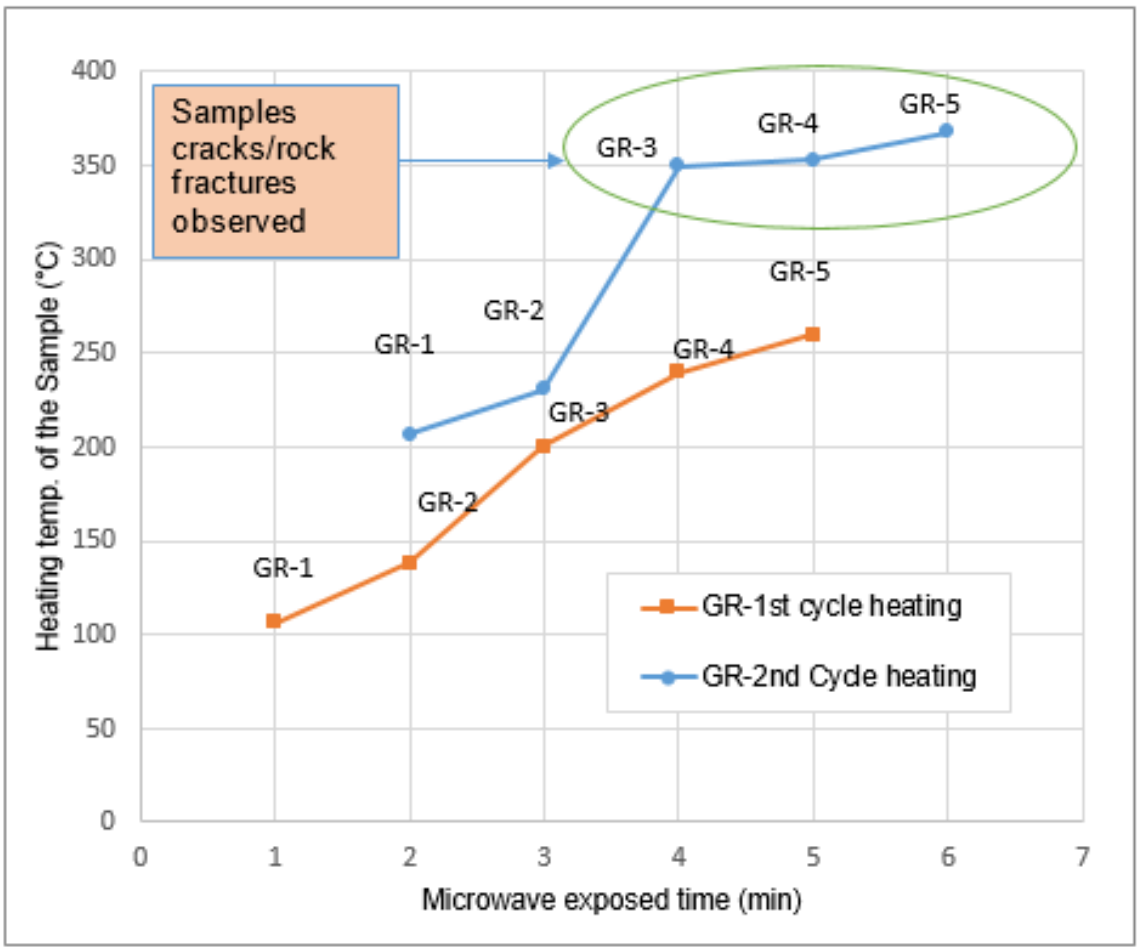

Figure 6–7. GR_Samples at 1st and 2nd heating cycle

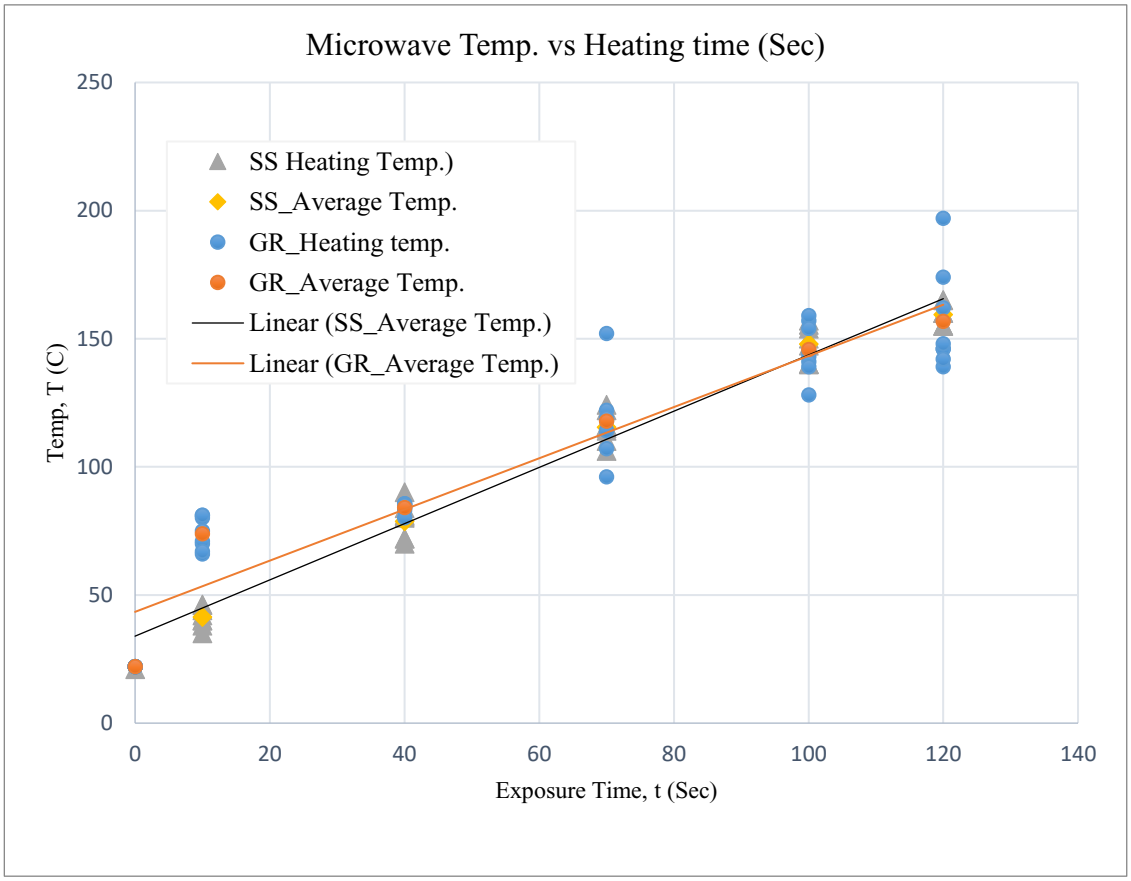

Figure 6–8. Microwave heating for IT Sample (SS and GR)

6.4.1.2 Microwave Irradiation Effects on the Ultrasound Wave Velocity

a. Fractures Induced on the Rock under Microwave Heating

The ultrasonic wave velocities, V_P and V_S, were observed to decrease as the exposure time increased because the fracture was initiated as the Sample absorbed more temperature. The cracks induced will cause a longer travel time and shorten the travel velocity. The visible cracks were observed after the set of ultrasonic wave samples was re-heated for the 2nd cycle. Figures 6-9 below show GR-3, GR-4, and GR-5 specimens with fractures.

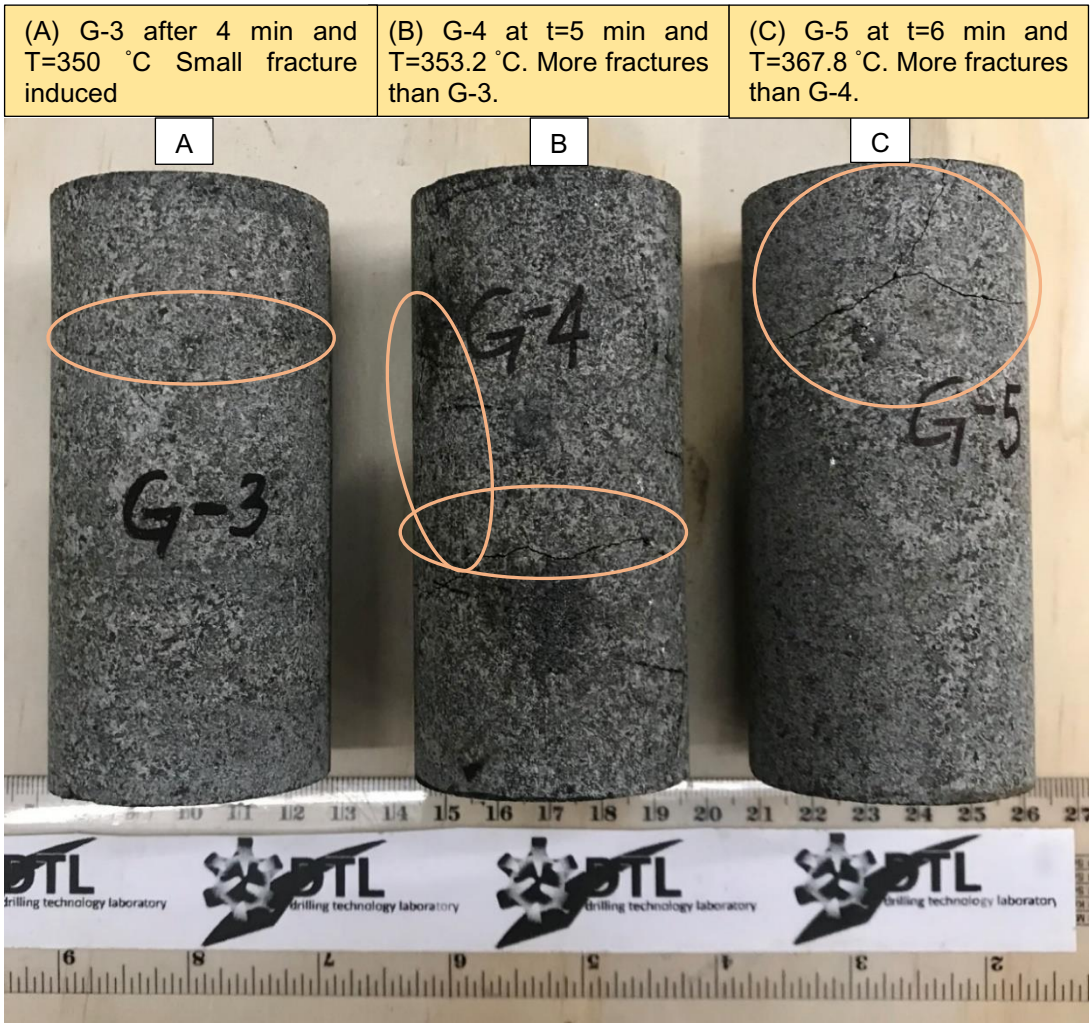

Figure 6–9. Fractures induced on 4in- GR Sample after the effect of re-heated

b. Effect of Microwave Heating on P & S Wave Velocity

Figure 6-10 below shows a plot of the GR-3 Sample showing time arrival for P and S-wave velocity pre-and post-microwave heating. Also, Tables 6-2 and 6-3 show the results of all samples tested for an ultrasound wave before and after microwave irradiation effects, respectively. Figure 6-9 shows V_P and V_S decreased after all the specimens were exposed to microwave radiation. In Figure 6-8, t_s- represents time arrival for shear wave and t_P- time arrival for compressional wave.

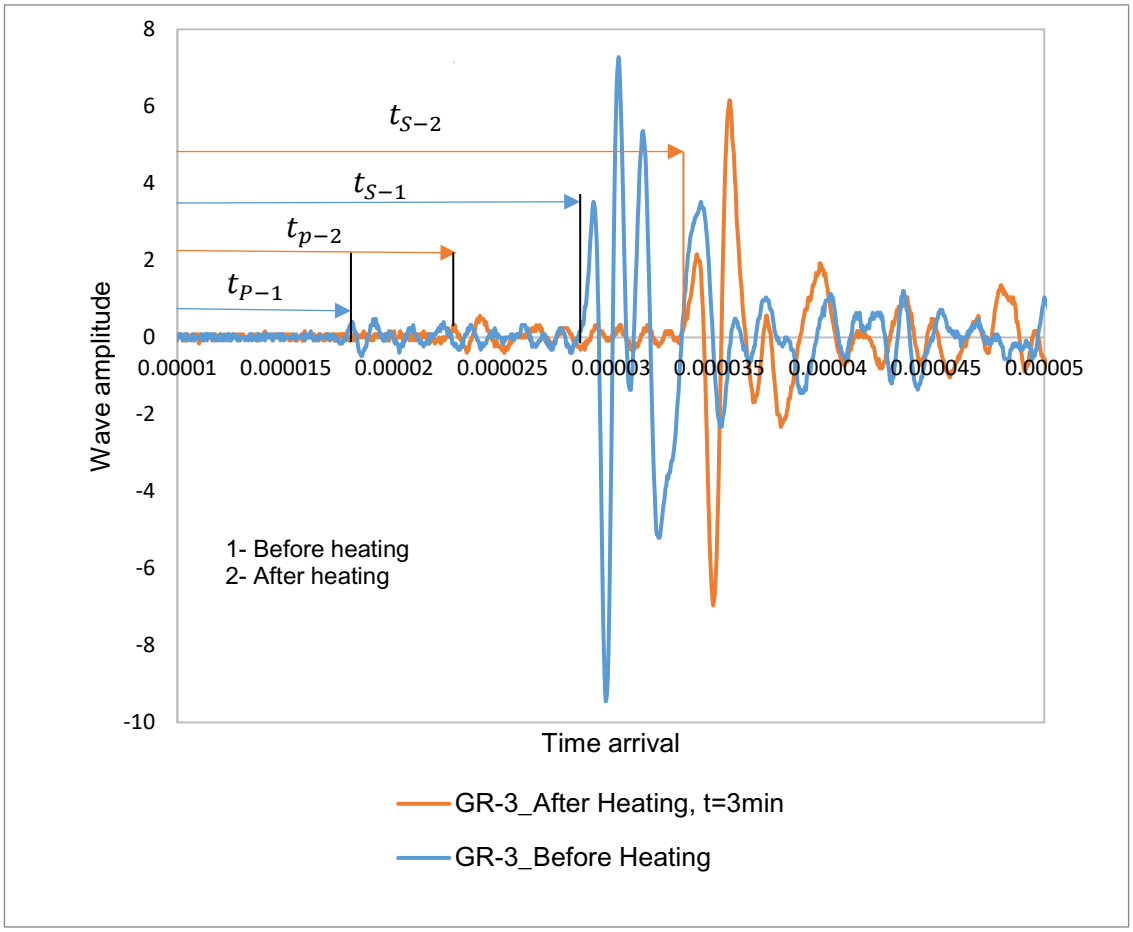

Figure 6–10. Time arrival for P&S wave velocity before and after microwave radiation for GR-3 Sample

Also, the elastic constants such as Young's Modulus (E) and Poisson's ratio (v) were calculated, as the results observed to decrease in elastic constants as MI exposure time increased as shown in Table 1. Elastic constants was computed using the following equations below:

$$V_P = L_P/T_P \qquad [6\text{-}2]$$

$$V_s = L_P/T_P \qquad [6\text{-}3]$$

Where: V_P & V_s = P- and S- wave velocity constants, respectively, m/s

$L\&T$ = Core sample length (m) and travel-time (sec), respectively.

$$E = [\rho V_s^2(3V_P^2 - 4V_s^2)]/(V_P^2 - V_s^2) \qquad [6\text{-}4]$$

Where: E = Young's modulus of elasticity (Pa), ρ = density, kg/m3

$$v = (V_P^2 - 2V_S^2)/[2(V_p^2 - V_S^2)] \qquad [6\text{-}5]$$

Where: v = *Poisson's ratio*

Table 6-1. Elastic properties of the rock before and after MI

Core Sample	Diameter	Length	Density	Arrival time (Sec)		Velocities		Young Modulus	Poissons ratio
4in	(m)	L(m)	kg/m3	tP-wave	tS-wave	Vp	Vs	E (Gpa)	v
GR_Before-MI	0.0473	0.0990	2885.73	0.000018	0.000029	5500	3414	79.82	0.187
GR-1_1m	0.0473	0.0990	2884.76	0.000018	0.000029	5500	3414	79.79	0.187
GR-2_2m	0.0473	0.0992	2881.37	0.000019	0.000030	5211	3300	73.12	0.165
GR-3_3m	0.0473	0.0998	2862.50	0.000023	0.000033	4348	3030	54.03	0.028
GR-4_4m	0.0473	0.0995	2871.33	0.000024	0.000035	4125	2829	48.53	0.056
GR-5_5m	0.0473	0.0992	2880.21	0.000025	0.000035	4060	2829	47.40	0.028

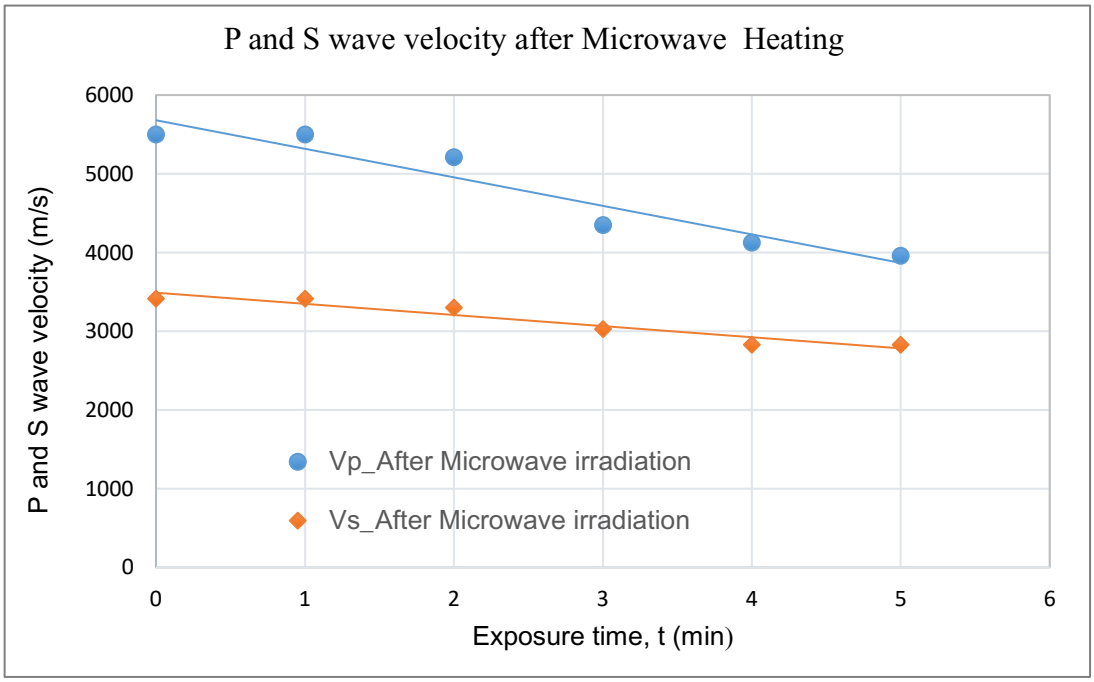

Figure 6–11. Effect of microwave irradiation on ultrasound wave velocity

6.4.2 Strength Tests Analysis

6.4.3 Effect of Microwave Heating on IT Strength of the Rock

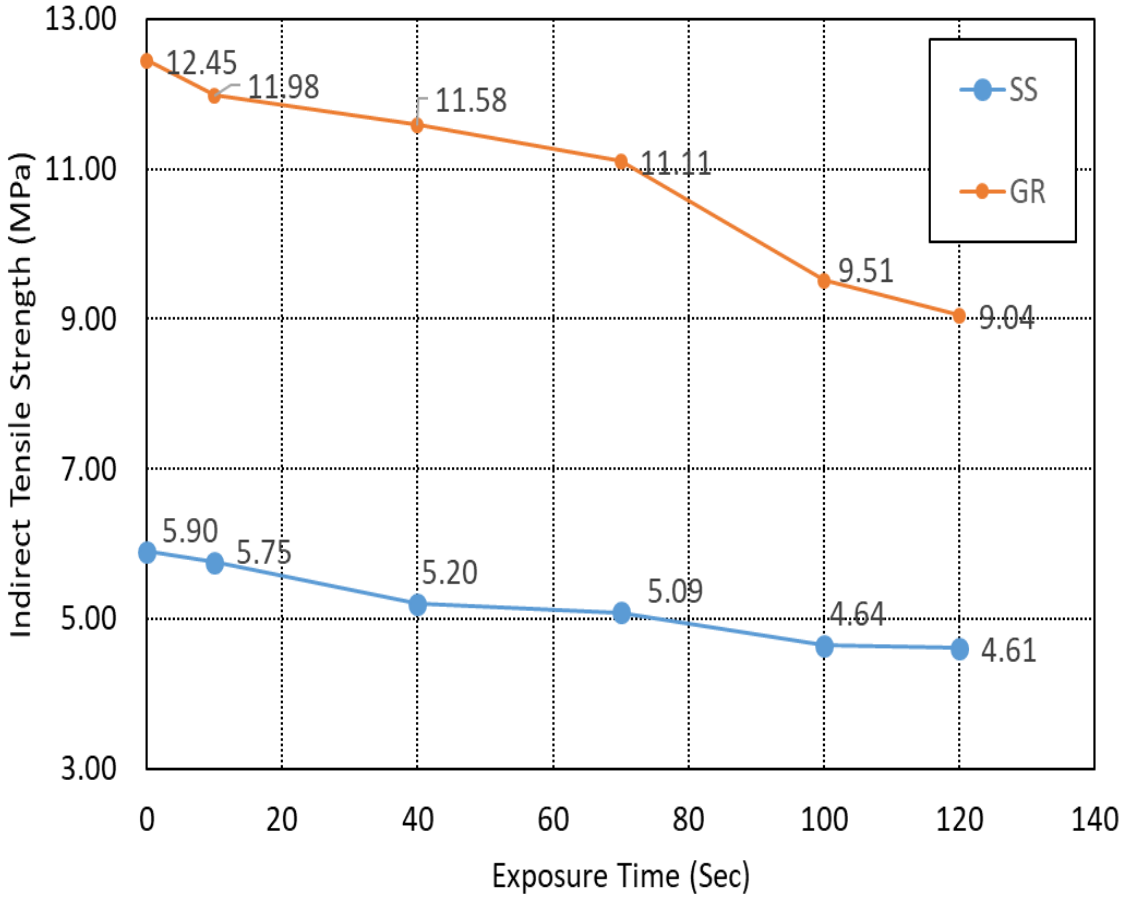

Figure 6–12. IT Strength or SS and GR as a function of Microwave exposure time.

The indirect tensile strength of the rock was determined following (ASTM-D3967). The rock strength decreased as Sample's heating temperature increased, as shown in figure 6-12 for SS and GR Samples. The decrease in rock strength is caused by the fracture initiation as the heating temperature increases, as shown in figure 6-9 for 4in-GR samples.

6.4.4 Drill-off-Test (DOT) Results

DOT was conducted for the granite samples without and after the samples exposed to MI. Figure 6-13 is showing the MI heating temperature of the rocks, where the room temperature was 22.2 for each sample and then with an increments of 75 seconds, the MI of each sample was observed to increase to the maximum of 1830 with 450 seconds.

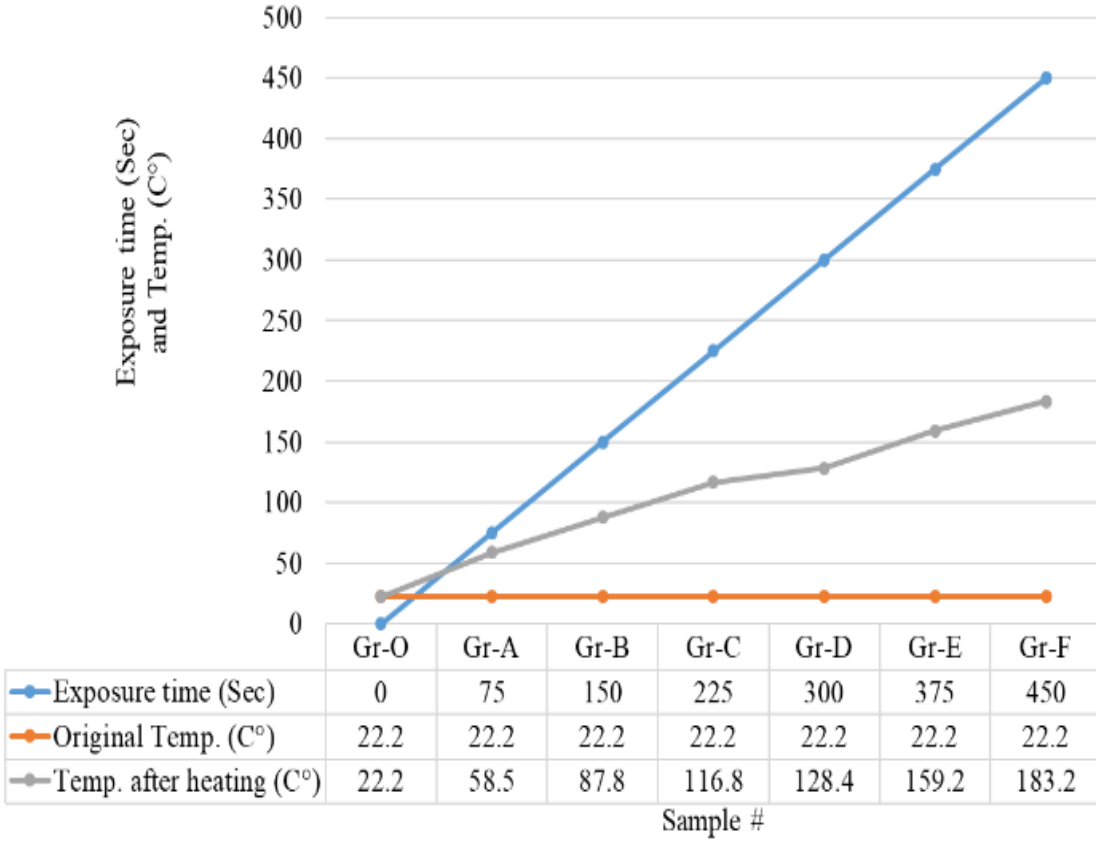

Figure 6–13. Heating of granite samples as a function of microwaves exposure time.

Then using dual PDC bit, DOT was conducted for granite samples. D-ROP was observed to increase as (i) the WOB increased and (ii) the MI heating effects increased for granite rock as shown in figure 6-14.

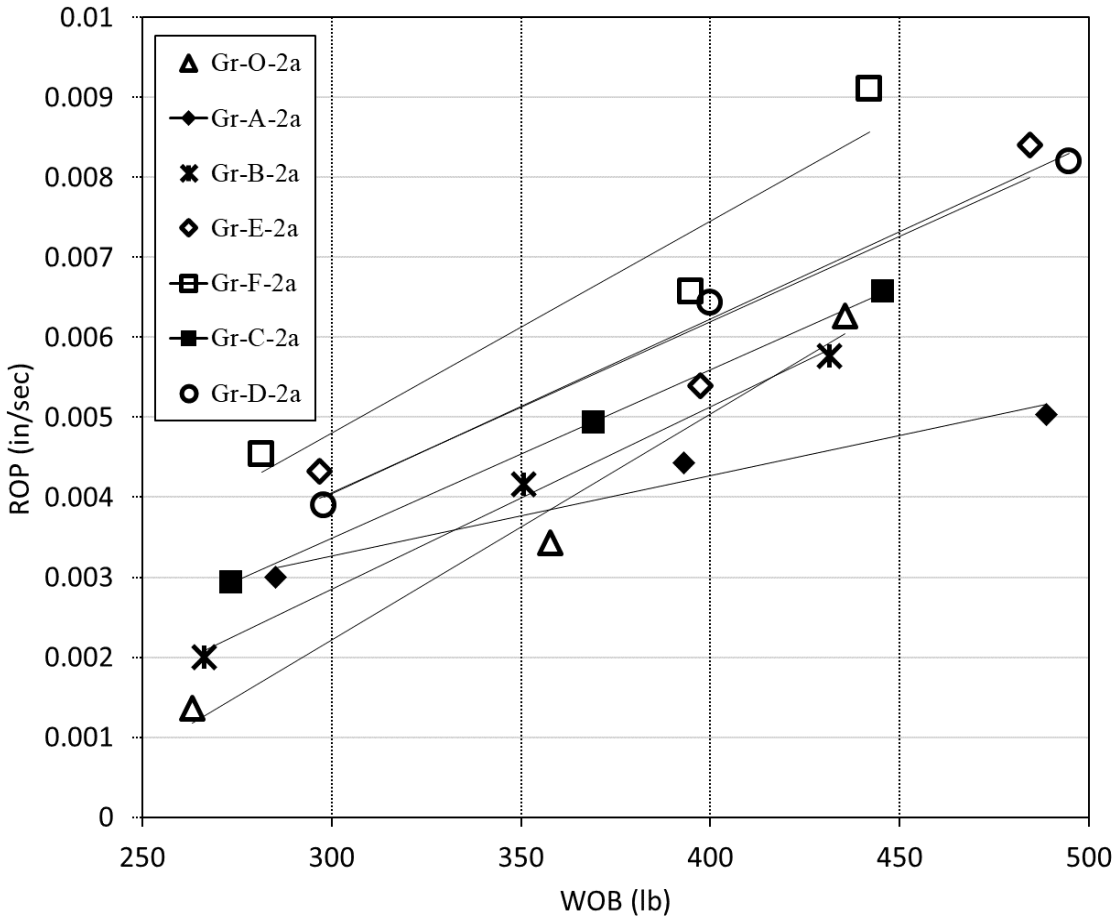

Figure 6–14. Drill-off-tests for granite samples with increasing irradiation time and temperature.

6.5 Conclusions

The current research explains the theory of weakening rock formation ahead of the tool that breaks, indents and fragments the rock, such as a drill bit for increasing ROP technique. Among the penetration rate optimization measures is analyzing and understanding rock properties such as strength and acoustic wave velocity. The summary of the work presented as follows:

- The heating temperature was observed to increase for all samples specimens after they were exposed to MI. In the 2nd heating cycle of 4-in GR samples, visible cracks were observed on GR-3, GR-4, and GR-5 when they reached 350 $^{\circ}$C, 353.2 $^{\circ}$C, and 367.8 $^{\circ}$C, respectively.
- The elastic properties of the rock including P-wave and S-wave velocities, Young's modulus (E) and Poisson's ration was observed to decrease as the MI of the rock increased.
- The indirect tensile strength of the rock was observed to decrease after the MI.
- Drilling ROP shows a remarkable increase after the samples exposed to MI heating, this shows a good indication of the MI weakening the rock.

Chapter 7 : Summary and Conclusion

This chapter concludes and summarizes the recommendations of the current work. Tremendous work was conducted on analyzing disk cutter drilling performance and optimization methods, rock strength correlations, and field data analysis at DTL Laboratory at MUN.

A part of this research explains the full-field trial of DDH and LDH drilling in the Sustainable Mining by Drilling (SMD) project. The drilling performance investigation was conducted to improve and optimize the drilling for the next phase. The drilling data was recorded on the site, and drill cuttings were collected. To complete the analysis, the experimental laboratory tests were conducted at MUN on the NQ core size representing the lithology of the drilling formation. The test results of the laboratory tests, including core logging, strength, hardness, and MLA technology, were then correlated with the field data. The observation at specific lithology intervals showed that high rock strength and hardness cause a reduction in drilling ROP performance. MLA analysis proved that increased strength is caused by microstructure alteration at that interval. Also, the cutting size results were compared with WOB and observed to increase parallel except at the depth intervals of low ROP where the grain sizes were finer.

Also, this work discusses the new methods of rock strength determination through a Semi-PLSI. The purpose was to simplify a testing method from standard PLSI. The research work was able to invent new techniques of rock strength estimation and correlate with other strength tests like UCS, ITS, and PLSI as destructive tests and V_P and V_S as non-destructive tests. The correlation results presented were very good for both tests. The DTL research

group expects to expand this work by conducting more tests and analyses using different rocks.

Additionally, this thesis includes an initial stage of experimental laboratory methods for investigating the rock properties conducted using microwave irradiation (MI). It is among the techniques that improve ROP by weakening the rock formation. The influence of rock properties, including strength and P&S-wave velocities, elastic constants i.e., Young's Modulus and poisson's ratio were analyzed and compared before and after MI. The results showed MI causes a decrease in strength, ultrasonic wave properties of the rock. Also, results from drill-off-test for drilling on a microwaved specimen of a granite rock shows a remarkable increase in ROP.

References

Abugharara, A. N., Alwaar, A. M., Butt, S. D., & Hurich, C. A. (2016, June). Baseline Development of Rock Anisotropy Investigation Utilizing Empirical Relationships Between Oriented Physical and Mechanical Measurements and Drilling Performance. In *International Conference on Offshore Mechanics and Arctic Engineering* (Vol. 49996, p. V008T11A016). American Society of Mechanical Engineers.

Abugharara, A. N., Hurich, C. A., Molgaard, J., & Butt, S. D. (2017, June). Implementation of circular wave measurements and multiple drilling parameter analysis in rock anisotropy evaluation. *In International Conference on Offshore Mechanics and Arctic Engineering* (Vol. 57762, p. V008T11A012). American Society of Mechanical Engineers.

Abugharara, A. N., Mohamed, B., Hurich, C., Molgaard, J., & Butt, S. D. (2019). Experimental Investigation of the Effect of Shale Anisotropy Orientation on the Main Drilling Parameters Influencing Oriented Drilling Performance in Shale. *Journal of Energy Resources Technology*, 141(10).

Abugharara, A., Butt, S., Molgaard, J., & Hurich, C. (2019). -Empirical Procedure Investigation for Sandstone Anisotropy Evaluation: Part I. *Influence of Formation Anisotropy and Axial Compliances on Drilling Performance*, 369.

Abugharara, A., Mafazy, S., & Butt, S. (2022, June). A New Approach for Rock Strength Estimation through a Semi-Point Load Strength Index and Correlation with Destructive and Non-destructive Tests. In *International Conference on Offshore Mechanics and Arctic Engineering* (Vol. 85956, p. V010T11A092). American Society of Mechanical Engineers.

Abugharara, A., Tytler, O., & Butt, S. (2022, June). Drilling Performance Evaluation Through Bit Cutters Reconfigurations and Micro Fractures Initiation. In *International Conference on Offshore Mechanics and Arctic Engineering* (Vol. 85956, p. V010T11A087). American Society of Mechanical Engineers.

Abzalov, M. (2016). Drilling Techniques and Drill Holes Logging. In *Applied Mining Geology* (pp. 39-77). Springer, Cham.

Ahmed, D., Xiao, Y., de Moura, J., & Butt, S. D. (2020, August). Drilling Cutting Analysis to Assist Drilling Performance Evaluation in Hard Rock Hole Widening Operation. In *International Conference on Offshore Mechanics and Arctic Engineering* (Vol. 84430, p. V011T11A082). American Society of Mechanical Engineers.

Allen, J. H. (1968). Drilling large diameter holes. *Australian Oil and Gas Review*.

Alsuwaidi, E. S. (2018). Cutting Transport Analysis in Horizontal Wells: A Computational Approach.

Altındag, R. (2003). Estimation of penetration rate in percussive drilling by means of coarseness index and mean particle size.

Armenta, M. (2008, September). Identifying inefficient drilling conditions using drilling-specific energy. In *SPE Annual Technical Conference and Exhibition*. OnePetro.

Asadi, A. (2015, October). Application of artificial neural networks in estimation of uniaxial compressive strength using indirect tensile strength data of limestone rocks. *In ISRM Regional Symposium-EUROCK 2015*. OnePetro.

Ashena, R., & Thonhauser, G. (2018). Jam Mitigation Coring. In *Coring Methods and Systems* (pp. 135-148). Springer, Cham.

ASME Shale Shaker Committee. (2011). *Drilling fluids processing handbook*. Elsevier.

ASTM D2845-08. (2008). Standard test method for laboratory determination of pulse velocities and ultrasonic elastic constants of rock. *American Society for Testing and Materials*, West Conshohocken, PA, USA.

ASTM D3967. (2017). Standard Test Method for Splitting Tensile Strength of Intact Rock Core Specimens. *American Society for Testing and Materials*, Pennsylvania, PA, USA.

ASTM D5731. (2016). Standard Test Method for Determination of the Point Load Strength Index of Rock and Application to Rock Strength Classifications. *American Society for Testing and Materials*, Pennsylvania, PA, USA.

ASTM D5873. (2014). Standard Test Method for Determination of Rock Hardness by Rebound Hammer Method. *American Society for Testing and Materials*, Pennsylvania, PA, USA.

ASTM D6913/6913M. (2017). Standard Test Methods for Particle-Size Distribution (Gradation) of Soils Using Sieve Analysis. *American Society for Testing and Materials*, Pennsylvania, PA, USA.

ASTM D7012. 92014). Standard Test Methods for Compressive Strength and Elastic Moduli of Intact Rock Core Specimens under Varying States of Stress and Temperatures. *American Society for Testing and Materials*, Pennsylvania, PA, USA.

ASTM. (2001). Standard Practices For Preparing Rock Core As Cylindrical Test Specimens And Verifying Conformance To Dimensional And Shape Tolerances. *American Society for Testing and Materials*, Pennsylvania, PA, USA.

Aston, M. S., Hearn, P. J., & McGhee, G. (1998, September). Techniques for solving torque and drag problems in today's drilling environment. In *SPE Annual Technical Conference and Exhibition*. OnePetro.

Basu, A., & Aydin, A. (2004). A Method for Normalization of Schmidt Hammer Rebound Values. *International Journal of Rock Mechanics & Mining Sciences*, 41: 1211-1214.

Breeds, C. D., & Conway, J. J. (1992). Rapid excavation. *SME mining engineering handbook*, *2*, 1871-1907.

Brooks, W. B., Dean, J. T., & Gravley, W. (1963). Mobile electronic recording system and drill-off data illustrating its use. *Journal of Petroleum Technology*, *15*(01), 11-16.

Butt, S. D. (2016). Drilling Technology Methods. In M. R. Riazi, Exploration and Production of Petroleum and Natural Gas, 197-231. *ASTM International*.

Cargill, J. S., & Shakoor, A. (1990, December). Evaluation of empirical methods for measuring the uniaxial compressive strength of rock. In *International Journal of Rock Mechanics and Mining Sciences & Geomechanics Abstracts* (Vol. 27, No. 6, pp. 495-503). Pergamon.

Carlos, L. J., Emilio, L. J., & Francisco, J. A. C. (2017). Drilling and blasting of rocks.

Chau, K. T., & Wong, R. H. C. (1996, February). Uniaxial compressive strength and point load strength of rocks. In *International journal of rock mechanics and mining sciences & geomechanics abstracts* (Vol. 33, No. 2, pp. 183-188). Pergamon.

Cigla, M., Yagiz, S., & Ozdemir, L. (2001, June). Application of tunnel boring machines in underground mine development. In *17th international mining congress and exhibition of Turkey* (pp. 155-164).

Cumming, J. D., & Smit, J. K. (1980). In Diamond drill handbook, 3rd Edition, Toronto.

De Moura Junior, J. (2021). Universal physics-based rate of penetration prediction model for rotary drilling (Doctoral dissertation, Memorial University of Newfoundland). *Thesis*.

de Moura, J., Xiao, Y., Yang, J., & Butt, S. D. (2021).An empirical model for the drilling performance prediction for roller-cone drill bits. Journal of Petroleum Science and *Engineering*, *204*, 108791.

Dupriest, F. E., & Koederitz, W. L. (2005, February). Maximizing drill rates with real-time surveillance of mechanical specific energy. In *SPE/IADC drilling conference*. OnePetro.

Ersoy, A., & Waller, M. D. (1997). Drilling detritus and the operating parameters of thermally stable PDC core bits. *International Journal of Rock Mechanics and Mining Sciences*, *34*(7), 1109-1123.

Farah, R. (2011). Correlations between index properties and unconfined compressive strength of weathered Ocala limestone. *Theses and Dissertations*.

Fjaer, E., Holt, R. M., Horsrud, P., & Raaen, A. M. (2008). *Petroleum related rock mechanics*. Elsevier.

Ghosh, D. K., & Srivastava, M. (1991). Point-load strength: an index for classification of rock material. Bulletin of the International Association of Engineering Geology, 44(1), 27-33.

Grant, D. C., Goudie, D. J., & Baird, E. (2018). Analysis of 98 individual− 200 mesh iron ore samples in a single scanning electron microscope-automated mineralogy session. *Applied Earth Science*, 127(1), 38-43.

Gwarek, W. K., & Celuch-Marcysiak, M. (2004, May). A review of microwave power applications in industry and research. *In 15th International Conference on Microwaves, Radar and Wireless Communications* (IEEE Cat. No. 04EX824) (Vol. 3, pp. 843-848). IEEE.

Hareland, G., Wu, A., Rashidi, B., & James, J. A. (2010, June). A new drilling rate model for tricone bits and its application to predict rock compressive strength. In *44th US Rock Mechanics Symposium and 5th US-Canada Rock Mechanics Symposium*. OnePetro.

Hartlieb, P., Kuchar, F., Moser, P., Kargl, H., & Restner, U. (2018). Reaction of different rock types to low-power (3.2 kW) microwave irradiation in a multimode cavity. *Minerals Engineering*, 118, 37-51.

Hassani, F., Nekoovaght, P. M., & Gharib, N. (2016). The influence of microwave irradiation on rocks for microwave-assisted underground excavation. *Journal of Rock Mechanics and Geotechnical Engineering*, 8(1), 1-15.

Hoek, E., Carranza-Torres, C., & Corkum, B. (2002). Hoek-Brown failure criterion-2002 edition. *Proceedings of NARMS-Tac*, 1(1), 267-273.

Holtz, R. D., Kovacs, W. D., & Sheahan, T. C. (1981). *An introduction to geotechnical engineering* (Vol. 733). Englewood Cliffs: Prentice-Hall.

Hong, Y., Lin, B. Q., Zhu, C. J., Wang, Z., Liu, J. Q., Saffari, P., & Nie, W. (2020). Image and ultrasonic analysis-based investigation of coal core fracturing by microwave energy. *International Journal of Rock Mechanics and Mining Sciences*, 127, 104232.

Horikoshi, S., Schiffmann, R. F., Fukushima, J., & Serpone, N. (2018). Microwave chemical and materials processing. *Springer*.

Huang, J., Xu, G., Liang, Y., Hu, G., & Chang, P. (2020). Improving coal permeability using microwave heating technology—*A review. Fuel*, 266, 117022.

Jaeger, J. C., Cook, N. G., & Zimmerman, R. (2009). *Fundamentals of rock mechanics*. John Wiley & Sons.

Johancsik, C. A., Friesen, D. B., & Dawson, R. (1984). Torque and drag in directional wells-prediction and measurement. *Journal of Petroleum technology*, *36*(06), 987-992.

Kahraman, S. A. İ. R. (2001). Evaluation of simple methods for assessing the uniaxial compressive strength of rock. *International Journal of Rock Mechanics and Mining Sciences*, 38(7), 981-994.

Kahraman, S., Canpolat, A. N., & Fener, M. (2020). The influence of microwave treatment on the compressive and tensile strength of igneous rocks. *International Journal of Rock Mechanics and Mining Sciences,* 129, 104303.

Karimi, M. (2013). Drill-Cuttings Analysis for Real-Time Problem Diagnosis and Drilling Performance Optimization. SPE Asia Pacific Oil and Gas Conference and Exhibition. *Society of Petroleum Engineers. SPE-165919-MS*.

Kolapo, P. (2021). Investigating the effects of mechanical properties of rocks on specific energy and penetration rate of borehole drilling. *Geotechnical and Geological Engineering*, 39(2), 1715-1726.

Krzysztof, K., & Piotr, M. (2019). Methods of mechanical mining of compact-rock—a comparison of efficiency and energy consumption. *Energies*, 12(18), 3562.

Lin, F., Feng, X. T., Yang, C., Li, S., Zhang, J., Su, X., & Tong, T. (2022). Microwave response characteristics and influencing factors of ores based on dielectric properties of synthetic samples. *Journal of Rock Mechanics and Geotechnical Engineering*, 14(2), 315-328.

Lu, G. M., Feng, X. T., Li, Y. H., Hassani, F., & Zhang, X. (2019). Experimental investigation on the effects of microwave treatment on basalt heating, mechanical strength, and fragmentation. *Rock Mechanics and Rock Engineering*, 52(8), 2535-2549.

Mafazy, S. K., Jamil, M. S., Tytler, O., Abugharara, A., & Butt, S. (2021). Mechanical Tests on R&J Rock Characterization. *Quarter 3-Sustainable Mining by Drilling (SMD) Interim Report. Memorial University of Newfoundland, St. John's, Canada.*

Mafazy, S. K., Marsh, M., Zijian, L., & Butt, S. (2022). Influence of Rock Microstructure on Rock Strength and Drilling Rate of Penetration. *75th Canadian Geotechnical Conference. Calgary, Alberta, CA.*

Mafazy, S. K., Tytler, O., Jamil, M. S., & Butt, S. (2022). Correlation of Rate of Penetration (ROP), Chip Size, Rock Properties & Lithology. *Quarter 1-Sustainable Mining by Drilling (SMD) Interim Report. Memorial University of Newfoundland, St. John's, Canada.*

Marland, S., Merchant, A., & Rowson, N. (2001). Dielectric properties of coal. *Fuel*, 80(13), 1839-1849.

Maurer, W. C. (1962). The perfect-cleaning theory of rotary drilling. *Journal of Petroleum Technology*, 14(11), 1270-1274.

McCormick, J. E., Evans, C. D., Le, J., & Chiu, T. (2012, February). The practice and evolution of torque and drag reduction: theory and field results. In *IPTC 2012: International Petroleum Technology Conference* (pp. cp-280). European Association of Geoscientists & Engineers.

Mishra, D. A., & Basu, A. (2012). Use of the block punch test to predict the compressive and tensile strengths of rocks. *International Journal of Rock Mechanics and Mining Sciences*, 51, 119-127.

Motlagh, P, N. (2009). An investigation on the influence of microwave energy on basic mechanical properties of hard rocks (Doctoral dissertation, Concordia University). *Thesis.*

Nazir, R., Momeni, E., Armaghani, D. J., & Amin, M. M. (2013). Correlation between unconfined compressive strength and indirect tensile strength of limestone rock samples. *Electron J Geotech Eng*, 18(1), 1737-1746.

NOV Inc. (2016). Agitator Technology, https://www.nov.com/products/agitator-technologies.

Novamera Inc. (2021). Method Statement Drilling Operations, Test Shaft Novamera Canada. Sustainable mining by Drilling (SMD) project. *Technical Report.*

Palchik, V. (2007). Use of stress-strain model based on Haldane's distribution function for prediction of elastic modulus. *International Journal of Rock Mechanics and Mining Sciences*, 44(4), 514-524.

Palmstrom, A. (2005). Measurements of and Correlations between Block Size and Rock Quality Designation (RQD). In W. Broere, S. Li, J. Rostami, & Q. Zhang, *Tunnelling and Underground Space Technology*, 20: 362-377. Norconsult AS, Vestfjordgaten 4, N-1338 Sandvika, Norway.

Pszonka, J., & Sala, D. (2018). Application of the mineral liberation analysis (MLA) for extraction of grain size and shape measurements in siliciclastic sedimentary rocks. In *E3S Web of Conferences* (Vol. 66, p. 02002). EDP Sciences.

Quan, W., Rasul, G., Abugharara, A., Zhang, Y., Rahman, M. A., & Butt, S. (2021). Empirical Correlations and A new Approach for Strength Evaluation of Isotropic Rocks. *Canadian Geotechnical Society*, Niagara Falls, Ontario, Canada.

Quan, W., Rasul, G., Abugharara, A., Zhang, Y., Rahman, M., & Butt, S. (2021). Tensile and Shear Fracture Examination for Optimal Drilling Performance Evaluation: part-II. *Canadian Geotechnical Society*. Niagara Falls, Ontario, Canada.

Rao, K. U. M., Bhatnagar, A., & Misra, B. (2002). Laboratory investigations on rotary diamond drilling. *Geotechnical & Geological Engineering*, *20*(1), 1-16.

Rasul, G., Quan, W., Abugharara, A., Zhang, Y., Azizur, M., & Rahman, S. B. (2021). 6. Chapter 6. Tensile and Shear Fracture Examination for Optimal Drilling Performance Evaluation. *Experimental and CFD Analyses of Cuttings Transport in Horizontal Annuli*, 95.

Rawal, R., Karmakar, N. C., Sharma, S. K., & Krishnamoorthi, S. (2022). Application of polymeric drilling fluids for reducing wearing of drill bit. *Journal of the Indian Chemical Society*, *99*(2), 100324.

Reich, M., Hoving, P. G., & Makohl, F. (1995, February). Drilling performance improvements using downhole thrusters. In *SPE/IADC Drilling Conference*. OnePetro.

Reyes, R., Kyzym, I., Rana, P. S., Molgaard, J., & Butt, S. D. (2015, June). Cuttings analysis for rotary drilling penetration mechanisms and performance evaluation. In *49th US Rock Mechanics/Geomechanics Symposium*. OnePetro.

Satish, H., Ouellet, J., Raghavan, V., & Radziszewski, P. (2006). Investigating microwave assisted rock breakage for possible space mining applications. *Mining technology*, 115(1), 34-40.

Schmalhorst, B. (1999, March). Dynamic behaviour of a bit-motor-thruster assembly. In *SPE/IADC drilling conference*. OnePetro.

Sheorey, P. R. (1997). *Empirical rock failure criteria*. AA Balkema.

Sulukcu, S., & Ulusay, R. (2001). Evaluation of the block punch index test with particular reference to the size effect, failure mechanism and its effectiveness in predicting rock strength. *International Journal of Rock Mechanics and Mining Sciences*, 38(8), 1091-1111.

Sylvester, P. J. (2012). Use of the mineral liberation analyzer (MLA) for mineralogical studies of sediments and sedimentary rocks. *Mineralogical Association of Canada Short Course*, *42*, 1-16.

Takbiri-Borujeni, A., Fathi, E., Sun, T., Rahmani, R., & Khazaeli, M. (2019). Drilling performance monitoring and optimization: a data-driven approach. *Journal of Petroleum Exploration and Production Technology*, *9*(4), 2747-2756.

Teale, R. (1965, March). The concept of specific energy in rock drilling. In *International journal of rock mechanics and mining sciences & geomechanics abstracts* (Vol. 2, No. 1, pp. 57-73). Pergamon.

Toasudjai, N., Lordkratok, C., Fecho, K., & Tipdontree, P. (2022, March). Improvement Drilling Efficiency by Using Mud Motor and Agitator Bha in 6 1/8-in. Hole: Gulf of Thailand. In *Offshore Technology Conference Asia*. OnePetro.

Tuğrul, A., & Gürpinar, O. (1997). A proposed weathering classification for basalts and their engineering properties (Turkey). *Bulletin of Engineering Geology and the Environment*, 55(1), 139-149.

Wei, W., Shao, Z., Zhang, Y., Qiao, R., & Gao, J. (2019). Fundamentals and applications of microwave energy in rock and concrete processing–A review. *Applied Thermal Engineering*, 157, 113751.

Xiao, Y., Zhong, J., Hurich, C., & Butt, S. D. 2015. Micro-Seismic Monitoring of PDC Bit Drilling Performance during Vibration Assisted Rotational Drilling, *49th US Rock Mechanics / Geomechanics Symposium*. San Francisco, CA, USA.

Xu, T., Yuan, Y., Heap, M. J., Zhou, G. L., Perera, M. S. A., & Ranjith, P. G. (2021). Microwave-assisted damage and fracturing of hard rocks and its implications for effective mineral resources recovery. *Minerals Engineering*, 160, 106663.

Zhao, K., Gu, S., Yan, Y., Li, Q., Xiao, W., & Liu, G. (2018). Rock mechanics characteristics test and optimization of high-efficiency mining in dajishan tungsten mine. *Geofluids*, *2018*.

Zhao, Q. H., Zhao, X. B., Zheng, Y. L., Li, J. C., He, L., He, J. L., & Zou, C. J. (2020). Heating characteristics of igneous rock-forming minerals under microwave irradiation. *International Journal of Rock Mechanics and Mining Sciences*, 135, 104519.

Znamenácková, I., Lovás, M., Hajek, M., & Jakabský, Š. (2003). Melting of andesite in a microwave oven. *Journal of Mining and Metallurgy*, Section B: Metallurgy, 39(3-4), 549-557.